



**Universidad**  
Zaragoza



**TESIS DOCTORAL**  
**POR COMPENDIO DE PUBLICACIONES**

**Exploring New Non-Destructive Techniques for the Study of Leaf  
Water Status: Air-Coupled Broadband Ultrasonic Spectroscopy  
and Microwave L-Band**

**Autor:**

Domingo Sancho Knapik

**Directores:**

Dr. Eustaquio Gil Pelegrín Centro de Investigación y Tecnología Agroalimentaria de Aragón	Dr. Tomas Gómez Álvarez-Arenas Consejo Superior de Investigaciones Científicas
---	--

**Departamento de Agricultura y Economía Agraria**

**UNIVERSIDAD DE ZARAGOZA**



### *Agradecimientos*

*Deseo expresar mi más profundo agradecimiento a todas las personas que han dedicado parte de su tiempo y dedicación a la elaboración de esta tesis doctoral:*

*En primer lugar, mi más amplio agradecimiento a los Doctores Eustaquio Gil Pelegrín y Tomás Gómez Álvarez Arenas, directores de la presente memoria, porque nunca he dejado de sentir su confianza y apoyo para guiar el desarrollo de esta investigación. Sus orientaciones y conocimientos han sido fundamentales para su finalización.*

*A los Doctores Javier Gismero y Alberto Asensio, colaboradores de este trabajo, con los que he aprendido cuestiones técnicas muy importantes que se reflejan en esta memoria.*

*También quisiera hacer patente mi agradecimiento a mis compañeros de laboratorio, el Dr. José Javier Peguero Pina, Dido Villarroya Lacarta y José María Alquezar Alquezar, por las valiosas aportaciones que me hicieron para mejorar la presente investigación y por su amistad. A ellos les deseo mucha suerte.*

*En especial quiero dar mi más profunda gratitud a mi familia. Ellos son los pilares de mi vida, los que me han transmitido siempre la fuerza necesaria para continuar, los que nunca me han fallado, los que me han acompañado en los buenos y malos momentos. En cada ejemplo, en cada línea y en cada palabra podría indicar la influencia de su apoyo, de sus sugerencias y de su compañía. Sólo espero ser capaz de devolverles algún día lo mucho que me han ayudado.*

*Por último, agradecer a los Proyectos INIA SUM2008-00004-C03-03, AGL2010-21153-C02-02 (Ministerio de Ciencia e Innovación), GA-LC-002/2010 (Departamento de Ciencia, Tecnología y Universidad) y al Gobierno de Aragón (grupo de investigación A54) por financiar el trabajo y servirme en todo momento de soporte económico.*

*A todos mi mayor reconocimiento y gratitud*



## ÍNDICE DEL CONTENIDO

<b>A. TESIS COMO COMPENDIO DE TRABAJOS PREVIAMENTE PUBLICADOS .....</b>	<b>5</b>
<b>B. INTRODUCCIÓN GENERAL .....</b>	<b>6</b>
<b>C. COPIA DE LOS TRABAJOS PUBLICADOS .....</b>	<b>15</b>
I. Air-coupled broadband ultrasonic spectroscopy as a new non-invasive and non-contact method for the determination of leaf water status .....	17
II. Relationship between ultrasonic properties and structural changes in the mesophyll during leaf dehydration. ....	25
III. Air-coupled ultrasonic resonant spectroscopy for the study of the relationship between plants leaves elasticity and their water content .....	35
IV. Microwave L-band (1730 MHz) accurately estimates the relative water content in poplar leaves. A comparison with a near infrared water index (R1300/R1450).....	43
<b>D. RESUMEN .....</b>	<b>49</b>
1. OBJETIVOS DE INVESTIGACIÓN.....	49
2. APORTACIONES DEL DOCTORANDO .....	49
3. METODOLOGÍA UTILIZADA .....	50
3.1 Espectroscopía ultrasónica de banda ancha acoplada al aire .....	52
3.2 Análisis de la respuesta espectral de la resonancia .....	54
3.3 La antena de microondas de telefonía móvil digital.....	58
3.4 Material vegetal y experimental .....	60
3.5 Curvas presión-volumen.....	61
3.6 Espesor y densidad .....	61
3.7 Microscopio electrónico de barrido por congelación .....	61
3.8 Análisis estadísticos .....	62
4. PRINCIPALES RESULTADOS .....	62
5. CONCLUSIONES FINALES.....	69
6. PERSPECTIVAS .....	71
7. BIBLIOGRAFÍA .....	71
<b>E. APÉNDICES .....</b>	<b>75</b>
APÉNDICE 1: Factor de impacto y Área temática de las revistas .....	77
APÉNDICE 2: Justificación de la contribución del doctorando.....	79

APÉNDICE 3: V. Noncontact and noninvasive study of plant leaves using air-coupled ultrasounds.....	81
APÉNDICE 4: VI. Determination of plant leaves water status using air coupled ultrasounds. ....	85

## ÍNDICE DE FIGURAS E IMÁGENES

<b>Figura 1:</b> Representación esquemática de la técnica de Espectroscopía ultrasónica.....	53
<b>Figura 2:</b> Procedimiento para calcular los valores de la velocidad, espesor, densidad y atenuación de la hoja.....	57
<b>Figura 3:</b> Representación esquemática de la antena y la técnica de microondas.....	59
<b>Figura 4:</b> Relación entre la frecuencia y la transmirtancia para <i>Populus x euramerica</i> y <i>Prunus laurocerasus</i> .....	63
<b>Figura 5:</b> Relación entre la frecuencia estandarizada y el contenido relativo en agua para <i>Populus x euramerica</i> y <i>Prunus laurocerasus</i> .....	64
<b>Figura 6:</b> Relación entre la frecuencia estandarizada y el potencial hídrico para <i>Populus x euramerica</i> y <i>Prunus laurocerasus</i> .....	64
<b>Figura 7:</b> Variación de la constante de elasticidad, el espesor y la densidad sobre la frecuencia estandarizada en <i>Quercus muehlenbergii</i> .....	65
<b>Figura 8:</b> Relaciones entre la presión de turgencia, el modulo de elasticidad de pared y la constante macroscopica de elasticidad para <i>Quercus muehlenbergii</i> .....	65
<b>Figura 9:</b> Respuesta espectral de la primera resonancia en <i>Platanus hispanica</i> a diferentes valores de contenido relativo en agua.....	67
<b>Figura 10:</b> Variación de la constante macroscópica de elasticidad con el contenido relativo en agua.....	68
<b>Figura 11:</b> Relación entre el contenido relativo en agua y los índices $R_{1300}/R_{1450}$ y $MWR_{1730}$ en <i>Populus x euroamericana</i> .....	69
<b>Imagen 1:</b> Detalle de los transductores.....	52
<b>Imagen 2:</b> Detalle del sistema de medida de microondas.....	58
<b>Imagen 3:</b> Hojas de <i>Quercus muehlenbergii</i> realizadas por el Microscopio electrónico de congelación.....	66

## A. TESIS COMO COMPENDIO DE TRABAJOS PREVIAMENTE PUBLICADOS

La presente tesis doctoral, de acuerdo con el informe correspondiente, autorizado por los Directores de Tesis y el Órgano Responsable del Programa de Doctorado, se presenta como un compendio de cuatro trabajos previamente publicados. Las referencias completas de los artículos que constituyen el cuerpo de la tesis son los siguientes:

- I. **Sancho-Knapik D**, Gómez Álvarez-Arenas T, Peguero Pina JJ, Gil-Pelegrín E. 2010. Air-coupled broadband ultrasonic spectroscopy as a new non-invasive and non-contact method for the determination of leaf water status. *Journal of Experimental Botany* 61, 1385-1391.
- II. **Sancho-Knapik D**, Gómez Álvarez-Arenas T, Peguero-Pina JJ, Fernández V, Gil-Pelegrin E. 2011. Relationship between ultrasonic properties and structural changes in the mesophyll during leaf dehydration. *Journal of Experimental Botany* 62, 3637-3645.
- III. **Sancho-Knapik D**, Calás H, Peguero-Pina JJ, Ramos Fernández A, Gil-Pelegrín E, Gómez Álvarez-Arenas T. 2012. Air-coupled ultrasonic resonant spectroscopy for the study of the relationship between plants leaves elasticity and their water content. *IEEE Transactions on Ultrasonics, Ferroelectrics and Frequency Control* 59, 319-325.
- IV. **Sancho-Knapik D**, Gismero J, Assensio A, Peguero-Pina JJ, Fernández V, Gómez Álvarez-Arenas T, Gil-Pelegrín E. 2011. Microwave L-band (1730 MHz) accurately estimates the relative water content in poplar leaves. A comparison with a near infrared water index (R1300/R1450). *Agricultural and Forest Meteorology* 151, 827-832.

Así mismo, se considera oportuno incluir en los apéndices 3 y 4 de la Tesis los siguientes artículos que han constituido parte de la base formativa del doctorando y en los cuales participa como coautor:

- V. Gómez Álvarez-Arenas TE, **Sancho-Knapik D**, Peguero-Pina JJ, Gil-Pelegrín E. 2009. Noncontact and noninvasive study of plant leaves using air-coupled ultrasounds. *Applied Physic Letters* 95, 193702.
- VI. Gómez Álvarez-Arenas TE, **Sancho-Knapik D**, Peguero-Pina JJ, Gil-Pelegrín E. 2009. Determination of plant leaves water status using air.coupled ultrasounds. *IEEE International Ultrasonics Symposium Proceedings* 771-774.

## B. INTRODUCCIÓN GENERAL

La vida está íntimamente asociada al agua y su importancia para las plantas es crucial. Además de ser considerada el componente principal y de ser el medio donde se producen la mayoría de los procesos bioquímicos (Larcher, 2003), el agua actúa como disolvente para muchas sustancias facilitando la absorción, el transporte y el movimiento de nutrientes desde el sistema radicular hasta los distintos tejidos que forman el vegetal. El motor del movimiento del agua es la transpiración, que puede ser considerada en esencia como un proceso de difusión en el que el vapor de agua pasa desde el interior de la hoja hasta la atmósfera libre. El grado de transpiración de una planta depende de factores tan diversos como son la radiación solar incidente, la temperatura, la humedad relativa del aire, el viento y el suministro de agua disponible para la planta. A pesar de que las variables anteriormente citadas pueden modular las tasas de transpiración del vegetal, el factor que más influye en este proceso es el grado de apertura estomática, que depende en gran medida de la disponibilidad de agua edáfica. Así, la disponibilidad de agua es uno de los principales factores que pueden limitar el crecimiento, ya que el cierre estomático hace disminuir las tasas de asimilación de CO<sub>2</sub> y, por lo tanto, la fotosíntesis neta. Esta situación, prolongada en el tiempo, puede llegar a comprometer la supervivencia de las plantas, debido a que la deshidratación de los tejidos vegetales por debajo de un nivel crítico viene acompañada por cambios irreversibles en la estructura y funcionamiento de la planta y, finalmente, por la muerte de la misma (Azcón-Bieto y Talón, 2000).

La existencia de una atmósfera seca predominante durante el periodo vegetativo en muchas regiones áridas y semiáridas del planeta, aumenta significativamente la tasa de transpiración de la planta y el agua consumida (Tognetti et al., 2009). Por consiguiente, muchos cultivos y plantaciones requieren de un aporte frecuente de agua para mantener la actividad fisiológica y lograr una buena producción. Para prevenir un excesivo consumo de agua en un cambio global de descenso del agua disponible, se han desarrollado bastantes métodos para maximizar el uso eficiente del agua, destacando la necesidad de desarrollar nuevos métodos de control y programación del riego más precisos (Jones, 2004). Para realizar una adecuada programación, además de estimar el estado de humedad del suelo se sugiere detectar el estrés en las plantas midiendo su

estado hídrico y su respuesta (Jones, 1990, 2004, 2007). Así mismo, la estimación del estado hídrico del vegetal puede materializarse en un valor susceptible de caracterizar el grado de hidratación de la misma a través de la medida del potencial hídrico o mediante la medida del contenido hídrico relativo.

El potencial hídrico ( $\Psi$ ) es un parámetro termodinámico empleado para describir el estado energético del agua en las plantas (Slatyer, 1967; Passiourara, 1982; Nobel 1983). Viene definido por la siguiente expresión (Pearcy et al., 1991):

$$\psi = \frac{\mu_w - \mu_w^*}{V_w}$$

donde  $\mu_w$  es el potencial químico o la energía libre por mol, del agua en algún punto del sistema a temperatura y presión constante,  $\mu_w^*$  es el potencial químico del agua pura a la misma temperatura y a presión atmosférica, y  $V_w$  es el volumen parcial molal de agua. En plantas,  $\Psi$  varía desde cero a valores negativos y viene dado por analogía en unidades de presión (MPa). Para una célula vegetal,  $\Psi$  puede ser expresado como la suma de tres componentes:

$$\psi = P + \pi + \tau$$

donde  $P$  es la presión hidrostática (o presión de turgencia),  $\pi$  es el potencial osmótico y  $\tau$  es el potencial matricial (Tyree y Jarvis, 1982).

Para la estimación de  $\Psi$  se han utilizado diferentes técnicas a lo largo de la historia de la fisiología vegetal basadas en distintos procedimientos experimentales (Barrs, 1968; Slavík, 1974; Turner, 1981; Tyree y Jarvis, 1982). Las primeras medidas de potencial hídrico sobre fragmentos de hoja se realizaban mediante un largo proceso de búsqueda del “potencial equivalente” a partir de disoluciones de concentración – o potencial hídrico – conocido. Para ello, los fragmentos de hoja se sumergían en una serie de disoluciones (tradicionalmente de sacarosa) de potencial osmótico conocido, y se valoraba en cuál de ellas no se había producido intercambio neto de líquido entre ambos sistemas (tejido vegetal y disolución). Cualquier flujo neto de agua entre ambos sistemas redundaba en un cambio en la densidad de la disolución, bien como ascenso (si el tejido había captado agua) o como descenso (si el tejido había aportado agua a la misma). Por lo tanto, la disolución en equilibrio sería aquella que no manifestara ni el más ligero cambio de densidad a lo largo del proceso. Para detectar de forma precisa

estos pequeños cambios en densidad se desarrolló un ingenioso procedimiento: la incorporación de minúsculas gotas de disoluciones de igual densidad que la original, aunque coloreadas (Knipling y Kramer, 1967). La disolución coincidente en este parámetro se revelaba inmediatamente al producirse una instantánea dispersión de las gotas. En el caso de que la densidad hubiera aumentado (por tratarse de disoluciones con un potencial menos negativo que el material vegetal) las gotas se mantenían coherentes durante un tiempo, ascendiendo hacia la superficie. Lo contrario ocurría en el caso de que la disolución captara agua del material, lo que sucedía en caso de que su potencial fuera originalmente más negativo que el del tejido. Esta técnica es aún teóricamente válida, aunque constituye, hoy en día, una reliquia metodológica dado el consumo de tiempo que requiere en comparación con otras más recientes. No se trata en ningún caso de una técnica que permita una rápida determinación del estado hídrico de la planta en condiciones de campo o en estudios muy dinámicos y, desde luego, descansa en la obtención de muestras de la hoja, por lo que constituye un típico caso de medida destructiva.

Una segunda aproximación, aún en uso, para la medida del potencial descansa en el empleo de psicrómetros de termopar, capaces de medir con notable precisión y sin apenas influencia, la temperatura y humedad relativa de una atmósfera confinada en contacto con la hoja (Spanner, 1951; Boyer y Knipling, 1963; Barrs, 1965; Boyer, 1966). La alta dependencia que el valor del potencial tiene de la temperatura hace que sea necesario trabajar en ambientes donde este parámetro esté muy controlado. Este hecho ya cuestionó, desde casi su génesis, la aptitud del método para el empleo como instrumento de campo (Knipling y Kramer, 1967). Por otro lado, los tiempos necesarios para el equilibrado del potencial hídrico de la atmósfera de referencia y el tejido son muy largos, citándose períodos de 17 horas (Boyer, 1966) o superiores. Como única forma de reducir estos largos períodos de equilibrado se han ensayado procedimientos de reducción de la resistencia de la cutícula a la difusión del vapor de agua mediante abrasión mecánica de la superficie foliar (Wullschleger y Oosterhuis, 1987), lo que impide la reutilización de ese material vegetal en posteriores medidas y, por lo tanto, su empleo para medidas repetidas en el tiempo.

Muchas de las limitaciones de estas dos anteriores técnicas son resueltas con la propuesta de medida del potencial hídrico mediante el uso de presiones positivas como forma de equilibrar la tensión generada en el agua del xilema debido a los potenciales negativos característicos en el funcionamiento del vegetal (Schollander et al., 1965). Básicamente, el procedimiento se basa en el empleo de un dispositivo susceptible de contener una hoja o brote, permitiendo que el extremo cortado de la estructura sobresalga (mediante un pasamuros o prensaestopas) y se mantenga así a presión atmosférica. La presión en el recipiente que encierra la estructura cuyo potencial se desea medir se eleva mediante la entrada de un gas (típicamente nitrógeno). Cuando el operario detecta la llegada del agua interna (agua del xilema) a la superficie del extremo cortado se registra la presión aplicada, asumiéndose que se ha alcanzado el equilibrio con la tensión (igual en magnitud, pero de signo contrario) previa en el xilema y que tal tensión equivale al potencial hídrico del tejido cuando se produjo su cosechado. Esta técnica tiene un recorrido amplísimo, sigue en perfecta vigencia pero adolece del mismo defecto que las anteriores, por cuanto la medida se realiza sobre un material que se desecha posteriormente, por lo que no permite el seguimiento continuo y no destructivo del estado hídrico en un mismo órgano. Por otro lado, la necesidad de emplear presiones, en ocasiones muy elevadas, convierte a la técnica en bastante peligrosa, exigiendo un cuidado y precaución muy elevado para evitar posibles accidentes.

El contenido hídrico relativo (RWC), el otro de los parámetros que también sirve para caracterizar la estimación del estado hídrico del vegetal, representa la cantidad de agua de un tejido en comparación con la que podría contener en hidratación completa. Su estimación se realiza comúnmente mediante un sencillo procedimiento basado en la estimación de un peso fresco (en el momento de la cosecha), un peso turgente (o valor máximo de hidratación) y un peso seco (tras mantener el material vegetal en estufa a temperaturas por encima de 60 ° C). La diferencia entre el peso en turgencia y el peso seco permite conocer el valor máximo de agua que el tejido puede contener. La diferencia entre el peso fresco, en cada momento, y el peso seco determina la cantidad real de agua que en ese estado el vegetal contiene. La relación entre ambos contenidos define la fracción de agua del vegetal, o contenido hídrico relativo.

Desde un punto de vista teórico, el contenido hídrico relativo se relaciona con el potencial hídrico mediante el establecimiento de las isotermas presión-volumen (Tyree y Hammel, 1972), de tal manera que, una vez tal relación ha sido establecida, la medida del contenido hídrico relativo permite aproximar con notable precisión el potencial hídrico del vegetal. Desde un punto de vista operativo, la medida del contenido hídrico relativo es simple exigiendo tan sólo instrumental básico de laboratorio (viales, balanza analítica). Exige además la recolección de parte o de todo el órgano sobre el que se realiza la medida lo que, de nuevo, lo convierte en medida destructiva y, por consiguiente, incapaz de ofrecer una visión continua de la fisiología de ese órgano.

El deseo de obviar la necesidad de extirpar una parte de la planta para conocer el estado hídrico de la misma – con las ventajas que ello reporta – ha llevado en las últimas décadas al desarrollo de diversos métodos aptos para la estimación del estado hídrico del vegetal de forma muy poco intrusiva y, en todos los casos, no destructivas. De esta forma se han impulsado nuevas técnicas que permitirían un seguimiento continuo, aunque relativo, de los cambios en el estado hídrico de la hoja mediante la monitorización de los cambios en su espesor (McBurney, 1992). En esta técnica, aunque se utiliza un transductor de desplazamiento de gran precisión, la baja repetibilidad y universalidad del método limita su empleo generalizado (Zimmermann et al., 2008). Posteriormente aparecieron otras técnicas (Lintilhac et al., 2000; Geitmann, 2006; Zimmermann et al., 2008) basadas en la estimación de la presión positiva ejercida sobre las paredes cuando la hoja aún conserva una turgencia positiva. Con independencia de los problemas metodológicos asociados a estas técnicas que también limitan notablemente su uso extensivo, la fase de turgencia positiva constituye tan sólo una parte del ciclo hídrico de una hoja, por lo que estas técnicas se limitarían a monitorizar una parte del mismo, sin alcanzar las fases críticas en el funcionamiento del vegetal.

Las ondas ultrasónicas también se han utilizado para determinar el contenido hídrico de la planta y han aparecido como técnicas no destructivas porque, además de su simplicidad y de no estar influenciadas por los cambios en las condiciones ambientales, mantienen la total integridad de la planta. Por primera vez Torii et al. (1988) mostraron una fuerte correlación entre varios parámetros ultrasónicos medidos en el tallo y el estado hídrico de la hoja de *Nicotiana tabacum*. Este hecho ya no es sorprendente

porque está bien reconocido que la propagación de las ondas ultrasónicas en sólidos porosos parcialmente saturados depende enormemente de su contenido de agua (Santos et al., 1990). Cualquier variación en el contenido del agua puede modificar la densidad y la rigidez del sólido poroso, y por lo tanto, también cambia la velocidad ultrasónica. Por otra parte, la variación del contenido de agua también puede cambiar la presencia de huecos en el sólido, lo que tiene una fuerte influencia en la dispersión de los ultrasonidos y en su coeficiente de atenuación. La técnica de Torii et al. (1988) cuenta con algunas desventajas: contacto con la muestra, solo se registra una frecuencia y no es apta para medir directamente en hojas. Desde entonces no se han vuelto a utilizar los ultrasonidos para monitorizar cambios en el estado hídrico de las hojas, desarrollándose únicamente técnicas para analizar sus características estructurales (Fukuhara et al., 2006). Es necesario, por lo tanto, encontrar un método que corrija los inconvenientes del uso de los ultrasonidos como técnica apta para el estudio del estado hídrico de las plantas.

En 1978, Sachse y Pao presentaron una técnica ultrasónica de espectroscopía, o técnica de pulso de banda ancha para la medida de la velocidad de fase de los ultrasonidos en materiales dispersos, basado en el análisis de un espectro de fases donde la fase y el conjunto de velocidades pueden ser obtenidos. En el mismo año, Haines et al. (1978) aplicó la espectroscopía ultrasónica de banda ancha a materiales de capas delgadas. En este caso, las muestras laminadas fueron sumergidas en agua y medidas a través de pulsos ultrasónicos transmitidos de banda ancha. Mas tarde, esta técnica fue ampliada para medir la atenuación y la velocidad de las ondas de corte (Kline, 1984; Wu, 1996). En la misma época, Pialucha et al. (1989) fueron capaces de determinar la velocidad de fase en sólidos de dispersión a partir de medidas en muestras planas basadas en el espectro de amplitudes en vez de en el de fases. El resultado de estos progresos fue una técnica llamada Espectroscopía Ultrasónica de Banda Ancha que está basada en el análisis del dominio de la frecuencia, utilizando la transformada de Fourier, de pulsos en banda ancha transmitidos a la muestra, o reflejados de ella, usada para medir la velocidad y la atenuación de las ondas ultrasónicas en los materiales. El desarrollo de nuevos transductores capaces de transmitir y recibir la señal a través del aire o de cualquier gas hizo posible utilizar el método de espectroscopia ultrasónica de banda ancha en la medida de materiales sin la inmersión de éstos en agua o sin utilizar

ningún otro tipo de líquido entre el transductor y la superficie del material. Este avance abrió el camino para investigar mediante ultrasonidos materiales como el papel, membranas microporosas, aerogeles o madera que no pueden ser mojados para llevar a cabo las medidas (Gómez Alvarez-Arenas, 2003a). En este sentido Gómez Alvarez-Arenas (2003b) aplicando la espectroscopía ultrasónica de banda ancha a diferentes tipos de filtros uniformes de membrana, encontró diferencias en la respuesta de la señal en cada filtro que dependían de su contenido en agua. Validando que existe una relación entre estos parámetros en filtros, es interesante probar la espectroscopía ultrasónica en hojas de árboles las cuales poseen una composición más compleja careciendo de la estructura uniforme de los filtros.

Por otra parte y en paralelo, la reflectancia en el dominio de la radiación infrarroja, y especialmente en las denominadas “bandas del agua” (970, 1450, 1940 nm) ha sido también relacionada con el contenido en agua del vegetal (Carter, 1991), habiéndose desarrollado índices capaces de aplicar la información aportada por sensores infrarrojos (Seelig et al., 2009) al estudio del estado hídrico de las plantas. Los resultados presentados hasta la fecha indican que se alcanzan adecuados niveles de precisión si se contempla todo el rango potencial de hidratación del tejido, desde su valor máximo hasta la deshidratación absoluta. Cuando el rango de valores reales de hidratación se reduce al fisiológico de hidratación (entre un 100 y un 65% de contenido relativo en agua) la precisión de la medida se reduce notablemente. Por otro lado, el instrumental necesario para efectuar las medidas en el vegetal, basados en el empleo de radiómetros en el rango del infrarrojo, son aún dispositivos con un coste de adquisición relativamente elevado. A pesar de que Seelig et al. (2009) concluyen que sus índices pueden utilizarse como señal de control en el riego, destacan que la reflectancia en el infrarrojo está influenciada por el espesor de la hoja, lo que implica tenerlo en cuenta en la medida.

Los avances en la tecnología referentes al infrarrojo pueden llevar a una mayor distribución en el uso de esta técnica en la medida del estado hídrico de las hojas. A parte de los complejos y relativamente caros equipos desarrollados principalmente para laboratorios, existen algunos modelos portátiles y más asequibles disponibles que

permiten trabajar a las mismas longitudes de onda bajo condiciones de campo (Zimmer et al., 2004)

Rangos de frecuencias electromagnéticas menores que las anteriores también han sido estudiadas con buenos resultados. Martínez et al. (1995) utilizó un reflectómetro en el dominio del tiempo (TDR) para estimar el estado hídrico de discos de hojas en la banda-X (7 a 12 GHz). Más recientemente Menzel et al. (2009) describió una técnica no invasiva basada en la medida de cambios en las propiedades dieléctricas en una cavidad de resonancia de microondas inducidas por el material vegetal introducido en él. A pesar de los buenos resultados obtenidos por Martínez et al. (1995) y Menzel et al. (2009) relacionados con el uso de microondas para estimar el estado hídrico de la planta, la complejidad del dispositivo experimental propuesto evita la aplicabilidad de tales métodos para el desarrollo de herramientas prácticas para caracterizar el estado hídrico de las plantas en condiciones de campo. Es interesante, por lo tanto, combinar la potencial eficacia de las microondas para estimar el estado hídrico con un instrumental y una tecnología más simple y portátil.

La idea de encontrar un nuevo método capaz de medir el estado hídrico en las plantas sin que éstas sufran perjuicio alguno, nos llevó, en paralelo, a experimentar tanto con la metodología ultrasónica como con las microondas. De esta forma esta idea se convirtió en la base de los cuatro trabajos presentados en la tesis.

El primer artículo presentado, conseciente de un trabajo anterior (Apéndice 3) donde se mostró que se podía utilizar la espectroscopía ultrasónica de banda ancha sobre hojas, se centró principalmente en destacar en el campo de la biología la aparición de los ultrasonidos como posible herramienta en el estudio del estado hídrico foliar. Este hecho fue consecuencia por un lado, del buen ajuste a un modelo sigmoidal de la relación entre la frecuencia de resonancia de la hoja y el contenido hídrico de la misma y por otro, de la coincidencia del punto de pérdida de turgencia calculado por métodos clásicos con el punto de inflexión de la relación sigmoidal. El posible motivo o la causa que explicara estas relaciones entre el parámetro ultrasónico y las variables fisiológicas fue la idea determinante para iniciar el trabajo que se presenta en el segundo de los artículos. En este estudio se escogieron los parámetros que sirven para determinar

teóricamente el valor de la frecuencia: espesor del material, densidad y constante elástica del material, con el fin de observar sus variaciones con respecto a los cambios en el contenido hídrico foliar. Del mismo modo, también se observaron los cambios estructurales de la hoja a nivel celular. El segundo trabajo reveló que era el cambio en la constante elástica el principal factor de influencia en la variación de la frecuencia. Como esta constante fue, en el segundo artículo, estimada a partir de otros parámetros y realmente no fue directamente medida sobre las hojas, el tercero de los trabajos se basó en la mejora del sistema de medida para obtener un análisis más detallado de la resonancia de la hoja con la que se pudiera medir en tiempo real dicha constante. Así pues, en el tercero de los artículos se muestra para varias especies la variación de esta constante elástica con respecto a cambios en el contenido hídrico. Por último, haciendo referencia a la otra técnica, el cuarto artículo presenta la utilización de una antena de telefonía móvil digital que funciona en el rango de las microondas para la medida del estado hídrico foliar. En este artículo se muestra una buena correlación lineal entre el índice obtenido por microondas y el contenido hídrico foliar, superando incluso a la correlación obtenida por un método ya comercial basado en el rango de los infrarrojos.

### **C. COPIA DE LOS TRABAJOS PUBLICADOS**



RESEARCH PAPER

# Air-coupled broadband ultrasonic spectroscopy as a new non-invasive and non-contact method for the determination of leaf water status

Domingo Sancho-Knapik<sup>1</sup>, Tomás Gómez Álvarez-Arenas<sup>2</sup>, José Javier Peguero-Pina<sup>1</sup> and Eustaquio Gil-Pelegrín<sup>1,\*</sup>

<sup>1</sup> Unidad de Recursos Forestales, Centro de Investigación y Tecnología Agroalimentaria, Gobierno de Aragón, Apdo. 727, E-50080 Zaragoza, Spain

<sup>2</sup> Departamento de Señales, Sistemas y Tecnologías Ultrasónicas, Instituto de Acústica, CSIC, E-28002 Madrid, Spain

\* To whom correspondence should be addressed: E-mail: egilp@aragon.es

Received 20 November 2009; Revised 22 December 2009; Accepted 4 January 2010

## Abstract

The implementation of non-destructive methods for the study of water changes within plant tissues and/or organs has been a target for some time in plant physiology. Recent advances in air-coupled ultrasonic spectroscopy have enabled ultrasonic waves to be applied to the on-line and real-time assessment of the water content of different materials. In this study, this technique has been applied as a non-destructive, non-invasive, non-contact, and repeatable method for the determination of water status in *Populus × euramericana* and *Prunus laurocerasus* leaves. Frequency spectra of the transmittance of ultrasounds through plant leaves reveal the presence of at least one resonance. At this resonant frequency, transmittance is at its maximum. This work demonstrates that changes in leaf relative water content (*RWC*) and water potential ( $\Psi$ ) for both species can be accurately monitored by the corresponding changes in resonant frequency. The differential response found between both species may be due to the contrasting leaf structural features and the differences found in the parameters derived from the *P–V* curves. The turgor loss point has been precisely defined by this new technique, as it is derived from the lack of significant differences between the relative water content at the turgor loss point ( $RWC_{TLP}$ ) obtained from *P–V* curves and ultrasonic measurements. The measurement of the turgor gradient between two different points of a naturally transpiring leaf is easily carried out with the method introduced here. Therefore, such a procedure can be an accurate tool for the study of all processes where changes in leaf water status are involved.

**Key words:** Drought, relative water content, turgor loss point, ultrasonic spectroscopy, water potential.

## Introduction

Several destructive methods have been used to characterize plant water status, either through water potential or relative water content (Barrs, 1968; Slavik, 1974; Turner, 1981; Tyree and Jarvis, 1982). These techniques preclude repetitive measurements in a given tissue (Bürquez, 1987) and, therefore, they are not suitable for studying dynamic water changes within the same plant tissue or organ. Attempts to find a non-destructive or non-invasive technique have been a challenge during recent decades.

Thermocouple psychrometers have been successfully used for measuring plant water potential (Savage and Wiebe, 1989). However, its accuracy is highly temperature dependent (Savage *et al.*, 1983) and the need for removing the waxy cuticle from the epidermis in order to reduce the water potential equilibration time (Savage *et al.*, 1984; Wullschleger and Oosterhuis, 1987) turns this method into a destructive technique. On the other hand, leaf or canopy temperature can also be used as an indicator of water stress

Abbreviations: *f*, standardized frequency; *P–V* curves, pressure–volume curves; *RWC*, relative water content;  $\Psi$ , water potential; TLP, turgor loss point.

© The Author [2010]. Published by Oxford University Press [on behalf of the Society for Experimental Biology]. All rights reserved.

For Permissions, please e-mail: journals.permissions@oxfordjournals.org

at different plant levels through the analysis of thermal imaging variables (Grant *et al.*, 2006a, b). Although methods such as infrared thermometry can be used for measurement at variable distances from the target (Sepulcre-Canto *et al.*, 2007), its accuracy is highly reduced by plant architecture (Grant *et al.*, 2006a), making this technique more suitable for use in crop science (Sepulcre-Canto *et al.*, 2007) than for accurate physiological measurements. Other authors related changes in canopy reflectance to leaf water status (Peguero-Pina *et al.*, 2008; Zarco-Tejada *et al.*, 2009). However, although these indexes are promising tools, the same concerns as for infrared thermometry can be raised. Another set of techniques are based on the continuous monitoring of turgor pressure changes as an estimator of the dynamic changes in plant water status, either controlling leaf thickness (McBurney, 1992) or by applying an external pressure. In this regard, ball tonometry is another non-destructive method that allows changes in water potential to be studied through the monitoring of cell turgor pressure (Lintilhac *et al.*, 2000; Geitmann, 2006). However, this technique can only be applied to superficial and relatively thin-walled cells, which constitutes a strong limitation for its widespread use (Lintilhac *et al.*, 2000). More recently, Zimmermann *et al.* (2008) have developed a high-precision pressure probe, which allows the online monitoring of water relations of intact leaves. Although this technique is very sensitive, versatile, and easy to handle, leaves must be clean and surface roughness must be avoided (Zimmermann *et al.*, 2008).

Among the non-destructive methods, the use of ultrasonic waves to determine the water content of a plant was first used by Torii *et al.* (1988). They found a strong correlation between ultrasonic velocity through the stem and leaf water status on *Nicotiana tabacum*. In fact, it is well known that the propagation of ultrasound waves in a partially saturated porous solid strongly depends on the water content (Santos *et al.*, 1990). Some of the disadvantages of this technique are that: (i) contact between the transducers and the stem is required, (ii) only one value of the frequency could be registered; and (iii) thin-layered samples could not be measured. Since then, the use of ultrasonic propagation through a plant organ has been developed to analyse leaf structural features (Fukuhara *et al.*, 2006). However, as far as is known, it has not been used for monitoring changes in leaf water status when there is no contact between the transducers and the sample, mostly due to the common use of water as the medium for the propagation of the signal.

An ultrasonic spectroscopy, or broadband pulse technique, was first presented by Sachse and Pao (1978) for the measurement of the phase velocity of ultrasounds in dispersive materials based on the analysis of the phase spectrum from which phase and group velocity of longitudinal waves can be obtained. At the same time, Haines *et al.* (1978) applied the broadband ultrasonic spectroscopy to thin-layered media. In this case, plate samples were immersed in water and the transmitted broadband ultra-

sonic pulses were measured. Later, this technique was extended to measure attenuation and velocity of shear waves (Kline, 1984; Wu, 1996). Afterwards, Pialucha *et al.* (1989) determined the phase velocity in dispersive solids from measurements in plate samples based on the amplitude instead of on the phase spectrum. Such developments allowed the implementation of a technique called 'Broadband ultrasonic spectroscopy', which is based on frequency-domain analysis, by using the Fourier transform, of broadband pulses transmitted or reflected through a sample. As a result, frequency, velocity, and attenuation of ultrasonic waves in materials can be measured. The development of new broadband ultrasonic emitters and receivers, able to transmit and receive ultrasonic signals to and from the air or any gas (air-coupled transducers) has made it possible to apply the broadband ultrasonic spectroscopic method to the measurement of materials without immersion of the sample in water, or the use of any coupling fluid to attach the transducer to the surface of the material. This opened the way to investigate by ultrasonic means, materials like paper, microporous membranes, aerogels or wood that cannot be wetted to carry out the measurements (Gómez Álvarez-Arenas, 2003a).

Compared with other ultrasonic techniques, broadband ultrasonic spectroscopy can be applied to dispersive materials and thin samples. In addition, unlike other conventional ultrasonic techniques, air-coupling requires neither any contact with the sample nor use of coupling fluids, so no contamination is introduced, and very rapid inspection is possible as well as an on-line and real-time assessment of the status of the sample. Air-coupled ultrasonic spectroscopy provides information not only from one of the surfaces of the membrane, but also about the whole volume. The back surface can also be used for precise time-delay measurements, even when pulses overlap in the time-domain and when strong dispersion takes place (Gómez Álvarez-Arenas, 2003a).

Gómez Álvarez-Arenas (2003b) found that the propagation of ultrasound waves in a partially saturated porous solid strongly depends on the water content. He applied broadband ultrasonic spectroscopy to several uniform membrane filters, finding a differential response signal in the transfer function of each membrane depending on the water content. Any variation of the water content may modify the density and the stiffness of the porous solid, hence, changing the ultrasound velocity. On the other hand, variation of the water content may also alter the presence and/or conformation of voids which has a strong influence on the scattering of ultrasounds and, as a consequence, on the attenuation coefficient. Consequently, our hypothesis is that ultrasonic waves could be a promising tool to determine leaf water content, in spite of the fact that propagation of ultrasounds in leaves is expected to be strongly dispersive due to its complex structure that comprises solid, fluid, and gas phases. Therefore, the main objective of this study is to apply the air-coupled broadband ultrasonic spectroscopy to leaves with different structural features, as a non-destructive, non-invasive, and

non-contact method, relating ultrasonic parameters with leaf water status.

## Materials and methods

### The broadband ultrasonic spectroscopy technique: experimental set-up

The broadband magnitude ultrasonic spectroscopy technique is described and schematically depicted in Gómez Álvarez-Arenas (2003a). Briefly, the experimental set-up (Fig. 1) consists of two pairs of specially designed air-coupled piezoelectric transducers; in this case with a centre frequency of 0.75 MHz, a working frequency range of 0.3–1.2 MHz, and with a radiating diameter area of 20 mm (Gómez Álvarez-Arenas, 2004). The active element is a disc made of piezoelectric fibres embedded in an epoxy matrix, poled in the thickness direction and with metalized surfaces (sputtered gold). These transducers are positioned facing each other at a distance of 2 cm. It should be noted that previous studies showed that the distance between the transducers had no influence on the signal obtained. A high voltage (100–400 V) square semicycle (duration 0.67 µs) is applied to the transmitter transducer which converts this electrical signal into an ultrasonic pulse and launches it into the air. The receiver transducer collects this signal and converts it into an electrical one, which is then amplified (up to 59 dB) and filtered (low-pass filter at 10 MHz). Eventually, an oscilloscope digitized it, averaged the number of waveforms to reduce the high frequency noise (typically up to 100 waveforms), performed Fast Fourier Transforms (FFT), both magnitude and phase, and transferred the data to a computer for storage.

The experimental procedure of the ultrasonic technique is as follows. First, transmission from a transmitter is directly measured into the receiver. This provides a calibration of the system, in particular, this permits the frequency-band response to be normalized, both magnitude  $-I_0(\omega)$ - and phase  $-\varphi_0(\omega)$ - of the whole system: transducers, electrical generator, and electrical receiver. Then the leaf is held with supports for a few seconds between the transducers at normal incidence. No contact between the leaf and the transducers is necessary.

When the ultrasounds impact normally on the leaf surface, part of the energy is reflected back while the rest is transmitted, propagates through the leaf, and reaches the back surface. Then part of the energy is reflected back while the rest is transmitted through the interface and received at the receiver transducer after travelling through an air gap. This process is repeated for each of

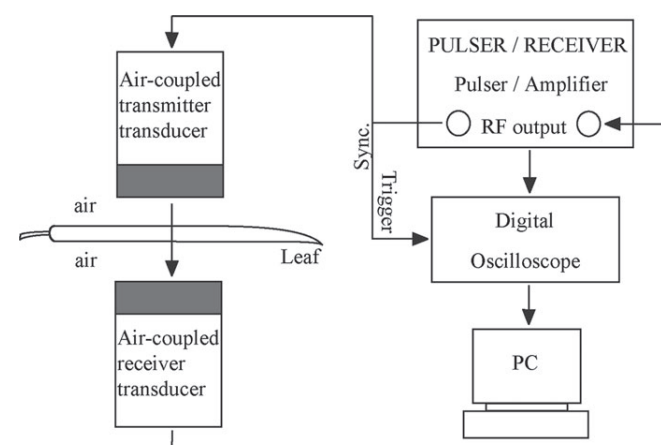


**Fig. 1.** Schematic representation of the experimental set-up.

the multiple internal reflections in the leaf until the attenuation of the ultrasounds in the material produces the decay of this reverberation. The data measured in this case are both magnitude  $-I(\omega)$ - and phase  $-\varphi(\omega)$ -spectra, obtaining the magnitude [ $T=I(\omega)/I_0(\omega)$ ] and the phase [ $\Phi=\varphi(\omega)-\varphi_0(\omega)$ ] of the transmittance. The use of magnitude and phase spectra simultaneously to obtain the thickness of the leaf, its density, and the velocity and the attenuation of the ultrasounds in it, is described in more detail by Gómez Álvarez-Arenas *et al.* (2009).

### Plant material and experimental conditions

In order to apply the broadband ultrasonic spectroscopy technique to species with very different leaf structural features, measurements were carried out in mature leaves collected from two different species, i.e. *Populus×euramericana* (Dode.) Guinier and *Prunus laurocerasus* L. (Table 1). For each species, branches were collected from a single tree; they were kept under water in order to avoid embolism and the leaves were taken with the whole petiole. Thereafter, leaves were rapidly introduced to plastic containers with water in order to ensure a water-vapour saturated atmosphere. After 24 h, weight, ultrasonic parameters, and water potential were individually measured per leaf at constant time intervals until values close to  $-3$  MPa for *P.×euramericana* and close to  $-5$  MPa for *P. laurocerasus* were reached. Leaves were subsequently dried in an oven and weighed when completely dry.

In order to test the repeatability of the technique, two different experiments were made in *P.×euramericana*. On the one hand, the same leaf location was measured ten times in a row at six different relative water content (*RWC*) values. On the other hand, one leaf at ten different locations was measured ten times in a row on and at six different *RWC* values.

### P–V analysis

*P–V* relationships were determined following the free-transpiration method described in previous studies (Dreyer *et al.*, 1990; Corcuera *et al.*, 2002; Brodribb and Holbrook, 2003). The water-relations parameters analysed were: leaf water potential at the turgor loss point,  $\Psi_{TLP}$ ; maximum bulk modulus of elasticity,  $\varepsilon_{max}$ ; maximum turgor; and the relative water content at the turgor loss point,  $RWC_{TLP}$ . Relative water content (*RWC*) was calculated as a ratio of the difference between leaf fresh weight minus leaf dry weight and the difference between leaf saturated weight minus leaf dry weight.

### Ultrasonic parameters measurements

The ultrasonic parameter directly measured was the transmitted pulse in the time domain. The Fourier transformation enabled the magnitude and phase to be obtained giving rise to a transmittance (*T*) versus frequency curve for each output. The value of the frequency associated with the maximum *T* at the peak curve was

**Table 1.** Leaf phenology and leaf morphological parameters [thickness, length, maximum width and leaf mass area (LMA)] for *Populus×euramericana* and *Prunus laurocerasus*

Data are expressed as mean  $\pm$ SE of five leaves for each species studied.

	<i>Populus×euramericana</i>	<i>Prunus laurocerasus</i>
Phenology	Deciduous	Evergreen
Thickness (µm)	$284 \pm 12$	$531 \pm 8$
Length (cm)	$11.8 \pm 0.6$	$11.6 \pm 0.2$
Maximum width (cm)	$13.8 \pm 0.3$	$3.9 \pm 0.1$
LMA (mg cm <sup>-2</sup> )	$13.88 \pm 0.08$	$19.32 \pm 0.22$

compared to the leaf water potential ( $\Psi$ , MPa) and to the  $RWC$ . In order to contrast the values obtained for both species, frequency values were standardized by means of dividing each single value between the maximum value obtained at  $RWC=1.00$  for each leaf studied.

#### Statistical analysis

The relationships between standardized frequency ( $f$ ) and  $RWC$  were adjusted to a cubic function ( $RWC=y_0+af+bf^2+cf^3$ ) for each leaf of both species. The turgor loss point was calculated as the inflection point of each regression equation. On the other hand, a Student's  $t$  test was used to compare (i) the parameters obtained from  $P-V$  analysis between both species and (ii) the  $RWC_{TLP}$  obtained from  $P-V$  analysis and those obtained from ultrasonic measurements. All statistical analyses were carried out using SAS version 8.0 (SAS, Cary, NC, USA).

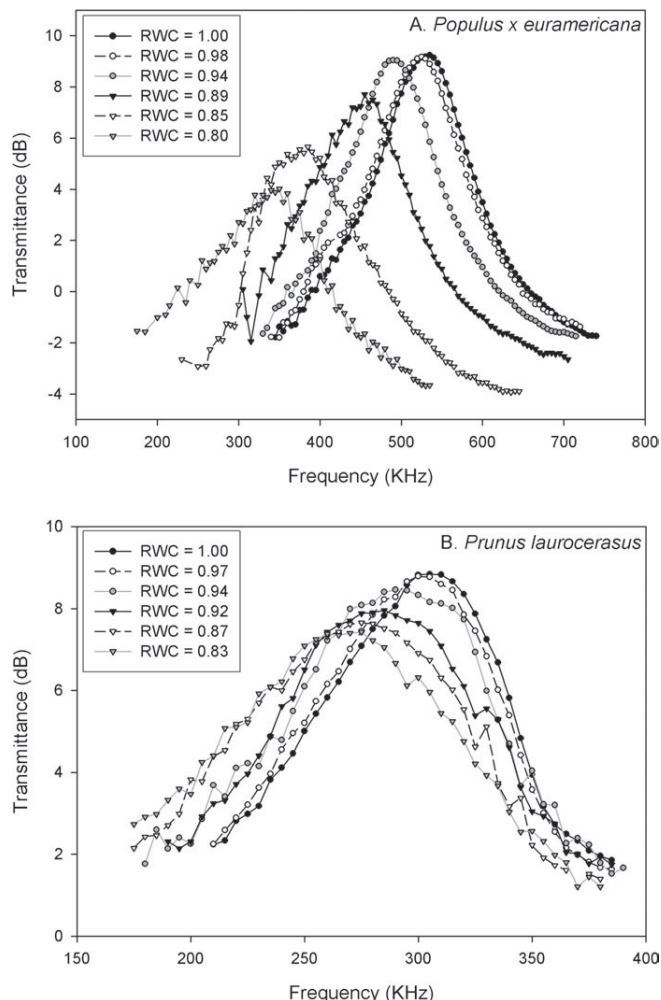
## Results

Table 2 shows the parameters derived from the pressure–volume curves for both species. It should be noted that *Prunus laurocerasus* showed higher values of  $\Psi_{TLP}$ ,  $\varepsilon_{max}$ , and  $\Pi_0$  than *Populus×euramericana* ( $P < 0.05$ ). However, the difference found in  $RWC_{TLP}$  between both species was negligible.

In Fig. 2, the relationship between frequency and transmittance for a single leaf of *P.×euramericana* and *P. laurocerasus* at different levels of  $RWC$  are represented. A drop in the maximum values of transmittance when leaf  $RWC$  decreased was observed for both species, as long as there was a movement of the whole curve to lower values of frequency. It is remarkable that, not only changes on the values of frequency and transmittance of the peak were observed, but that changes on curve shape also occurred. While  $RWC$  decreased, the signal of transmittance gained more noise and the shape of the curve got wider at a constant vertical distance from the peak. In this way, the curves at 0.80 and 0.85 of  $RWC$  for *P.×euramericana* and at 0.87 and 0.83 of  $RWC$  for *P. laurocerasus* showed more dispersion and they were wider than curves obtained for higher values of  $RWC$  (Fig. 2).

Figure 3 shows the relationships between the mean values of  $f$  and  $RWC$  for the leaves of *P.×euramericana*

and *P. laurocerasus*. It should be noted that the differences found in the frequency values measured for both species (Fig. 2) made the use of the standardized frequency ( $f$ ) necessary in order to compare them. The relationship between  $f$  and  $RWC$  was adjusted to a cubic function ( $R^2=0.99$ ,  $P < 0.0001$  for both species), which is characterized by the existence of an inflection point. In our experiment, the inflection point determines a change in the evolution of  $f$  as  $RWC$  decreases. This point can be compared with the intersection point of the two-phase linear equation for the relationship between leaf water potential and  $RWC$  found by Brodribb and Holbrook (2003). These authors considered that the intersecting point can be associated with the turgor loss point, such as for the inflection point in the  $f-RWC$  relationships. For *P.×euramericana*, the  $RWC_{TLP}$  found from the  $f-RWC$  relationships was  $0.89 \pm 0.01$ , whereas it was  $0.88 \pm 0.01$  from the analysis of  $P-V$  curves. For *P. laurocerasus*, the  $RWC_{TLP}$  found from the  $f-RWC$  relationships and from



**Fig. 2.** Relationship between the frequency (KHz) and transmittance (dB) for (A) *Populus×euramericana* and (B) *Prunus laurocerasus* for a single leaf of each species at different levels of relative water content ( $RWC$ ).

**Table 2.** Parameters derived from the pressure–volume curves for *Populus×euramericana* and *Prunus laurocerasus*: water potential at the turgor loss point ( $\Psi_{TLP}$ , MPa), relative water content at the turgor loss point ( $RWC_{TLP}$ ), maximum bulk modulus of elasticity ( $\varepsilon_{max}$ , MPa), and maximum turgor (MPa)

Data are expressed as mean  $\pm$  SE. Different letters indicate significant differences at  $P < 0.05$ .

	<i>Populus×euramericana</i>	<i>Prunus laurocerasus</i>
$\Psi_{TLP}$ (MPa)	$1.72 \pm 0.11$ a	$2.66 \pm 0.21$ b
$RWC_{TLP}$	$0.88 \pm 0.01$ a	$0.89 \pm 0.01$ a
$\varepsilon_{max}$ (MPa)	$11.34 \pm 0.63$ a	$17.53 \pm 0.87$ b
Maximum turgor (MPa)	$1.54 \pm 0.04$ a	$2.72 \pm 0.11$ b

the analysis of  $P-V$  curves were  $0.89 \pm 0.01$ . However, the differences in  $RWC_{TLP}$  values obtained from both techniques ( $P-V$  curves and ultrasonic measurements) were not statistically significant at  $P < 0.05$ .

In Fig. 4, the relationships between the mean values of  $f$  and  $\Psi$  for the leaves of *P. × euramericana* and *P. laurocerasus* is represented. The relationship between  $f$  and  $\Psi$  was also adjusted to a cubic function ( $R^2=0.99$ ,  $P < 0.0001$  for both species). Although the relationship for *P. × euramericana* could also be adjusted to a linear correlation equation ( $R^2=0.97$ ,  $P < 0.0001$ ), we have considered that the cubic function reflected better the relationship between  $f$  and  $\Psi$  for this species.

The repeatability of the technique was checked with *P. × euramericana* leaves. On the one hand, the value of the frequency measured in the same leaf location remained

fairly constant and the differences were not statistically significant at  $P < 0.01$ , for the six  $RWC$  values considered (data not shown). On the other hand, the differences found in the frequency values measured for the same leaf at ten different locations were not statistically significant at  $P < 0.05$ , for the six  $RWC$  values considered (data not shown).

## Discussion

In this study, the broadband ultrasonic spectroscopy technique has been proven as a non-destructive, non-invasive, non-contact, and reproducible method for the dynamic determination of leaf water status. The procedure is based on the excitation of thickness resonances on the leaves, specifically, changes in the frequency at the maximum transmittance (leaf resonant condition) have been revealed as an optimum indicator of changes in  $RWC$  of leaves with contrasting structural features. The frequency-transmittance output curves were surprisingly well explained by an ultrasonic model, assuming the medium as continuous and non dispersive, specifically those with higher values of  $RWC$  (Fig. 2), in spite of the high complexity and heterogeneity of the structure of leaves. However, when the frequency values of *P. × euramericana* and *P. laurocerasus* were compared, they were very different in range (Fig. 2), which may be related to the differences found in leaf structural parameters between both species (Table 1). The strong relationship found between  $RWC$  and the frequency associated with the maximum transmittance is mainly due to the mechanical softening of the leaf as it loses water. This produces a reduction in the velocity of ultrasounds that eventually leads to the observed reduction of the resonant frequency of the leaf.

The relationship between  $f$  and  $RWC$  was characterized by the existence of an inflection point. This point could be related to the intersecting point found by Brodribb and Holbrook (2003) for the relationship between  $\Psi$  and  $RWC$ , which has been associated with the turgor loss point. The turgor loss point has been considered to be a threshold for many physiological processes (Brodribb and Holbrook, 2003; Thomas *et al.*, 2006; Mitchell *et al.*, 2008). In our study, there were no statistically significant differences between  $RWC_{TLP}$  derived from the analysis of  $P-V$  isotherms and those obtained from the relationship between  $f$  and  $RWC$  for both species. Therefore, the turgor loss point could be estimated through the calculation of the inflection point of the  $f-RWC$  relationship. However, the data presented are preliminary and need to be confirmed in future attempts by incorporating results obtained from a larger range of plant species and tissues.

The decrease in the frequency associated with the maximum transmittance (thickness resonance of the leaf) before the turgor loss point can be explained by the mechanical softening of the leaf. This softening overcomes the effect of density reduction due to the loss of water and gives rise to a decrease in the velocity of ultrasounds in the leaf. The slope

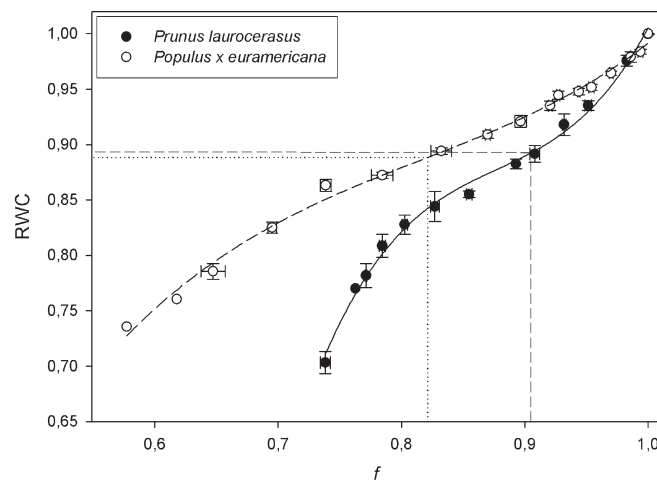


**Fig. 3.** Relationship between standardized frequency ( $f$ ) and relative water content ( $RWC$ ) for *Populus × euramericana* and *Prunus laurocerasus*. Data are expressed as mean  $\pm$ SE of ten leaves for each species studied.

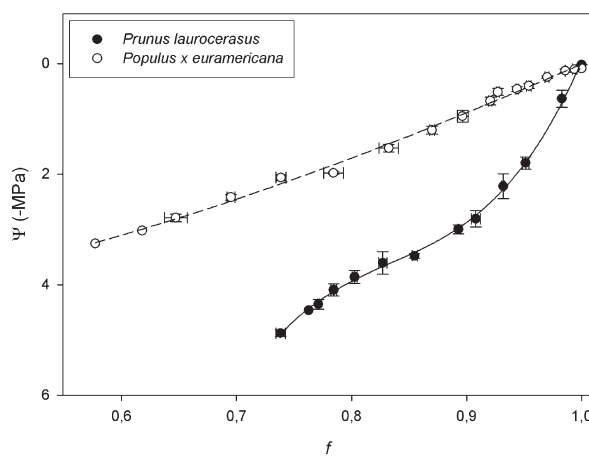


**Fig. 4.** Relationship between standardized frequency ( $f$ ) and water potential (-MPa) for *Populus × euramericana* and *Prunus laurocerasus*. Data are expressed as mean  $\pm$ SE of ten leaves for each species studied.

of the relationship between  $f$  and  $RWC$  during this phase is clearly higher in *P. laurocerasus* because the loss of turgor in this species is sharper than in *P. × euramericana*. This fact can be explained by the higher value of  $\varepsilon_{\max}$  recorded for *P. laurocerasus*. A simple mathematical model to explain this behaviour can be developed, assuming the leaf cells as a compact arrangement of fluid droplets, each one surrounded by an elastic membrane (or fluid-filled microballoons). Compressibility of such an arrangement, which is determined by the deformation of such cells at the point of contact with others, is used to determine the overall compressibility of granular media (Duran, 2000). It is proposed that compressibility increased when leaf water potential became more negative and the tension decreased, which would bring about a reduction in the frequency associated with the maximum transmittance.

The turgor loss point (associated with the inflection point) determines a change in the evolution of  $f$  as  $RWC$  decreases (Fig. 3). This change coincided with a strong increase in the noise of the transmittance signal (Fig. 2). This new phase deserves a different physical explanation than the former one. It is proposed that an increment in the leaf internal heterogeneity may underlie the change in the acoustic properties of the leaf, which are associated with an increase in signal attenuation. The higher irregularity in the acoustic pathway could be related to an increment in the gas-filled spaces in the internal tissues. The cavitation of minor veins has been proposed as a common phenomenon during water stress (Trifilo *et al.*, 2003), which could explain the formation of gas-filled obstacles to acoustic propagation. However, the changes in frequency during the dehydration process remained quite progressive, although cavitation is a sharper process that may have a sudden change in the acoustic signal. Another mechanism that could explain the increment in the gas-filled spaces is the lateral shrinkage of mesophyll cells, as shown by cryoscanning observation of dehydrated leaf tissues (McBurney, 1992). However, we consider that a full explanation of the structural changes experimented by the leaf during dehydration deserves further investigation, in order to obtain a definitive mechanistic explanation.

In spite of this and from a methodological point of view, the broadband ultrasonic technique proves to be a promising new method for the determination of the turgor loss point, as the inflection point of the relationship between the standardized frequency and  $RWC$  during drying, in a non-contact and non-destructive way. The advantage of this procedure, as compared to the classical analysis of the  $P-V$  isotherms (Corcuera *et al.*, 2002) is that it is outstanding in terms of simplicity and time consumption. Moreover, when the frequency is standardized, the accuracy of this new technique seems to be dependent on the natural heterogeneity existing in a set of leaves, as it is shown for the  $P-V$  isotherms method. However, nowadays, this method cannot be applied to species with leaves smaller than the radiating area of the transducer. To solve this problem, transducers with a radiating diameter area lower than 20 mm are now being developed.

The ability for registering rapid changes in turgor values, under conditions of free leaf transpiration, may constitute a tool of paramount importance for the study of dynamic processes associated with this variable. Thomas *et al.* (2006) suggested that the cell pressure probe is the only available method for the direct measurement of turgor in plant cells, due to the possible artefacts related to the use of isopiestic psychrometers. The changes in frequency along the positive turgor phase can be effectively used as an indicator of the changes experienced by the leaf tissues examined by the waves. Although a direct estimation of a single cell cannot be achieved, the smaller the area exposed to the ultrasonic waves, which can be optically modified, the bigger the spatial resolution of the method. The measurement of the turgor gradient between two different points of the leaf blade, in order to relate such a gradient with water transport within an attached, naturally transpiring leaf can easily be carried out with the method presented here.

## Acknowledgements

The authors are very grateful to Professor Dr MT Tyree for his very valuable comments of a preliminary draft of this manuscript and to Dr V Fernández for her help with the English language. This study was partially supported by INIA project SUM2008-00004-C03-03 (Ministerio de Ciencia e Innovación). Financial support from Gobierno de Aragón (A54 research group) is also acknowledged.

## References

- Barrs HD.** 1968. Determination of water deficits in plant tissues. In: Kozlowski TT, ed. *Water deficits and plant growth*, Vol. I. London, New York: Academic Press, 235–368.
- Brodrribb TJ, Holbrook NM.** 2003. Stomatal closure during leaf dehydration, correlation with other leaf physiological traits. *Plant Physiology* **132**, 2166–2173.
- Búrquez A.** 1987. Leaf thickness and water deficit in plants: a tool for field studies. *Journal of Experimental Botany* **38**, 109–114.
- Corcuera L, Camarero JJ, Gil-Pelegrín E.** 2002. Functional groups in *Quercus* species derived from the analysis of pressure–volume curves. *Trees, Structure and Function* **16**, 465–472.
- Dreyer E, Bousquet F, Ducrey M.** 1990. Use of pressure volume curves in water relations analysis on woody shoots: influence of rehydration and comparison of four European oak species. *Annales des Sciences Forestières* **47**, 285–297.
- Duran J.** 2000. *Sands, powders, and grains: an introduction to the physics of granular materials*. New York: Springer.
- Fukuhara M, Gupta SD, Okushima L.** 2006. Acoustic characteristics of plant leaves using ultrasonic transmission waves. In: Gupta SD, Ibaraki Y, eds. *Plant tissue culture engineering*. Dordrecht: Springer, 427–439.
- Geitmann A.** 2006. Experimental approaches used to quantify physical parameters at cellular and subcellular levels. *American Journal of Botany* **93**, 1380–1390.

- Grant OM, Chaves MM, Jones HG.** 2006 b. Optimizing thermal imaging as a technique for detecting stomatal closure induced by drought stress under greenhouse conditions. *Physiologia Plantarum* **127**, 507–518.
- Grant OM, Tronina L, Chaves MM.** 2006 a. Exploring thermal imaging variables for the detection of stress responses in grapevine under different irrigation regimes. *Journal of Experimental Botany* **58**, 815–825.
- Gómez Álvarez-Arenas TE.** 2003 a. Air-coupled ultrasonic spectroscopy for the study of membrane filters. *Journal of Membrane Science* **213**, 195–207.
- Gómez Álvarez-Arenas TE.** 2003 b. A non-destructive integrity test for membrane filters based on air-coupled ultrasonic spectroscopy. *IEEE Transactions on Ultrasonics, Ferroelectrics and Frequency Control* **50**, 676–685.
- Gómez Álvarez-Arenas TE.** 2004. Acoustic impedance matching of piezoelectric transducers to the air. *IEEE Transactions on Ultrasonics, Ferroelectrics and Frequency Control* **51**, 624–633.
- Gómez Álvarez-Arenas TE, Sancho-Knapik D, Peguero-Pina JJ, Gil-Pelegrín E.** 2009. Noncontact and noninvasive study of plant leaves using air-coupled ultrasounds. *Applied Physics Letters* **95**, 193702.
- Haines NF, Bell JC, McIntyre PJ.** 1978. The application of broadband ultrasonic spectroscopy to the study of layered media. *Journal of the Acoustical Society of America* **76**, 498–504.
- Kline RA.** 1984. Measurement of attenuation and dispersion using an ultrasonic spectroscopy technique. *Journal of the Acoustical Society of America* **76**, 498–504.
- Lintilhac PM, Wei C, Tanguay JJ, Outwater JO.** 2000. Ball tonometry: a rapid, non-destructive method for measuring cell turgor pressure in thin-walled plant cells. *Journal of Plant Growth Regulation* **19**, 90–97.
- McBurney T.** 1992. The relationship between leaf thickness and plant water potential. *Journal of Experimental Botany* **43**, 327–335.
- Mitchell PJ, Veneklass EJ, Lambers H, Burgess SSO.** 2008. Leaf water relations during summer water deficit: differential responses in turgor maintenance and variation in leaf structure among different plant communities in south-western Australia. *Plant, Cell and Environment* **31**, 1791–1802.
- Peguero-Pina JJ, Morales F, Flexas J, Gil-Pelegrín E, Moya I.** 2008. Photochemistry, remotely sensed physiological reflectance index and de-epoxidation state of the xanthophyll cycle in *Quercus coccifera* under intense drought. *Oecologia* **156**, 1–11.
- Pialucha T, Guyott CCH, Cawley P.** 1989. Amplitude spectrum method for the measurement of phase velocity. *Ultrasonics* **27**, 270–279.
- Sachse W, Pao YH.** 1978. On the determination of phase and group velocities of dispersive waves in solids. *Journal of Applied Physics* **49**, 4320–4327.
- Santos JE, Douglas JJ, Corberó JM, Lovera OM.** 1990. A model for wave propagation in a porous medium saturated by a two-phase fluid. *Journal of the Acoustical Society of America* **87**, 1439–1448.
- Savage MJ, Wiebe HH.** 1989. Practical aspects of the effect of leaf conductance on thermocouple hygrometric leaf water potential measurements. In: Kreeb KH, Richter H, Thomas MH, eds. *Structural and functional responses to environmental stresses*. The Hague, Netherlands: SPB Academic Publishing, 45–54.
- Savage MJ, Wiebe HH, Cass A.** 1983. *In situ* field measurements of leaf water potential using thermocouple psychrometers. *Plant Physiology* **73**, 609–613.
- Savage MJ, Wiebe HH, Cass A.** 1984. Effect of cuticular abrasion on thermocouple psychrometric *in situ* measurement of leaf water potential. *Journal of Experimental Botany* **35**, 36–42.
- Sepulcre-Canto G, Zarco-Tejada PJ, Jimenez-Munoz JC, Sobrino JA, Soriano MA, Fereres E, Vega V, Pastor M.** 2007. Monitoring yield and fruit quality parameters in open-canopy tree crops under water stress. Implications for ASTER. *Remote Sensing of Environment* **107**, 455–470.
- Slavík B.** 1974. *Methods of studying plant water relations*. Berlin: Springer.
- Thomas TR, Matthews MA, Shackel KA.** 2006. Direct *in situ* measurement of cell turgor in grape (*Vitis vinifera* L.) berries during development and in response to plant water deficits. *Plant, Cell and Environment* **29**, 993–1001.
- Torii T, Okamoto T, Kitani O.** 1988. Non-destructive measurement of water content of a plant using ultrasonic technique. *Acta Horticulturae* **230**, 389–396.
- Trifilo E, Gascó A, Raimondo F, Nardini A, Salleo S.** 2003. Kinetics of recovery of leaf hydraulic conductance and vein functionality from cavitation-induced embolism in sunflower. *Journal of Experimental Botany* **54**, 2323–2330.
- Turner NC.** 1981. Techniques and experimental approaches for the measurement of plant water status. *Plant and Soil* **58**, 339–366.
- Tyree MT, Jarvis PG.** 1982. Water in tissues and cells. In: Lange OL, Nobel PS, Osmond CB, Ziegler H, eds. *Encyclopedia of plant physiology*, New series, Vol. 12b. Berlin: Springer-Verlag, 35–77.
- Wu J.** 1996. Determination of velocity and attenuation of shear waves using ultrasonic spectroscopy. *Journal of the Acoustical Society of America* **99**, 2871–2875.
- Wullschleger SD, Oosterhuis DM.** 1987. Electron microscope study of cuticular abrasion on cotton leaves in relation to water potential measurements. *Journal of Experimental Botany* **38**, 660–667.
- Zarco-Tejada PJ, Berni JA, Suárez L, Sepulcre-Cantó G, Morales F, Miller JR.** 2009. Imaging chlorophyll fluorescence with an airborne narrow-band multispectral camera for vegetation stress detection. *Remote Sensing of Environment* **113**, 1262–1275.
- Zimmermann D, Reuss R, Westhoff Gebner P, Bauer W, Bamberg Bentrup FW, Zimmermann U.** 2008. A novel, non-invasive, online-monitoring, versatile and easy plant-based probe for measuring leaf water status. *Journal of Experimental Botany* **59**, 3157–3167.



## RESEARCH PAPER

# Relationship between ultrasonic properties and structural changes in the mesophyll during leaf dehydration

Domingo Sancho-Knapik<sup>1</sup>, Tomás Gómez Álvarez-Arenas<sup>2</sup>, José Javier Peguero-Pina<sup>3</sup>, Victoria Fernández<sup>4</sup> and Eustaquio Gil-Pelegrín<sup>1,\*</sup>

<sup>1</sup> Unidad de Recursos Forestales, Centro de Investigación y Tecnología Agroalimentaria, Gobierno de Aragón, E-50059, Zaragoza, Spain

<sup>2</sup> Grupo de Señales, Sistemas y Tecnologías Ultrasónicas., CSIC, E-28002 Madrid, Spain

<sup>3</sup> Departament de Biología, Universitat de les Illes Balears, Carretera de Valldemossa, km 7.5, E-07071 Palma de Mallorca, Balears, Spain

<sup>4</sup> Forest Genetics and Ecophysiology Research Group, ETS Forest Engineering, Technical University of Madrid, Ciudad Universitaria s/n, E-28040 Madrid, Spain

\* To whom correspondence should be addressed: E-mail: egilp@aragon.es

Received 2 December 2010; Revised 20 January 2011; Accepted 15 February 2011

Downloaded from jxb.oxfordjournals.org by guest on March 21, 2011

## Abstract

The broad-band ultrasonic spectroscopy technique allows the determination of changes in the relative water content (RWC) of leaves with contrasting structural features. Specifically, the standardized frequency associated with the maximum transmittance ( $f/f_0$ ) is strongly related to the RWC. This relationship is characterized by the existence of two phases separated by an inflection point (associated with the turgor loss point). To obtain a better understanding of the strong relationship found between RWC and  $f/f_0$ , this work has studied the structural changes experienced by *Quercus muehlenbergii* leaves during dehydration in terms of ultrasounds measurements, cell wall elasticity, leaf thickness, leaf density, and leaf structure. The results suggest that the decrease found in  $f/f_0$  before the turgor loss point can be attributed to the occurrence of changes in the estimation of the macroscopic effective elastic constant of the leaf ( $c_{33}$ ), mainly associated with changes in the bulk modulus of elasticity of the cell wall ( $\epsilon$ ). These changes are overriding or compensating for the thickness decreases recorded during this phase. On the other hand, the high degree of cell shrinkage and stretching found in the mesophyll cells during the second phase seem to explain the changes in the acoustic properties of the leaf beyond the turgor loss point. The formation of large intercellular spaces, which increased the irregularity in the acoustic pathway, may explain the increase of the attenuation coefficient of ultrasounds once the turgor loss point threshold is exceeded. The direct measurement of  $c_{33}$  from ultrasonic measurements would allow a better knowledge of the overall biomechanical properties of the leaf further than those derived from the P–V analysis.

**Key words:** Cell wall elasticity, leaf thickness, relative water content, turgor loss point, ultrasonic spectroscopy, water potential.

## Introduction

The broad-band ultrasonic spectroscopy technique has been proven as a non-destructive, non-invasive, non-contact, and reproducible method for the dynamic determination of leaf water status. It is based on the excitation of thickness resonances on the leaves, specifically, changes in the standardized frequency ( $f/f_0$ ) at the maximum transmittance

(leaf resonant condition). This parameter has been revealed as an optimum indicator of the relative water content (RWC) of leaves with contrasting structural features (Gómez Álvarez-Arenas *et al.*, 2009a). The relationship between  $f/f_0$  and RWC is characterized by the existence of two phases separated by an inflection point, which has been

Abbreviations:  $c_{33}$ , macroscopic effective elastic constant;  $\epsilon$ , bulk modulus of elasticity of the cell wall;  $f/f_0$ , standardized frequency; P–V curves, pressure–volume curves; RWC, relative water content;  $\Psi$ , water potential; TLP, turgor loss point.

© The Author [2011]. Published by Oxford University Press [on behalf of the Society for Experimental Biology]. All rights reserved.

For Permissions, please e-mail: journals.permissions@oup.com

associated with the turgor loss point (Sancho-Knapik *et al.*, 2010).

The existence of two phases in the physics of leaf dehydration was firstly reported by Tyree and Hammel (1972) regarding the analysis of the leaf P–V relationships. During the first phase, when the leaf is water-saturated ( $RWC=1.00$ ), the protoplast of the cell exerts a positive pressure over the cell wall, which is maximally distended (maximum turgor pressure) (Tyree and Jarvis, 1982). Loss of water during the first phase, which is modulated by the elasticity of the cell wall, leads to a reduction in the cellular volume and, as a consequence, to a direct decrease in the pressure over the cell wall. The cell volume progressively diminishes until a threshold value, beyond which the protoplast does not exert pressure over the cell wall (Larcher, 2003; Pritchard, 2007).

During this first phase, before the turgor loss point, Sancho-Knapik *et al.* (2010) reported a decrease in  $f/f_0$  when the leaf is dehydrated. According to Temkin (1981), the resonant frequency of an elastic plate, when wave dispersion phenomena can be considered negligible, is given by the following equation:

$$f = v_z/2l \quad (1)$$

where  $f$  is the resonant frequency,  $v_z$  is the velocity of the ultrasonic longitudinal wave in the leaf along the direction normal of the leaf plane ( $z$ -axis) and  $l$  is the leaf thickness (Gómez Álvarez-Arenas *et al.*, 2003a). This velocity, which is dependent on elastic constants of the measured material (Auld, 1990), is given by:

$$v_z = (c_{33}/\rho)^{1/2} \quad (2)$$

where  $c_{33}$  is the macroscopic effective elastic constant of the material for compression waves in the  $z$  direction and  $\rho$  is the density (Auld, 1990).  $c_{33}$  determines the bulk macroscopic elastic stiffness of the material in the  $z$  direction. The relationship between  $c_{33}$  and the microscopic features of a material is not straightforward. In composites, for example,  $c_{33}$  depends on the components, their volumetric concentration and spatial distribution (Christensen, 2005). In foams, there are several mechanisms that contribute to furnish the overall response of  $c_{33}$  (e.g. compression and bending of the struts) (Gibson and Ashby, 1997). In this sense, it could be expected that the macroscopic  $c_{33}$  of plant leaves can be the result of a number of contributions. Among them, the effect of the tissue stiffness can be assessed independently by comparing  $c_{33}$  with the bulk modulus of elasticity ( $\epsilon$ ) calculated from the P–V curves. Therefore, it is expected that the reduction of  $\epsilon$  may cause a variation of  $c_{33}$ . This fact will cause a variation in  $v_z$  (equation 2) and, as a consequence, the reduction in  $f$ , which will be consistent with the experimental data showed by Gómez Álvarez-Arenas *et al.* (2009a).

In addition, the loss of turgor may produce a decrease of the leaf thickness (Burquez, 1987) and a slight increase in leaf density (Ogaya and Peñuelas, 2006). These changes in leaf anatomical properties may have an influence on the

resonant frequency at the higher values, according to equations 1 and 2. However, the shift of the resonant frequency towards lower values (Gómez Álvarez-Arenas *et al.*, 2009a) suggests that the changes in  $c_{33}$  exert a dominant effect over the changes in the leaf resonant frequency during this first phase.

Once the turgor loss point is exceeded, a new phase starts in the leaf dehydration process, which is characterized by the absence of cell turgor. Thus, it is assumed that cell walls are not under positive pressure during this phase (Tyree, 1976; Pritchard, 2007). Therefore, changes in pressure can no longer determine the variation of the acoustic properties of the leaf observed after the turgor loss point. Subsequent leaf dehydration increases the concentration of the sap cell, inducing changes in the osmotic potential and, as a consequence, in the water potential of the whole cell (Mitchell *et al.*, 2008). These physiological adjustments may induce morphological changes in the mesophyll cells of the leaf. In this way, it has been suggested that, at this point, the cell walls are drawn inward and may shrivel (Larcher, 2003). These conformational changes may be similar to the elastic buckling found in cellular solids subjected to a strong compression (Gibson and Ashby, 1997). It is known that the elastic buckling causes a decrease in  $c_{33}$ , which could explain the further decrease found in the resonant frequency beyond the turgor loss point. On the other hand, an additional effect to these conformational changes is the formation of gas-filled spaces in the internal tissues, which could be explained by the lateral shrinkage of mesophyll cells, as shown by Cryo-SEM observations of dehydrated leaf tissues (McBurney, 1992). Thus, the strong increase in the leaf internal heterogeneity during this phase may underlie the change in the acoustic properties of the leaf, which are associated with an increase in signal attenuation (Sancho-Knapik *et al.*, 2010).

Therefore, the main objective of this work is to study in depth the structural changes experimented by the leaf during dehydration, in order to obtain a better understanding for the strong relationship found between RWC and  $f/f_0$ , interpreting the ultrasonic measurements in terms of leaf structure, composition and water status. For this purpose, the changes occurring during different leaf dehydration steps were assessed in terms of ultrasounds measurements, P–V analysis, leaf thickness, and leaf structure.

## Materials and methods

### Plant material and experimental conditions

Measurements were carried out in ten mature leaves collected from *Quercus muehlenbergii* Engelm, the species selected for this study. In the early morning, branches were collected from the north side of the trees, placed in plastic bags and carried out to the laboratory. Once there, leaf petioles were re-cut under water to avoid embolism and kept immersed (avoiding the wetting of leaves) for 24 h at 4 °C until full leaf rehydration. It was considered that over-rehydration did not take place because changes in leaf optical properties were not observed (i.e. dark spots or dark areas in the leaf lamina). After 24 h, weight and

ultrasonic parameters were individually measured per leaf at constant time intervals following the methodology described in Gómez Álvarez-Arenas *et al.* (2009a) and Sancho-Knapik *et al.* (2010). Leaves were weighed and measured at different levels of RWC, starting at full saturation (turgid weight, TW). Leaf dry weight (DW) was estimated after keeping the plant material in a stove (24 h, 60 °C). The RWC was then calculated following the expression:  $RWC = (FW - DW) / (TW - DW)$ , FW being the sample fresh weight at any moment.

#### P–V analysis

P–V relationships were determined following the free-transpiration method described in previous studies (Clifford *et al.*, 1998; Corcuera *et al.*, 2002; Burghardt and Riederer, 2003; Vilagrosa *et al.*, 2003). The water relations parameters analysed were leaf water potential at the turgor loss point,  $\Psi_{TLP}$ ; maximum bulk modulus of elasticity,  $\varepsilon_{max}$ ; maximum turgor,  $\pi$ ; and the relative water content at the turgor loss point,  $RWC_{TLP}$ . The symplastic water loss (RWL, %) was calculated in order to obtain the Höfler diagram. Moreover, the dynamic changes in the bulk modulus of elasticity ( $\epsilon$ ) associated to changes in turgor pressure were analysed.

#### Leaf thickness and leaf density measurements

Leaf thickness was determined using a digital contact sensor GT-H10L coupled to an amplifier GT-75AP (GT Series, Keyence Corporation, Japan). This ultra-low force sensor (having a measuring force of 0.2 N when installed facing up) applies a clamp pressure of 7 kPa, which is *c.* ten times lower than the one used by Zimmermann *et al.* (2008) for a similar purpose. Thereby, it is ensured that determinations did not disturb leaf thickness measurements due to an excess of pressure over the leaf. The loss of thickness per leaf is expressed as the ratio between the thickness measured for every particular RWC and the thickness determined at full turgor.

Leaf density ( $\rho$ ,  $\text{kg m}^{-3}$ ) was calculated by measuring, in another set of leaves, the variation in leaf area, thickness, and weight during the dehydration process. In addition to the other parameters already mentioned, the area was obtained through the realization of digital images of the leaves and posterior analysis using the public domain NIH Image program (developed at the US National Institutes of Health and available at <http://rsb.info.nih.gov/nih-image/>). The volume of the leaf was calculated as the product between the leaf thickness and the area.  $\rho$  was then obtained as the ratio between leaf weight and leaf volume.

#### Cryo-scanning electron microscopy (SEM) observations

*Quercus muehlenbergii* leaves at three different RWC levels (i.e. at full turgor, around the turgor loss point, and at a RWC of *c.* 0.72) were observed with a low temperature scanning electron microscope (LTSEM, DSM 960 Zeiss, Germany, acceleration potential 15 kV, working distance 10 mm and probe current 5–10 nA). Fresh transverse sections were frozen in liquid N<sub>2</sub>, gold sputtered and subsequently observed by this microscopic technique. Micrographs were analysed using the public domain NIH Image program (developed at the US National Institutes of Health and available at <http://rsb.info.nih.gov/nih-image/>). The length and width of the 20 palisade and 20 spongy parenchyma cells were measured at the three different RWC levels studied.

#### The broad-band ultrasonic spectroscopy technique: experimental set-up and parameters measured

The experimental set-up consists of two pairs of specially designed air-coupled piezoelectric transducers (Fig. 1A); in this case with a centre frequency of 0.75 MHz, a working frequency range of 0.3–1.2 MHz, and with a radiating diameter area of 20 mm (Gómez

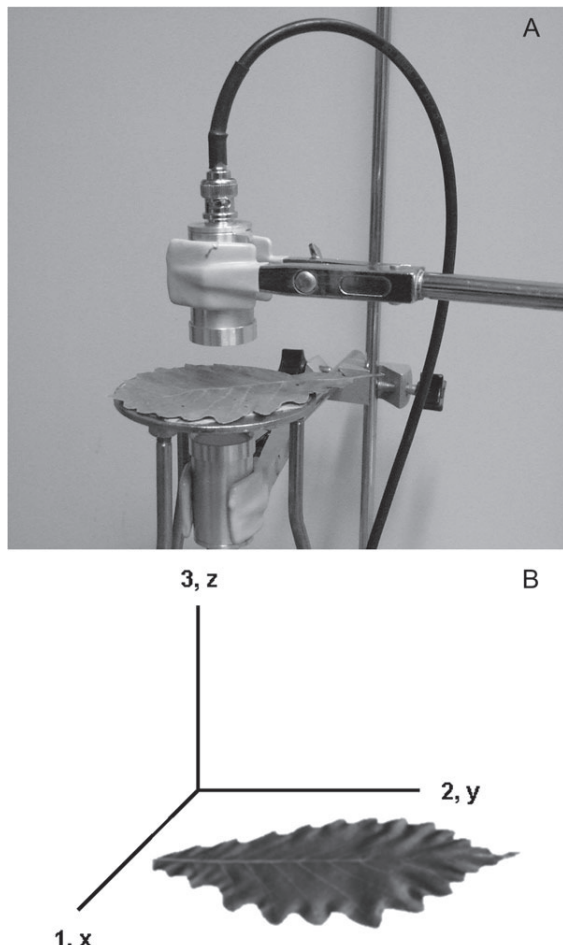


**Fig. 1.** Experimental set-up (A) and reference frame for the assessment of the measurements of the leaf rigidity (B).

Álvarez-Arenas, 2003a, 2004). These transducers are positioned facing each other at a distance of 2 cm. A high voltage (100–400 V) square semicycle (duration of 0.67 µs) is applied with a Panametrics 5077 pulser-receiver (Olympus, USA) to the transmitter transducer which converts this electrical signal into an ultrasonic pulse and launches it into the air. The receiver transducer collects this signal and converts it into an electrical one, then it is amplified (up to 59 dB) and filtered (low-pass filter at 10 MHz). Eventually, an oscilloscope (Tektronix 5052 TDS, Tektronix Inc., USA) digitizes it, averages a number of waveforms to reduce the high frequency noise (typically up to 100 waveforms), performs the Fast Fourier Transform (FFT) and transfers the data to a computer for storage. The sample rate of the oscilloscope was set to 25 Ms s<sup>-1</sup> with a total length of 5000 points. The experimental procedure of the ultrasonic technique is as follows. First, transmission from a transmitter is directly measured into the receiver, providing a calibration of the system. Then a leaf is held for a few seconds between the transducers at normal incidence. When the ultrasounds impact normally on the leaf surface, part of the energy is transmitted through the leaf, and reaches the back surface. Then part of the energy is transmitted through the interface (air) and received at the receiver transducer.

The ultrasonic parameter directly measured was the transmitted pulse in the time domain. The Fourier transformation enabled obtaining a transmittance ( $T$ ) versus frequency curve for each output. The value of the frequency associated with the maximum  $T$  at the peak curve was compared to the relative water content (RWC). The frequency values were standardized ( $f/f_0$ ) by means of

dividing each single value ( $f$ ) by the maximum value obtained at RWC=1.00 ( $f_0$ ) for each leaf studied (Sancho-Knapik *et al.*, 2010). Moreover, to estimate the attenuation of sound in the samples, the inverse of the quality factor ( $Q$ ) was employed, since  $1/Q$  is directly proportional to it. An increase in  $1/Q$  reflects an increase in the irregularity in the acoustic pathway. The  $Q$  factor is defined as the ratio between the resonance frequency and the width of the resonance peak measured at 3 dB below the maximum value (Gómez Álvarez-Arenas, 2003b).

#### The ultrasonic mechanical model

For normal incidence of plane waves on a homogeneous plate, the transmission is made up by the transmitted signal plus the contribution of all the reverberations inside the plate that are, eventually, transmitted to the air at the rear face of the plate. When all these reverberations arrive to the rear face of the plate in phase between them and with the through transmitted signal, a constructive interference is established: the transmitted energy is maximal. This is called a thickness resonance (Gómez Álvarez-Arenas, 2003a, 2009a). When attenuation in the plate can be considered negligible, then the resonance condition is obtained by:

$$f = m(v_z/2l) \quad (3)$$

where  $f$  is the resonant frequency,  $m$  is the order of the resonance, and  $v$  is the velocity of the ultrasonic longitudinal wave in the plate along the direction normal to the plate ( $z$ -axis). For non-normal incidence it is necessary to consider the presence of shear stresses and shear waves in the solid plate.

Spectra of the transmission coefficient of ultrasonic pulses through plant leaves revealed the presence of resonances. Gómez Álvarez-Arenas *et al.* (2009a) demonstrated that these resonances are thickness resonances and that there is no evidence of the appearance of shear waves in plant leaves, even when working at non normal incidence. Gómez Álvarez-Arenas *et al.* (2009b) shows, for the study of these resonances on leaves, a comparison between a one-layered model and a more detailed model based on a four-layered model (upper epidermis, palisade parenchyma, spongy mesophyll, and lower epidermis). The work demonstrates that, apart from the greater ease in obtaining the data in the one-layered model, the deviation of the one-layer model with respect to the four-layered model for the first thickness resonance ( $m=1$ ) is very small. Therefore, the one-layer model is a reasonable, accurate, and practical model that has been used in this study as in previous works (Sancho-Knapik *et al.*, 2010).

#### The macroscopic effective elastic constant ( $c_{33}$ )

The linearized relationship between the stress ( $\sigma$ ) and the strain ( $\gamma$ ) produced in an object is given in terms of elastic constants ( $c$ ) (Auld, 1990):

$$\sigma_i = c_{ij}\gamma_j$$

In this way,  $c_{33}$  relates the compressional deformation in the 3 direction with the stress applied in the same direction, an ultrasonic beam in this case (Fig. 1B).  $c_{33}$ , named as the macroscopic effective elastic constant of the leaf, represents the elasticity of the whole leaf and it is given in MPa.  $c_{33}$  was estimated using equations 1 and 2 and the absolute values of leaf frequency, thickness, and leaf density.

#### Statistical analysis

The relationship between RWC and  $f/f_0$  was adjusted to a four parameter logistic curve

$$(f = a + (b - a) / (1 + (RWC/c)^d))$$

for each leaf studied. Although the relationship between RWC and  $f/f_0$  for *Q. muehlenbergii* leaves could also be adjusted to a cubic

function ( $<B>=0.99$ ,  $P <0.0001$ ), the use of the sigmoid function was preferred because the inflection point is directly inferred from the equation. This function was selected because it describes the evolution between two 'equilibrium states', before and after the turgor loss point.

The relationships RWC versus PLT and RWC versus  $1/Q$  were adjusted to a linear segmented model (Schabenberger and Pierce, 2002) for each leaf studied. This is a non-linear model that fit a curve compound of two lineal models with slopes different to zero. The point at which the switch between the two functions occurs is generally called a joint-point, which can easily be associated with a change in the trend of the studied variable during the dehydration process. On the other hand, the relationship between RWC and  $p$  was adjusted to a square function ( $f=a+bx+cx^2$ ) for each leaf studied.

The turgor loss point was calculated as the inflection point (coefficient  $c$ ) of the regression equation for the relationship between RWC and  $f/f_0$ . On the other hand, the turgor loss point was associated with the joint-point of the relationships RWC versus PLT and RWC versus  $1/Q$ . Finally, the turgor loss point was also calculated as the maximum value of the square function for the relationship between RWC and  $p$ . A Student's  $t$  test was used to compare the  $RWC_{TLP}$  values obtained from P–V analysis and those recorded from ultrasonic measurements and leaf thickness and density. On the other hand, one-way ANOVAs were performed to compare the evolution of the width and length of the palisade and spongy parenchyma cells as RWC decreased. Multiple comparisons were carried out among the exposition times for the physiological variables using the *post-hoc* Tukey's Honestly Significant Difference test. All statistical analyses were performed with the program SAS version 8.0 (SAS, Cary, NC, USA).

## Results

The parameters derived from the pressure–volume curves for *Q. muehlenbergii* are shown in Table 1 and Figs 2 and 3. According to the Höfler diagram (Fig. 2), the symplastic water loss (RWL, %) at the turgor loss point corresponded to 26.6%. Figure 3 shows the strong decrease in the bulk modulus of elasticity ( $\epsilon$ , MPa), when turgor pressure (MPa) decreases due to leaf dehydration.

The relationship between the RWC and the percentage of loss of thickness (PLT) was adjusted to a linear segmented model (Fig. 4;  $<B>=0.93$ ,  $P <0.0001$ ; all coefficients were statistically significant,  $P <0.0001$ ). It can be observed that thickness strongly decreases until a certain RWC threshold ( $0.79 \pm 0.03$ ), which is associated with the turgor loss point

**Table 1.** Parameters derived from the pressure–volume curves for *Quercus muehlenbergii*: water potential at the turgor loss point ( $\Psi_{TLP}$ , MPa), relative water content at the turgor loss point ( $RWC_{TLP}$ ), maximum bulk modulus of elasticity ( $\epsilon_{max}$ , MPa), and maximum turgor ( $\pi$ , MPa)

Data are mean  $\pm$ SE.

#### *Quercus muehlenbergii*

$\Psi_{TLP}$ (MPa)	$2.80 \pm 0.05$
$RWC_{TLP}$	$0.83 \pm 0.01$
$\epsilon_{max}$ (MPa)	$17.09 \pm 0.58$
$\pi_0$ (MPa)	$2.15 \pm 0.07$

and close to that derived from P-V curves (Table 1). Once this RWC point is reached, the loss of thickness remains fairly constant. However, leaf density, which was adjusted to a square function (Fig. 5;  $R_{\text{adj}}^2=0.88$ ,  $P=0.002$ ), shows a slight increase (*c.* 9%) until  $\text{RWC}=0.82\pm 0.01$ , followed by a slight decrease once this point is exceeded. The loss of leaf thickness is caused by the sharp reduction in the width and length of both spongy and palisade mesophyll cells (Table 2). This process can be observed in the Cryo-SEM micrographs of leaf tissue at full turgor (Fig. 6A, C) and at  $\text{RWC}=0.72$  (Fig. 6B, D). Moreover, Fig. 6D shows the buckling experienced by the mesophyll cells when the turgor loss point is exceeded (Fig. 6D).

In Fig. 7 the mean values of  $f/f_0$  obtained from ultrasonic measurements are represented against different levels of RWC. The relationship between RWC and  $f/f_0$  was adjusted to a four parameter logistic curve ( $R_{\text{adj}}^2=0.99$ ,  $P < 0.0001$ ; all

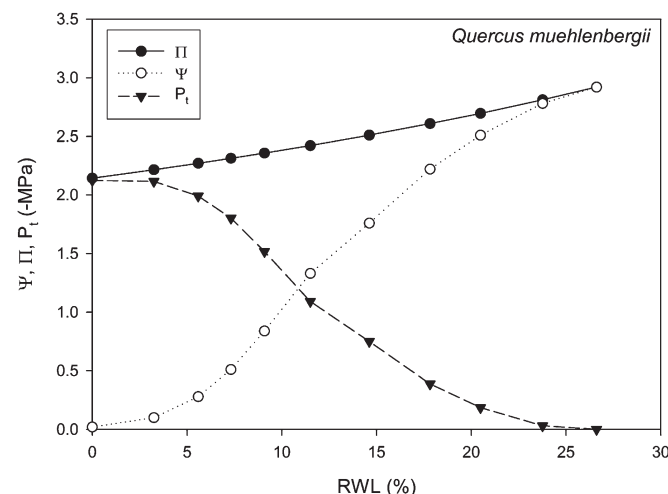


**Fig. 2.** Höfler diagrams relating symplastic water loss (RWL, %) to turgor pressure ( $P_t$ ), osmotic potential ( $\pi_0$ ), and leaf water potential ( $\Psi$ ) in *Quercus muehlenbergii*.

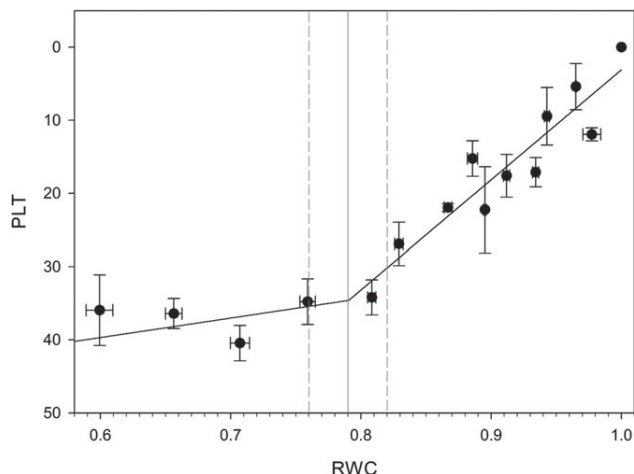


**Fig. 3.** Relationship between the turgor pressure (MPa) and the bulk modulus of elasticity ( $\epsilon$ , MPa) for *Quercus muehlenbergii*. Data are expressed as mean  $\pm$  SE.

coefficients were statistically significant,  $P < 0.0001$ ), which is characterized by the existence of an inflection point, corresponding to the turgor loss point (Sancho-Knapik *et al.*, 2010). The turgor loss point for *Q. muehlenbergii* leaves estimated by the standardized frequency corresponded to a RWC of  $0.84\pm 0.01$ . Figure 8 represents the RWC versus the inverse of the quality factor of the leaf first thickness resonance ( $1/Q$ ), which was adjusted to a linear segmented model ( $R_{\text{adj}}^2=0.97$ ,  $P < 0.0001$ ; all coefficients were statistically significant,  $P < 0.0001$ ). The  $\text{RWC}_{\text{TLP}}$  derived from  $1/Q$  values was  $0.82\pm 0.01$ . It can be observed

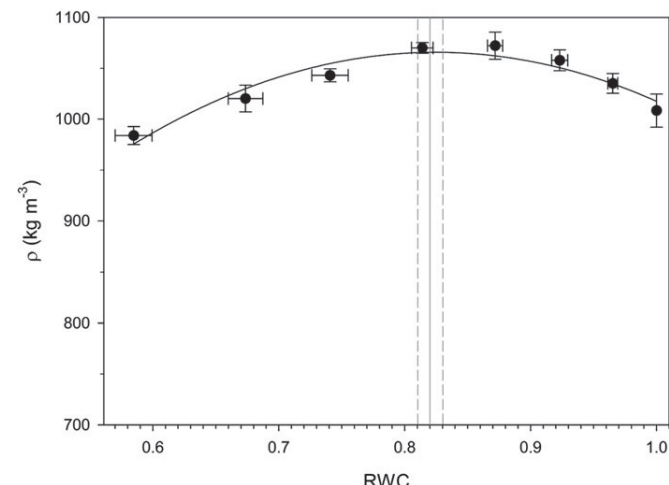


**Fig. 4.** Relationship between the percentage of loss of thickness (PLT) and the relative water content (RWC) for *Quercus muehlenbergii*. Data are expressed as mean  $\pm$  SE of ten leaves. Solid line and dashed lines indicates, respectively, the estimated relative water content at the turgor loss point ( $\text{RWC}_{\text{TLP}}$ ) and the standard error of this estimation.

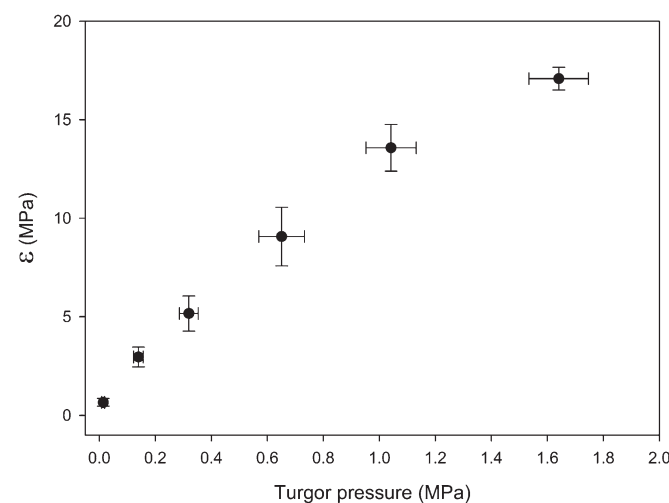


**Fig. 5.** Relationship between the leaf density ( $\rho$ , kg m<sup>-3</sup>) and the relative water content (RWC) for *Quercus muehlenbergii*. Data are expressed as mean  $\pm$  SE of ten leaves. Solid line and dashed lines indicates, respectively, the estimated relative water content at the turgor loss point ( $\text{RWC}_{\text{TLP}}$ ) and the standard error of this estimation.

that at high RWC values, up to the turgor loss point,  $1/Q$  remains nearly constant (*c.* 0.3), while it dramatically increases once this point is exceeded. The results indicate that there is an increase of the attenuation coefficient of ultrasounds, once the leaf is below the RWC threshold determined by the turgor loss point.

The RWC<sub>TLP</sub> values derived from P–V curves and those estimated from PLT,  $\rho$ , and ultrasonic measurements ( $f/f_0$  and  $1/Q$ ) were not statistically different at all levels of significance of  $P < 0.05$  (Table 3). It should be noted that

**Table 2.** Width ( $x$ ,  $\mu\text{m}$ ) and length ( $y$ ,  $\mu\text{m}$ ) of the palisade and spongy parenchyma cells of *Quercus muehlenbergii* leaves at three different RWC levels

Data are mean  $\pm$  SE. Different letters within columns indicate significant differences at  $P < 0.05$  among the three RWC levels.

RWC	Palisade parenchyma cells		Spongy parenchyma cells	
	$x$ ( $\mu\text{m}$ )	$y$ ( $\mu\text{m}$ )	$x$ ( $\mu\text{m}$ )	$y$ ( $\mu\text{m}$ )
1.00	17 $\pm$ 1 a	142 $\pm$ 1 a	20 $\pm$ 1 a	51 $\pm$ 3 a
0.83	7 $\pm$ 0 b	63 $\pm$ 1 b	8 $\pm$ 0 b	24 $\pm$ 2 b
0.72	6 $\pm$ 0 b	53 $\pm$ 1 c	8 $\pm$ 0 b	16 $\pm$ 1 c

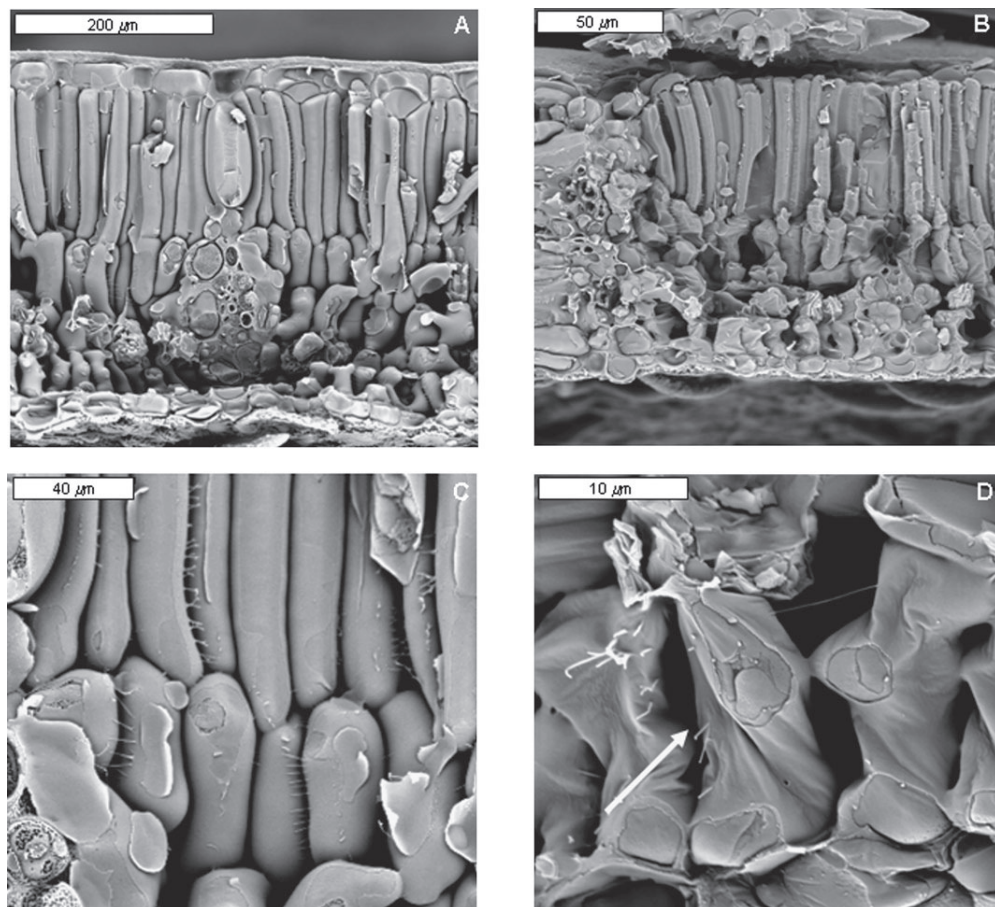


**Fig. 6.** Cryo-SEM micrographs of leaves of *Quercus muehlenbergii* at full turgor (A, C) and at RWC = 0.72 (B, D). White arrow indicates the cell buckling phenomenon.

ultrasonic measurements showed correlation coefficients higher than leaf thickness and density (Table 3).

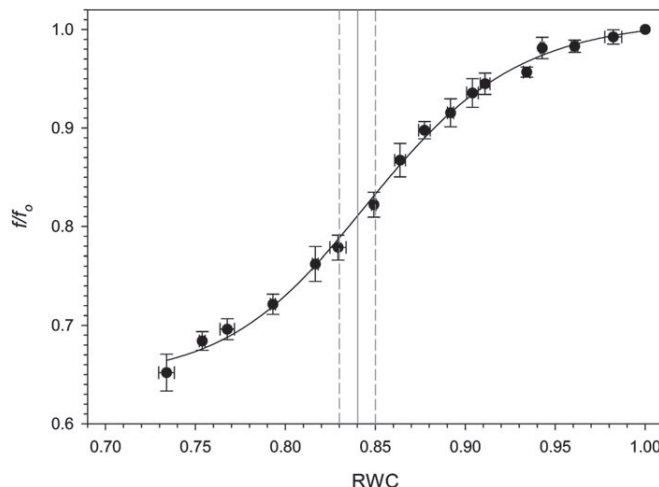
Figure 9 compares the changes in the bulk modulus of elasticity ( $\varepsilon$ , MPa) and the estimated macroscopic effective elastic constant ( $c_{33}$ ) associated with changes in turgor pressure (MPa). Both parameters decreased in a similar way, from full turgor to turgor loss point. However, when turgor is lost,  $\varepsilon$  was *c.* 0 MPa whereas  $c_{33}$  did not reach this value.

Figure 10 shows the influence of the macroscopic effective elastic constant ( $c_{33}$ ), leaf thickness, and leaf density on the standardized frequency ( $f/f_0$ ) for *Quercus muehlenbergii* leaves. It can be observed that  $c_{33}$  is the main factor affecting the changes in  $f/f_0$ . On the other hand,  $f/f_0$  was slightly affected by changes in leaf thickness at high  $f/f_0$  values (i.e. at high RWC values, before the turgor loss point), whereas leaf density always had a negligible influence on  $f/f_0$  values.

## Discussion

In this investigation, the changes occurring during different dehydration steps were assessed in terms of ultrasounds measurements, P–V analysis, leaf thickness, leaf density,

and leaf structure. Although all the studied parameters were sensitive to changes in plant water status and allowed the estimation of the turgor loss point for *Q. muehlenbergii* leaves (Table 3), most of them showed some drawbacks. Leaf thickness requires contact with the leaf so it is more invasive than the broad-band ultrasonic spectroscopy. Moreover, the absence of changes in leaf thickness after the turgor loss point prevents its use for the estimation of leaf water status beyond this point (Fig. 4). In this way, the variation of leaf density was almost negligible during the



**Fig. 7.** Relationship between the relative water content (RWC) and the standardized frequency ( $f/f_0$ ) for *Quercus muehlenbergii*. Data are expressed as mean  $\pm$  SE of ten leaves. Solid line and dashed lines indicates, respectively, the estimated relative water content at the turgor loss point ( $RWC_{TLP}$ ) and the standard error of this estimation.

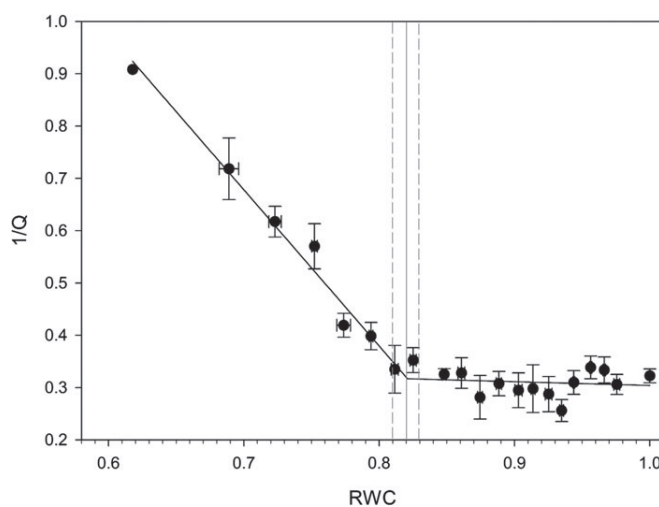


**Fig. 8.** Relationship between the relative water content (RWC) and the inverse of Q-factor ( $1/Q$ ) for *Quercus muehlenbergii*. Data are expressed as mean  $\pm$  SE of ten leaves. Solid line and dashed lines indicates, respectively, the estimated relative water content at the turgor loss point ( $RWC_{TLP}$ ) and the standard error of this estimation.

**Table 3.** Relative water content at the turgor loss point ( $RWC_{TLP}$ ) estimated from the relationships between RWC and (i) percentage of loss of thickness (PLT), (ii) density ( $\rho$ ), (iii) standardized frequency ( $f/f_0$ ), and (iv) the inverse of Q-factor ( $1/Q$ ) for *Quercus muehlenbergii* leaves

The adjusted correlation coefficient ( $R^2_{adj}$ ) and the  $P$ -value are shown for each studied relationship. All estimated  $RWC_{TLP}$  values were not statistically different from  $RWC_{TLP}$  derived from P–V curves.

	$RWC_{TLP}$	$R^2_{adj}$	$P$
RWC versus PLT	$0.79 \pm 0.03$	0.93	<0.0001
RWC versus. $\rho$	$0.82 \pm 0.01$	0.88	0.002
RWC versus $f/f_0$	$0.84 \pm 0.01$	0.99	<0.0001
RWC versus $1/Q$	$0.82 \pm 0.01$	0.97	<0.0001

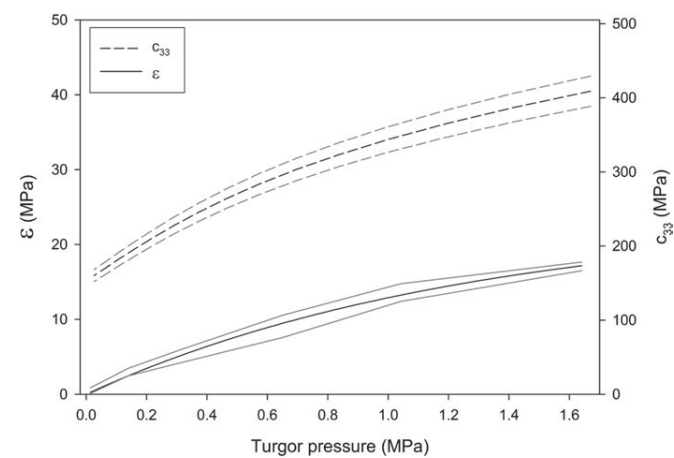


**Fig. 9.** Relationships turgor pressure (MPa) versus the bulk modulus of elasticity ( $\epsilon$ , MPa) (solid line) and turgor pressure (MPa) versus the estimated macroscopic effective elastic constant ( $c_{33}$ ) (dashed line) for *Quercus muehlenbergii*. Grey solid lines and grey dashed lines represent, respectively, the standard errors of  $\epsilon$  and  $c_{33}$ .

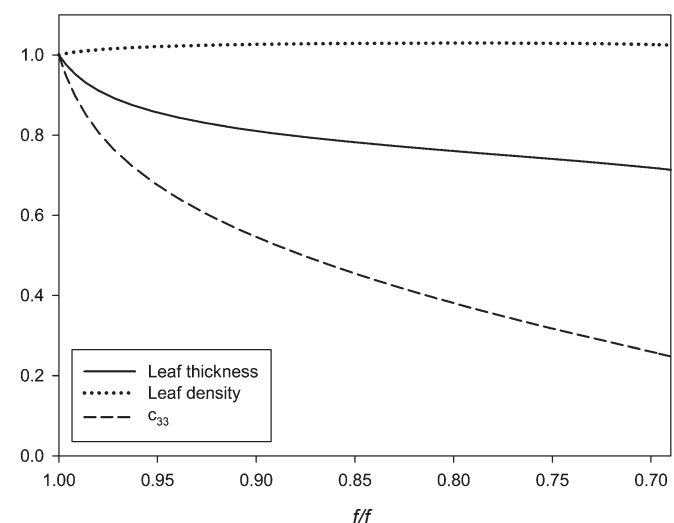


**Fig. 10.** Variation of the macroscopic effective elastic constant ( $c_{33}$ ), leaf thickness and leaf density on the standardized frequency ( $f/f_0$ ) for *Quercus muehlenbergii*. All the variables have been standardized by dividing each value by its value at  $RWC=1.00$ .

dehydration process (Fig. 5) due to the existence of compensation between the loss of weight induced by water loss and the reduction in leaf thickness. On the other hand, regarding ultrasonic parameters, the use of the frequency is more suitable than  $1/Q$  to estimate plant water status because (i) the frequency is a parameter directly measured while  $1/Q$  is a calculated parameter over a certain frequency range, which can be affected by any distortion of the leaf resonance present in the measurement, and (ii) the turgor loss point calculated from frequency data is the inflection point of a full process of changes (Fig. 7), which is more accurate than the estimation of a point at the beginning of a change process (Fig. 8). For these reasons, it is considered that the frequency is an optimum parameter for the estimation of plant water status. Sancho-Knapik *et al.* (2010) showed that the turgor loss point can be accurately determined by the measurement of the frequency associated with the maximum transmittance. It should be noted that the turgor loss point has been considered a threshold for many physiological processes (Brodrribb and Holbrook, 2003; Thomas *et al.*, 2006; Mitchell *et al.*, 2008). Again, no significant differences were found between the RWC<sub>TLP</sub> derived from analysis of P–V isotherms and those obtained by ultrasounds. The turgor loss point established the separation in two differential phases of the performance of  $f/f_0$  as a function of RWC variations.

The first phase, corresponding to high RWC, is characterized by a progressive loss of turgor pressure (Fig. 2), a reduction in the bulk modulus of elasticity of the leaf ( $\epsilon$ ) (Fig. 3) and a loss of thickness (Fig. 4). The decrease found in  $\epsilon$  showed a similar trend to that found for the macroscopic effective elastic constant ( $c_{33}$ ) of the leaf (Fig. 9). This fact indicates that changes in  $\epsilon$  could be associated with changes in  $c_{33}$ . It should be noted that  $\epsilon$  has been mainly recognized as an indicator of the elastic properties of the cell walls (Tyree and Jarvis, 1982; Saito *et al.*, 2006), whereas  $c_{33}$  can be associated with the elasticity of the whole leaf. Thus, there are other factors that could contribute to  $c_{33}$ , which may explain the differences found between the values of  $\epsilon$  and  $c_{33}$  (Fig. 9). This is a matter that deserves further investigations. The decrease in  $c_{33}$  (Fig. 9) and the slight increase in  $\rho$  (Fig. 5) during the first phase are directly traduced in a reduction of the ultrasound velocity (equation 2) and hence a displacement of the resonance of the leaf towards lower frequencies (equation 1). This fact could explain the sharp decline found in  $f/f_0$  during this first phase (Fig. 7). On the other hand, it can be argued that the  $f/f_0$  variations determined could be associated with leaf thickness reductions during leaf dehydration (Fig. 4). However, due to the inverse relationship between thickness and frequencies, higher  $f/f_0$  values could theoretically be expected during dehydration (equation 1), while, by contrast, lower  $f/f_0$  values were recorded. Therefore, it can be concluded that the changes in  $c_{33}$  (that can be attributed to changes in  $\epsilon$ ) are the main causal factor for the changes found in  $f/f_0$  during this first phase, exceeding the effect caused by the loss of thickness during leaf dehydration or density variations (Fig. 10).

The second phase, once the turgor loss point is exceeded, is characterized by the existence of an additional decrease in  $f/f_0$  as the leaf dehydration process goes on (Fig. 7), which cannot be caused by changes in the turgor pressure as assumed so far. The further observed reduction of  $f/f_0$  beyond the turgor loss point must be justified in terms of a reduction in  $c_{33}$ , but now, this  $c_{33}$  reduction cannot be produced by the loss of turgor. At the early stages of this procedure, the most likely mechanism is the occurrence of partial elastic buckling of the solid structure (Gibson and Ashby, 1997). This leads to a reduction of  $c_{33}$  and hence a reduction of the velocity and a shift of the resonant frequency towards lower frequencies. Therefore, this could explain the further decrease found in the resonant frequency beyond the turgor loss point (Fig. 7). As a first approach to verify this hypothesis, Cryo-SEM micrographs of tissue subjected to differential dehydration stages were obtained and it was indeed observed that water loss induced the occurrence of a high degree of cell shrinkage and stretching (Fig. 6). Around the turgor loss point, both spongy and palisade mesophyll cells experienced a reduction in length and width of c. 54% and 59%, respectively. This reduction was more dramatic at 0.72 RWC, where maximum reductions were observed regarding cell length (from 62% to 68%) in contrast to cell width (c. 63%). Therefore, it can be concluded that the changes found in  $f/f_0$  during this second phase (Fig. 7) are mainly due to the conformational changes of mesophyll cells. Furthermore, these changes caused the formation of large intercellular spaces, which increased the irregularity in the acoustic pathway. This fact may explain the increase of the attenuation coefficient of ultrasounds due to the ultrasound scattering produced by these irregularities and hence the increase of the damping of the leaf thickness (Fig. 8), once the turgor loss point threshold is passed.

## Conclusions

In this work  $c_{33}$  has been estimated through independent measurements of frequency, thickness, and density. The decrease in  $c_{33}$  is the main factor explaining the decrease found in  $f/f_0$  before the turgor loss point. The physical changes found in the mesophyll may explain the variations in the ultrasonic properties of the leaf during the second phase. Finally, the knowledge derived from this study can serve for the development of tools for the continuous monitoring of plant water status, in order to maximize water use efficiency in crop plants.

## Acknowledgements

This study was partially supported by INIA project SUM2008-00004-C03-03 (Ministerio de Ciencia e Innovación). Financial support from Gobierno de Aragón (A54 research group) is also acknowledged. Work of José Javier Peguero-Pina is supported by a ‘Juan de la Cierva’-MICIIN post-doctoral contract.

## References

- Auld BA.** 1990. *Acoustic fields and waves in solids*, 2nd edn. Malabar, FL: Krieger Publishing Company.
- Brodribb TJ, Holbrook NM.** 2003. Stomatal closure during leaf dehydration, correlation with other leaf physiological traits. *Plant Physiology* **132**, 2166–2173.
- Burghardt M, Riederer M.** 2003. Ecophysiological relevance of cuticular transpiration of deciduous and evergreen plants in relation to stomatal closure and leaf water potential. *Journal of Experimental Botany* **54**, 1941–1949.
- Bürquez A.** 1987. Leaf thickness and water deficit in plants: a tool for field studies. *Journal of Experimental Botany* **38**, 109–114.
- Christensen RM.** 2005. *Mechanics of composite materials*. Dover Publications.
- Clifford SC, Arndt SK, Corlett JE, Joshi S, Sankhla N, Popp M, Jones HG.** 1998. The role of solute accumulation, osmotic adjustment and changes in cell wall elasticity in drought tolerance in *Ziziphus mauritiana* (Lamk). *Journal of Experimental Botany* **49**, 967–977.
- Corcuera L, Camarero JJ, Gil-Pelegrín E.** 2002. Functional groups in *Quercus* species derived from the analysis of pressure–volume curves. *Trees, Structure and Function* **16**, 465–472.
- Gibson LJ, Ashby MF.** 1997. *Cellular solids*. Cambridge University Press.
- Gómez Álvarez-Arenas TE.** 2003a. Air-coupled ultrasonic spectroscopy for the study of membrane filters. *Journal of Membrane Science* **213**, 195–207.
- Gómez Álvarez-Arenas TE.** 2003b. A nondestructive integrity test for membrane filters based on air-coupled ultrasonic spectroscopy. *IEEE Transactions on Ultrasonics, Ferroelectrics and Frequency Control* **50**, 676–685.
- Gómez Álvarez-Arenas TE.** 2004. Acoustic impedance matching of piezoelectric transducers to the air. *IEEE Transactions on Ultrasonics, Ferroelectrics and Frequency Control* **51**, 624–633.
- Gómez Álvarez-Arenas TE, Sancho-Knapik D, Peguero-Pina JJ, Gil-Pelegrín E.** 2009a. Noncontact and noninvasive study of plant leaves using air-coupled ultrasounds. *Applied Physics Letters* **95**, 193702.
- Gómez Álvarez-Arenas TE, Sancho-Knapik D, Peguero-Pina JJ, Gil-Pelegrín E.** 2009b. Determination of plant leaves water status using air-coupled ultrasounds. *IEEE International Ultrasonics Symposium Proceedings* 771–774.
- Larcher W.** 2003. *Physiological plant ecology. Ecophysiology and stress physiology of functional groups*. Berlin, Heidelberg, New York: Springer-Verlag.
- McBurney T.** 1992. The relationship between leaf thickness and plant water potential. *Journal of Experimental Botany* **43**, 327–335.
- Mitchell PJ, Veneklass EJ, Lambers H, Burgess SSO.** 2008. Leaf water relations during summer water deficit: differential responses in turgor maintenance and variation in leaf structure among different plant communities in south-western Australia. *Plant, Cell and Environment* **31**, 1791–1802.
- Ogaya R, Peñuelas J.** 2006. Contrasting foliar responses to drought in *Quercus ilex* and *Phillyrea latifolia*. *Biologia Plantarum* **50**, 373–382.
- Pritchard J.** 2007. Plant tissues and cells: turgor pressure. In: Roberts K, ed. *Handbook of plant science*, Vol. I. Chichester, England: Wiley, 148–151.
- Saito T, Soga K, Hoson T, Terashima I.** 2006. The bulk elastic modulus and the reversible properties of cell walls in developing *Quercus* leaves. *Plant and Cell Physiology* **47**, 715–725.
- Sancho-Knapik D, Gómez Álvarez-Arenas T, Peguero-Pina JJ, Gil-Pelegrín E.** 2010. Air-coupled broadband ultrasonic spectroscopy as a new non-invasive and non-contact method for the determination of leaf water status. *Journal of Experimental Botany* **61**, 1385–1391.
- Schabenberger O, Pierce FJ.** 2002. *Contemporary statistical models for the plant and soil sciences*. Boca Raton, FL: CRC Press, 252–259.
- Temkin S.** 1981. Elements of acoustics. New York: John Wiley & Sons.
- Thomas TR, Matthews MA, Shackel KA.** 2006. Direct *in situ* measurement of cell turgor in grape (*Vitis vinifera* L.) berries during development and in response to plant water deficits. *Plant, Cell and Environment* **29**, 993–1001.
- Tyree MT.** 1976. Negative turgor pressure in plant cells: fact or fallacy? *Canadian Journal of Botany* **54**, 2738–2746.
- Tyree MT, Hammel HT.** 1972. The measurement of the turgor pressure and the water relations of plants by the pressure-bomb technique. *Journal of Experimental Botany* **23**, 267–282.
- Tyree MT, Jarvis PG.** 1982. Water in tissues and cells. In: Lange OL, Nobel PS, Osmond CB, Ziegler H, eds. *Encyclopedia of plant physiology, New series*, Vol. 12b. Berlin: Springer-Verlag, 35–77.
- Vilagrosa A, Bellot J, Vallejo VR, Gil-Pelegrín E.** 2003. Cavitation, stomatal conductance, and leaf dieback in seedlings of two co-occurring Mediterranean shrubs during an intense drought. *Journal of Experimental Botany* **54**, 2015–2024.
- Zimmermann D, Reuss R, Westhoff Gebner P, Bauer W, Bamberg Bentrup FW, Zimmermann U.** 2008. A novel, non-invasive, online-monitoring, versatile and easy plant-based probe for measuring leaf water status. *Journal of Experimental Botany* **59**, 3157–3167.



# Correspondence

---

## Air-Coupled Ultrasonic Resonant Spectroscopy for the Study of the Relationship Between Plant Leaves' Elasticity and Their Water Content

Domingo Sancho-Knapik, Hector Calás,  
Jose Javier Peguero-Pina, Antonio Ramos Fernández,  
Eustaquio Gil-Pelegrín,  
and Tomas E. Gómez Álvarez-Arenas

**Abstract**—Air-coupled wideband ultrasonic piezoelectric transducers are used in the frequency range 0.3 to 1.3 MHz to excite and sense first-order thickness resonances in the leaves of four different tree species at different levels of hydration. The phase and magnitude spectra of these resonances are measured, and the inverse problem solved; that is, leaf thickness and density, ultrasound velocity, and the attenuation coefficient are obtained. The elastic constant in the thickness direction ( $c_{33}$ ) is then determined from density and velocity data. The paper focuses on the study of  $c_{33}$ , which provides a unique, fast, and noninvasive ultrasonic method to determine leaf elasticity and leaf water content.

### I. INTRODUCTION

ULTRASONIC spectroscopy was first suggested in the early 1960s as a method of obtaining information about size and orientation of discrete defects in metals [1]. Later, this technique was used in many different contexts. In 1978, Haines *et al.* used magnitude and phase spectral analysis, with a pulse-echo water immersion technique, to study reflection from multilayered materials in a frequency range in which thickness resonances appeared [2]. Sachse and Pao proposed a method to determine the phase velocity of dispersive materials in the absence of thickness resonances by using the phase spectrum and a water immersion and through-transmission technique [3]. Later, this method was extended to include the information of the magnitude spectra and to obtain both velocity and attenuation [4]. Pialucha *et al.* proposed a magnitude spectrum method to measure phase velocity [5]; they used water immersion, a through transmission technique, and the magnitude spectral analysis of the thickness resonances.

Manuscript received April 15, 2011; accepted December 5, 2011. The authors acknowledge funding by the Spanish Ministry for Science through projects DPI2008-05213 and DPI2011-22438.

D. Sancho-Knapik and E. Gil-Pelegrín are with the Unidad de Recursos Forestales, Centro de Investigación y Tecnología Agroalimentaria, Zaragoza, Spain.

H. Calás, A. Ramos Fernández, and T. E. Gómez Álvarez-Arenas are with the Ultrasound for Medical and Industrial Applications (UMEDIA) research group, Consejo Superior de Investigaciones Científicas (CSIC), Madrid, Spain (e-mail: tgomez@ia.cetef.csic.es).

J. J. Peguero-Pina is with the Departament de Biología, Universitat de les Illes Balears, Palma de Mallorca, Spain.

Digital Object Identifier 10.1109/TUFFC.2012.2194

Use of air-coupled ultrasound to obtain material properties is especially interesting for those materials that cannot be wetted, or those situations where avoiding the use of water or other coupling liquids may be an advantage. This technique was first used to study paper using through transmission and plate wave resonances by Luukkala *et al.* [6]. Thickness and plate resonances have been largely used as a means to enhance the amount of transmitted energy. For example, Hutchins *et al.* used this technique for poly(methyl methacrylate) and carbon fiber reinforced polymers (FRPs) [7]. Later, Schindel and Hutchins used air-coupled ultrasound to measure the ultrasound velocity in plates by comparing time of flight measurements with measurements of the frequency of the thickness resonance [8]. Air-coupled techniques in the time domain have also been used to measure velocities or attenuation coefficients and to calculate elastic constants or other material properties for a variety of materials including porous rocks [9], textiles [10], FRPs [11], polymers during polymerization [12], and wood [13].

A more detailed analysis of the spectrum of the thickness resonances permit the density of the plate and the velocity and the attenuation coefficient of ultrasound in the plate to be obtained if the thickness is known. This technique has been applied to silicone rubber plates, filtration membranes, and paper [14]–[16]. Later, this resonant technique in the frequency domain was extended for oblique incidence to obtain, in addition, the velocity and attenuation coefficient of shear waves and viscoelastic constants [17]. Analysis of more complex resonances of finite-sized materials has also been used to determine the elastic properties of drug tablets [18]. More recently, a method that uses both phase and magnitude spectra of thickness resonances has been proposed. It requires no independent determination of the thickness and has been applied to composite materials, membranes, and leaves [19]. Later, improvements of this technique were applied to determine plate thickness and density and velocity and attenuation of ultrasound in polypropylene ferroelectret films and vacuum-packaged cured ham [20], [21].

Development and use of non-invasive techniques to determine the status and properties of plants is a key issue in fields such as applied botany and plant physiology. In particular, there is a rising need for non-invasive sensing of plants' watering needs to control horticultural and agricultural water application and irrigation systems [22], [23].

Ultrasonic techniques represent a good alternative for this purpose; actually, ultrasonic water immersion techniques have already been used [24], [25]. However, these techniques are not useful to determine the leaf's water status. Noncontact ultrasonic spectroscopy has recently been used to measure the transmission coefficient of plant leaves over the frequency range 0.2 to 2.5 MHz at normal incidence [26]. Later, the frequency location of the first

thickness resonance ( $f_{\text{TR}}$ ) and the quality factor of the resonance ( $Q$ ) were measured through the desiccation process of some leaves; these data were compared with relative water content (RWC) measurements, pressure-volume curves [27], and cryo-scanning electron microscopy images [28]. Very high correlation factors have been found between  $f_{\text{TR}}$  and the RWC, and between  $f_{\text{TR}}$  and the water potential. Moreover, it has been possible to establish that the point of null turgor pressure and the point of inflection in the curve of  $f_{\text{TR}}$  versus RWC appear at the same RWC value.

However, the identification of the underlying physical mechanisms which permit explanation of this observed behavior is not straightforward. The main reason is that  $f_{\text{TR}}$  depends on several leaf properties that are affected, in different and complex ways, by the modifications produced in the leaves by the variation of the RWC, including thickness, density, elastic constant, and cell structure.

To avoid this problem, a more detailed analysis of the leaf resonances is presented in this paper. This analysis is based on the solution of the inverse problem, as explained in [19], and a subsequent improvement of the fitting of the theoretically calculated thickness resonance curve into the experimentally measured one, as presented in [20]. Toward this end, an effective model for the leaf has been used, based on the assumption that thickness resonances in leaves can be represented by the thickness resonances of a homogeneous plate with effective properties. For this analysis, we have developed a fast, efficient, and automatic processing of the spectra that is performed *in situ*, right after the measurement. This provides, almost in real time: leaf density and thickness, and velocity and attenuation coefficient of ultrasound in the leaves. *In situ* processing of the data is a key issue considering the large number of samples and measurements to be taken. This procedure is applied to study the desiccation process of leaves of four different tree species (two evergreen and two deciduous species): *Prunus laurocerasus*, *Ligustrum lucidum*, *Populus x euroamericana*, and *Platanus hispanica*.

## II. ANALYSIS OF THE SPECTRAL RESPONSE OF THE LEAVES' THICKNESS RESONANCE

Elastic response of plant leaves is largely determined by the water contained in them and by the air-filled pore space. Most of the water contained in plant leaves is enclosed within the leaf cells at a pressure greater than the atmospheric pressure because of the mechanical stress stored in the cell membrane. This membrane stress in the densely packed cell structure of the leaf is the main factor responsible for the leaf's elastic properties. When a fully hydrated leaf loses water, the volume of water contained by each cell is reduced and, consequently, the stress stored in the cell membranes is also reduced. On the macroscopic scale, these changes give rise to leaf shrinkage and a loss of rigidity. The elastic constants ( $c_{ij}$ ) are expected to decrease as a result of both the loss of mechanical stress in the cells membrane and the deformation of the cell structure.

Leaves' first thickness resonance spectra are analyzed, considering the leaves as a homogeneous plate with effective properties. A multilayered model, closer to the real leaf structure, was proposed in [29]. However, this model is currently of little practical use because it introduces a much larger set of parameters which are difficult to determine. In addition, the one-layer model provides a reasonable fitting into the experimental data if the analysis is limited to the vicinity of the first-order thickness resonance and it is not extended to higher resonance orders. The transmission coefficient,  $T$ , at normal incidence for a single solid plate of homogeneous material embedded in a fluid is given by  $T = |\xi|^2$ , where

$$\xi = \frac{2r\Gamma}{2r\Gamma \cos(k_2 l) - i(1 + r^2\Gamma^2)\sin(k_2 l)}, \quad (1)$$

where  $l$  is the thickness of the plate;  $r$  is the ratio of wave numbers (fluid to solid),  $r = k_1/k_2$ ; and  $\Gamma = \rho_1/(r^2\rho_2)$ , where  $\rho$  is the density [30]. Plate roughness can be introduced by considering a modification of the transmission and reflection coefficients [31]. The transmission coefficient is measured using a through-transmission technique, then the following relations between the measured modulus and phase of the transmission coefficient ( $T$  and  $\Delta\phi$ ) and the calculated  $\xi$  [magnitude,  $|\xi|$ , and phase,  $\phi(\xi)$ ] hold:

$$T = |(\xi \exp(\alpha_1 l))|^2 \cong |\xi|^2 \quad (2)$$

$$\Delta\phi = \phi(\xi) - lk_1, \quad (3)$$

where  $\alpha_1$  is the attenuation coefficient in air.

The analysis of the experimentally measured resonance spectra follows the procedure explained in [18] and [19]. Using (4) and (5), this procedure permits us to get a first estimation of the ultrasonic velocity ( $v_2$ ) and the thickness of the plate ( $l$ ) from the measured values of the frequency location of the first thickness resonance ( $f_{\text{TR}}$ ) and the value of the phase spectra  $\Delta\phi$  at this frequency  $\Delta\phi(f_{\text{TR}}) = \Delta\phi_1$ .

$$v_2(f_{\text{TR}}) = 2f_{\text{TR}} \quad (4)$$

$$v_2(f_{\text{TR}}) = l/(l/v_1 - \Delta\phi_1/(2\pi f_{\text{TR}})), \quad (5)$$

where  $v_1$  is the velocity of ultrasound in the fluid in which the plate is immersed (air in this case). In this work, a first estimation of the density of the leaves  $\rho_2^0 = 950 \text{ g/m}^3$  was considered. The attenuation of the ultrasonic waves in the plate at  $f_{\text{TR}}$  ( $\alpha_2^0(f_{\text{TR}})$ ) can be estimated from the leaf impedance and the  $Q$ -factor of the thickness resonance (see [15] and [16]). The variation of the attenuation with the frequency ( $\alpha_2(f)$ ) can be described by a power law, as has been done in the past for a large number of porous materials and biological tissues (see [17] and [20]):

$$\alpha_2'(f) = \alpha_2^0 \left( \frac{f}{f_{\text{TR}}} \right)^{1.5}. \quad (6)$$

Velocity is assumed to be constant, which is a reasonable assumption considering the frequency range in which measurements are performed.

The values of  $v_2^0$ ,  $\alpha'_2(f)$ ,  $\rho_2^0$ , and  $l^0$  so obtained are considered a first approach. We then calculate  $k_2$  according to

$$k_2(f) = \frac{\omega}{v_2} + i\alpha_2(f), \quad (7)$$

where, in this case,  $v_2 = v_2^0$  and  $\alpha_2(f) = \alpha'_2(f)$ .

These values are introduced in (1), and then  $\xi$  is calculated. From  $\xi$ , we get  $T(f)^{\text{theo}} = |\xi|^2$  and  $\Delta\phi(f)^{\text{theo}} = \phi(\xi) - lk_1$ . The estimation of the quality of the agreement is given by  $\tau^T$  and  $\tau^\phi$ , defined as:

$$\tau^T = \frac{1}{N} \sum_{n=1}^N ((T(f_n)^{\text{exp}} - T(f_n)^{\text{theo}})/T(f_n)^{\text{exp}})^2 \quad (8a)$$

$$\tau^\phi = \frac{1}{N} \sum_{n=1}^N ((\Delta\phi(f_n)^{\text{exp}} - \Delta\phi(f_n)^{\text{theo}})/\Delta\phi(f_n)^{\text{exp}})^2, \quad (8b)$$

where  $f_n$  are the frequencies at which  $T$  and  $\Delta\phi$  are measured and  $N$  is the number of measurements (length of vector  $f_n$ ).

To improve this agreement, we changed the values of velocity, attenuation, thickness, and density; for each set of these values, we calculated  $T$  and then we estimated the quality of the agreement (8). The set of input parameters that maximizes this agreement is taken as the final result. To avoid having to change the four parameters simultaneously, which is a very time-consuming approach, we have designed a procedure based on the knowledge of the effect that each one of these parameters produces on  $T$ . So, this procedure has two main steps, in the first one only attenuation and density are changed, and (8a) is taken as the optimization criterion. In the second step, velocity and thickness are changed in such a way that we kept the location of the resonant frequency constant, and (8b) is taken as the optimization criterion. The procedure is shown in Fig. 1.

These operations are implemented in a Matlab function (The MathWorks, Natick, MA) loaded in the Windows-based (Microsoft Corp., Redmond, WA) oscilloscope used for the measurements; the function runs right after the measurement is taken, permitting us to obtain, practically in real time (run time about 1.0 s), the estimation of the leaf's effective parameters. The value of this simple fitting routine is that it runs fast enough so that the full resonance analysis can be performed *in situ* and almost in real time, and it is efficient enough so that it provides a satisfactory curve fitting for all measurements performed in this work. Our experience has shown that final results do not depend on the initial guess values, but that the time for the calculations increases when the initial guess is less accurate or when the interval for the variation of the magnitudes is enlarged.

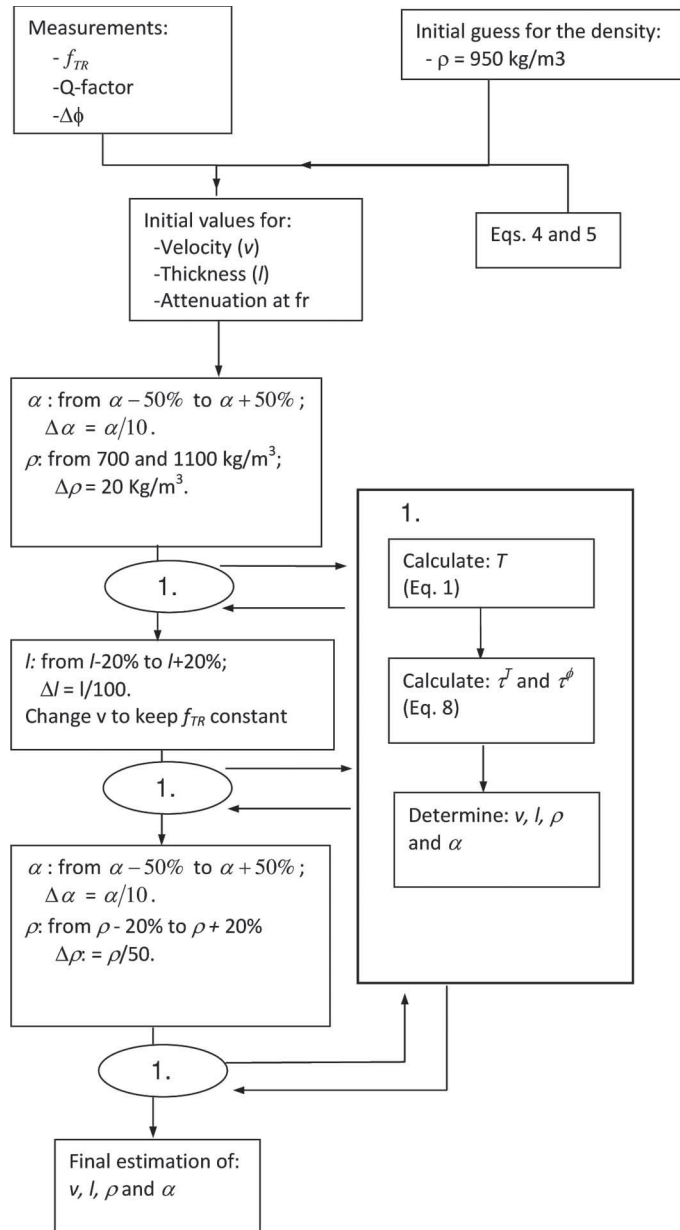


Fig. 1. Procedure to calculate the value of the velocity, the thickness, and the density, and the attenuation coefficient of the leaf from the measured magnitude and phase of the transmission coefficient and the theoretical expression of the transmission coefficient of a homogeneous plate.

### III. PLANT MATERIAL AND EXPERIMENTAL SETUP AND PROCEDURE

#### A. Plant Material and Conventional Measurements

The study was carried out using four different tree species: *Populus x euramericana*, *Prunus laurocerasus*, *Platanus hispanica*, and *Ligustrum lucidum*. A set of eight leaves per species was used for the measurements. Leaves were allowed to dry under environmental conditions; they were weighed and ultrasonically measured at constant time intervals and for a time period between 4 and 6 h. The measurements in this paper are represented in leaf RWC intervals. Within each interval, we only represent

the mean value and the error bars correspond to the standard deviation. RWC was measured as explained in [28].

The thickness of the leaves was measured through the desiccation process using a conventional micrometer and also by using a digital contact sensor GT-H10L coupled to an amplifier GT-75AP (GT Series, Keyence Corp., Osaka, Japan). To determine the density, 9 circular samples of each species (30 mm diameter) were cut. Thickness, diameter, and weight were measured throughout the desiccation process (12 to 15 measurements for each sample).

### B. Ultrasonic Measurements

The experimental procedure is based on a conventional through-transmission technique at normal incidence to measure the amplitude and the phase of the transmission coefficient in the frequency domain; toward this end, Fourier analysis is performed.

Ultrasonic measurements were performed using a pair of air-coupled piezoelectric transducers [32]. Two pairs of transducers with center frequencies of 0.25 and 1.0 MHz and circular aperture of 25 and 20 mm, respectively, were used for the evergreen and deciduous species, respectively. For a few measurements in some *Platanus hispanica* leaves at low RWC, it was necessary to use an additional pair of transducers with an intermediate center frequency at 0.5 MHz and 20 mm aperture diameter. For the study of plant leaves, the available frequency band for each pair of transducers is the band that fulfills that the SNR > 20 dB. This is, approximately, 0.19 to 0.34 MHz, 0.3 to 0.7 MHz, and 0.5 to 1.3 MHz for the 0.25-, 0.5-, and 1.0-MHz pairs of transducers, respectively. Transmitter and receiver transducers were located facing each other along the vertical at a distance of 2 to 4 cm (1 and 0.5 MHz) and 4 to 6 cm (0.25 MHz). A Panametrics P/R 5077 (Panametrics, Waltham, MA) was used to drive the transmitter and to amplify the received signal. A Tektronix 5052 oscilloscope (Beaverton, OR) was used to digitize the received signal. Scheme and further details of the experimental set-up can be found in [27] and [28]. Fig. 2 shows the through-transmitted signal (time and frequency domain) for the 1.0-MHz pair of transducers.

Air temperature and pressure were simultaneously measured. The velocity of sound in air ( $v_1$ ), the attenuation coefficient ( $\alpha_1$ ), and the air density ( $\rho_1$ ) were determined according to

$$v_1 = \left( 331.3 + \frac{T(\text{°C})}{1.6502(\text{°C})} \right) (\text{m/s}) \quad (9)$$

$$\alpha_1 (\text{dB/m}) = 1.6 \times 10^{-10}(f(\text{Hz}))^2 \quad (10)$$

$$\rho_1 = \frac{P}{RT}, \quad (11)$$

where  $P$  is the pressure,  $R$  is the gas constant, and  $T$  is the absolute temperature

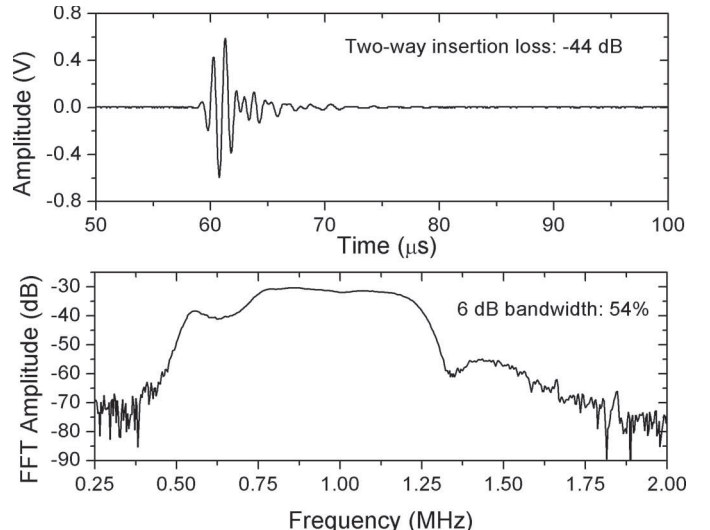


Fig. 2. Response (top: time domain; bottom: frequency domain) of the pair of transducers with center frequency at 1 MHz, separation 20 mm, excitation 200 V, 1 semicycle of a square wave, gain at reception 0 dB. Insertion loss is calculated from the ratio of the peak-to-peak voltage measured at the receiver transducer to the peak-to-peak voltage applied to the transmitter transducer.

## IV. EXPERIMENTAL RESULTS

### A. Thickness and Density

Thickness and density of the leaves were obtained using the proposed ultrasonic technique and also the conventional methods explained in Section II-A. The comparison is used as a test of the accuracy of the proposed ultrasonic technique. The results of both techniques are in agreement within the experimental error range. For one measurement on one particular leaf, typical deviation of ultrasonic and conventional thickness measurements is about 5 to 10  $\mu\text{m}$ , whereas typical deviation of ultrasonic and conventional density measurements is about 50 to 100  $\text{kg/m}^3$  (see [26]). For all the leaves of a given species at a given value of RWC, maximum observed standard deviation for the ultrasonic thickness and density measurements is  $\pm 50 \mu\text{m}$  and  $\pm 100 \text{ kg/m}^3$ , respectively. The large thickness standard variation reveals the fact that different leaves of a given species may have quite different thicknesses; however, variability of density measurements is much smaller. For all the species, the loss of water produces a reduction of the thickness. For a reduction of RWC from 1 to 0.75, the averaged thickness of *Prunus laurocerasus* leaves is reduced from 405 to 310  $\mu\text{m}$ ; for *Ligustum lucidum* leaves, an RWC reduction from 1 to 0.7 corresponds to a thickness reduction from 320 to 205  $\mu\text{m}$ ; for *Platanus hispanica* and *Populus x euroamericana* leaves, an RWC reduction from 1 to 0.6 produces a thickness reduction from 260 to 190  $\mu\text{m}$  and from 230 to 175  $\mu\text{m}$ , respectively.

This thickness reduction compensates the loss of mass of the leaf (resulting from the loss of water), hence the density remains rather constant with some local variations. Density of the *Prunus laurocerasus* leaves slightly

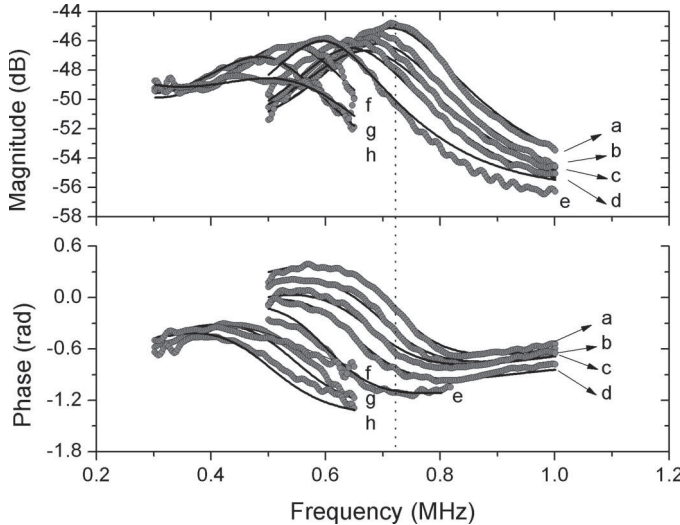


Fig. 3. Spectral response (top: magnitude; bottom: phase) of the first thickness resonance of a *Platanus hispanica* leaf at different values of the relative water content (RWC); a: 1.00, b: 0.97, c: 0.95, d: 0.94, e: 0.92, f: 0.85, g: 0.77, and h: 0.72.

increased from  $835 \text{ kg/m}^3$  (RWC = 1) to  $890 \text{ kg/m}^3$  (RWC = 0.75). Density of *Ligustrum lucidum* leaves increased from  $850 \text{ kg/m}^3$  (RWC = 1) to  $950 \text{ kg/m}^3$  (RWC = 0.7). Density of *Platanus hispanica* leaves first slightly decreased from  $820 \text{ kg/m}^3$  (RWC = 1) to  $780 \text{ kg/m}^3$  (RWC = 0.9) and then to  $670 \text{ kg/m}^3$  (RWC = 0.66). Finally, density of *Populus x euroamericana* slightly decreased from  $960 \text{ kg/m}^3$  (RWC = 1) to  $815 \text{ kg/m}^3$  (RWC = 0.63). These two parameters (thickness and density) can be hardly used to determine RWC because of the large variability of the thickness between different leaves of the same species and because of the very small variations in the density with the RWC.

#### B. Variation of the Spectra of the First Thickness Resonance

Magnitude and phase spectra of the transmission coefficient were measured along the desiccation process. Fig. 3 shows the theoretical (solid line) and experimental (dots) phase and magnitude spectra of the ultrasonic transmission coefficient versus frequency in the vicinity of the first thickness resonance at several values of RWC for one of the *Platanus hispanica* leaves measured. A similar behavior was observed for the other species. As the leaves lose water, the resonant frequency shifts toward lower frequencies and the damping increases. It is interesting to observe the low frequency location of the first thickness resonance, especially when considering the typical leaf thicknesses. This is due, as we will show, to a very low value of the propagation velocity, which originates from a very low value of the elastic constant resulting from the leaf's porosity and internal structure.

These spectra are processed according to the procedure previously outlined to obtain the variation with RWC in: 1) the relative displacement of the resonant frequency

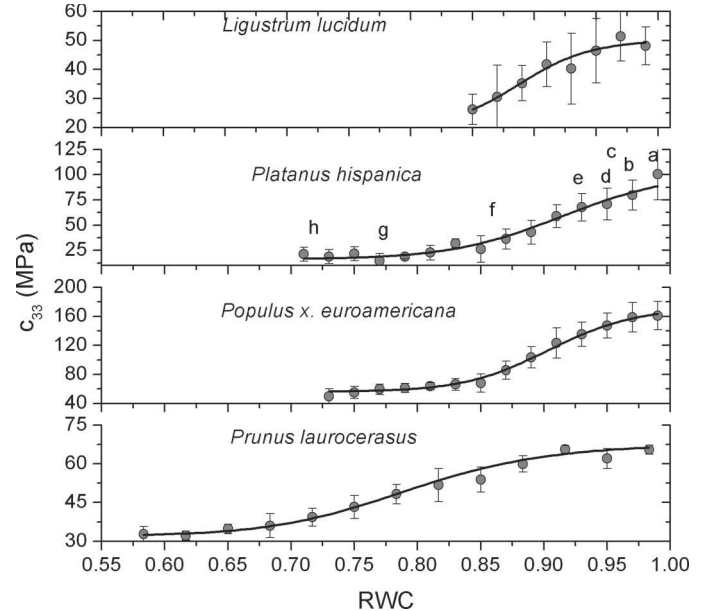


Fig. 4. Variation in the leaf's elastic constant in the thickness direction versus the relative water content (RWC). In the case of the *Platanus hispanica*, the letters a-h indicate the RWC location of the resonances shown in Fig 3.

$(\Delta f_{\text{TR}}/f_{\text{TR}}^0)$ ; 2) the leaf thickness; 3) the leaf density; 4) the velocity of ultrasound in the leaf; and 5) the attenuation coefficient of ultrasound in the leaf. From velocity and density data, the elastic constant is determined. The subsequent analysis of the results focuses on the elastic constant.

#### C. Variation in the Leaves Elastic Constant ( $c_{33}$ ) With RWC

Calculated  $c_{33}$  are shown in Fig. 4. A sigmoid-like behavior is observed, which is typical of a transition between two states (wet and dry in this case). This sigmoid evolution has also been previously observed in  $\Delta f_{\text{TR}}/f_{\text{TR}}^0$  versus RWC graphs ([27], [28]).

The observed total variations in  $c_{33}$  with RWC (that is, from wet to dry states) are larger than the variations observed in  $\Delta f_{\text{TR}}/f_{\text{TR}}^0$  (14% to 37%) or in the ultrasound velocity (35% to 49%) because the influence of the thickness and the density is eliminated for the  $c_{33}$  measurements. This result suggests that this parameter can provide a better way to estimate the RWC of the leaves.

In addition, a common trend of the variation in  $c_{33}$  depending on the leaf phenology is observed: the largest relative variation in  $c_{33}$  is observed in the deciduous species (85% and 68%, for *Platanus hispanica* and *Populus x. euroamericana*, respectively, and 53% and 59% for the evergreen species *Prunus laurocerasus* and *Ligustrum lucidum*). This difference could be explained by the more resistant leaves required by the evergreen species.

Previous works have demonstrated that the point of inflection of  $\Delta f_{\text{TR}}/f_{\text{TR}}^0$  versus RWC graphs corresponds to the point of null turgor pressure obtained from pressure-

TABLE I. LOCATION OF THE INFLECTION POINT, STANDARD ERROR, AND COEFFICIENT OF DETERMINATION OF THE FITTING ( $R^2$ ) OF THE  $c_{33}$  VERSUS RELATIVE WATER CONTENT (RWC) AND  $\Delta f_{\text{TR}}/f_{\text{TR}}^0$  VERSUS RWC CURVES.

	$x_0 = \text{RWC}_0$ .	$R^2$
<i>Prunus laurocerasus</i>		
$c_{33}$	$0.790 \pm 0.013$	0.99
$\Delta f_{\text{r}}/f_{\text{r}}^0$	$0.828 \pm 0.011$	0.93
<i>Platanus hispanica</i>		
$c_{33}$	$0.918 \pm 0.034$	0.92
$\Delta f_{\text{r}}/f_{\text{r}}^0$	$0.896 \pm 0.004$	0.99
<i>Ligustrum lucidum</i>		
$c_{33}$	$0.890 \pm 0.019$	0.96
$\Delta f_{\text{r}}/f_{\text{r}}^0$	$0.905 \pm 0.008$	0.99
<i>Populus x euroamericana</i>		
$c_{33}$	$0.905 \pm 0.008$	0.99
$\Delta f_{\text{r}}/f_{\text{r}}^0$	$0.895 \pm 0.003$	0.99

volume relationships determined by the free-transpiration method [27]; given the special significance of this point in terms of leaf physiology, it is of interest to obtain a measurement of the location of this point in the  $c_{33}$  versus RWC curves. Toward this end, the sigmoid-growth function

$$y = y_U + \frac{y_L - y_U}{1 + (x/x_0)^p} \quad (12)$$

is used, where  $x_0$  corresponds to the point of inflection and  $y_U$  and  $y_L$  are the upper and the lower bounds of  $y$ , respectively.

Table I shows the obtained parameters from these fittings. For purposes of comparison, the parameters obtained for the  $\Delta f_{\text{TR}}/f_{\text{TR}}^0$  versus RWC curves are also shown. The obtained location of  $\text{RWC}_0$  according to both measurements is similar, which is an expected result because the dominant factor in the variation in  $\Delta f_{\text{TR}}/f_{\text{TR}}^0$  with RWC is the variation of the leaf elastic constants ( $f_{\text{TR}} = 1/2l\sqrt{c_{33}/\rho}$ ). The advantage of using  $c_{33}$  instead of  $\Delta f_{\text{TR}}/f_{\text{TR}}^0$  is two-fold:  $c_{33}$  measurements are more sensitive and they do provide a correlation between the absolute value of the two magnitudes (RWC and  $c_{33}$ ), and not a correlation between relative variations.  $\text{RWC}_0$  data in Table I also show a good agreement with  $\text{RWC}_0$  data for *P. laurocerasus* and *P. x euroamericana* obtained from pressure-volume relationships determined by the free-transpiration method [27].

## V. CONCLUSIONS

This paper demonstrates that magnitude and phase spectra of the thickness resonances of plant leaves, excited and sensed using air-coupled piezoelectric transducers, can be well described by an effective medium approach, and that this can be used to obtain, among other leaf properties, the elastic constant in the thickness direction ( $c_{33}$ ), which provides a very good indicator of the leaf status.

The known low values of ultrasound velocity in plant leaves (from 150 to 300 m/s) are explained by the very low value of the elastic constant ( $c_{33}$ ) measured in this work. This is due to both the porosity and the microstructure of the leaves. The overall or macroscopic deformation of this microstructure is made of local bending and twisting of the microscopic components (fibers and cells), which are similar to those found in cellular solids; this gives rise to very low values of the  $c_{33}$ , even for intermediate porosity values [33].

The elastic constant,  $c_{33}$ , decreases when the leaves lose water, following a sigmoid shape; this can be attributed to the loss of tension in the cell membranes and by the deformation of the cell structure. Observed relative variations in  $c_{33}$  are larger than the observed variations in the resonant frequency ( $\Delta f_{\text{TR}}/f_{\text{TR}}^0$ ), the velocity, the density, or the thickness, so monitoring of  $c_{33}$ -variations can be a better procedure to determine the RWC of leaves.

The sigmoid-like variation in  $c_{33}$  with RWC is very similar to that observed for the variation in  $\Delta f_{\text{TR}}/f_{\text{TR}}^0$  with RWC and the point of inflection of both curves is located at approximately the same RWC value. This is an expected result because eventually  $\Delta f_{\text{TR}}/f_{\text{TR}}^0$  depend on  $c_{33}$  and this is the dominant factor in the variation in  $\Delta f_{\text{TR}}/f_{\text{TR}}^0$  with RWC. Considering the intrinsic complexity in the biological nature of plant leaves, each species should be treated as a different problem and should be carefully checked; however, for the cases studied thus far, the point of turgor loss can be ultrasonically determined and the best technique, because it provides better sensitivity and absolute values, is the one based on the measurement of the point of inflection in the variation of the elastic constant ( $c_{33}$ ) versus RWC curve.

## REFERENCES

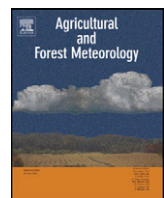
- [1] O. R. Gericke, "Determination of the geometry of hidden defects by ultrasonic pulse analysis testing," *J. Acoust. Soc. Am.*, vol. 35, no. 3, pp. 364–368, 1963.
- [2] N. F. Haines, J. C. Bell, and P. J. McIntyre, "The application of broadband ultrasonic spectroscopy to the study of layered materials," *J. Acoust. Soc. Am.*, vol. 64, no. 6, pp. 1645–1651, 1978.
- [3] W. Sachse and H. Y. Pao, "On the determination of phase and group velocities of dispersive waves in solids," *J. Appl. Phys.*, vol. 49, no. 8, pp. 4320–4327, 1978.
- [4] R. A. Kline, "Measurement of attenuation and dispersion using an ultrasonic spectroscopy technique," *J. Acoust. Soc. Am.*, vol. 76, no. 2, pp. 498–504, 1984.
- [5] T. Pialucha, C. C. H. Guyott, and P. Cawley, "Amplitude spectrum method for the measurement of phase velocity," *Ultrasonics*, vol. 27, no. 5, pp. 270–279, 1989.
- [6] M. Luukkala, P. Heikkila, and J. Surakka, "Plate wave resonance—A contactless test method," *Ultrasonics*, vol. 9, no. 4, pp. 201–208, 1971.
- [7] D. A. Hutchins, W. M. D. Wright, and D. W. Schindel, "Ultrasonic measurements in polymeric materials using air-coupled capacitance transducers," *J. Acoust. Soc. Am.*, vol. 96, no. 3, pp. 1634–1642, 1994.
- [8] D. W. Schindel and D. A. Hutchins, "Through-thickness characterization of solids by wideband air-coupled ultrasound," *Ultrasonics*, vol. 33, no. 1, pp. 11–17, 1995.
- [9] P. B. Nagy, "Slow wave propagation in air-filled permeable solids," *J. Acoust. Soc. Am.*, vol. 93, no. 6, pp. 3224–3234, 1993.

- [10] T. E. Gómez Álvarez-Arenas, L. Elvira-Segura, and E. Riera Franco de Sarabia, "Generation of the slow wave to characterize air-filled porous fabrics," *J. Appl. Phys.*, vol. 78, no. 4, pp. 2843–2845, 1995.
- [11] B. Hosten, D. A. Hutchins, and D. W. Schindel, "Measurement of elastic constants in composite materials using air-coupled ultrasonic bulk waves," *J. Acoust. Soc. Am.*, vol. 99, no. 4, pp. 2116–2123, 1996.
- [12] F. Lionetto, A. Tarzia, and A. Maffezzoli, "Air-coupled ultrasound: A novel technique for monitoring the curing of thermosetting matrices," *IEEE Trans. Ultrason. Ferroelectr. Freq. Control*, vol. 54, no. 7, pp. 1437–1444, 2007.
- [13] S. Dahmen, H. Ketata, M. H. Ben Ghzlen, and B. Hosten, "Elastic constants measurement of anisotropic Olivier wood plates using air-coupled transducers generated Lamb wave and ultrasonic bulk wave," *Ultrasonics*, vol. 50, no. 4–5, pp. 502–507, 2010.
- [14] S. P. Kelly, G. Hayward, and T. E. Gómez, "An air-coupled ultrasonic matching layer employing half wavelength cavity resonance," in *Proc. IEEE Ultrasonics Symp.*, 2001, pp. 965–968.
- [15] T. E. Gómez Álvarez-Arenas, "Air-coupled ultrasonic spectroscopy for the study of membrane filters," *J. Membr. Sci.*, vol. 213, no. 1–2, pp. 195–207, 2003.
- [16] T. E. Gómez Álvarez-Arenas, "A nondestructive integrity test for membrane filters based on air-coupled ultrasonic spectroscopy," *IEEE Trans. Ultrason. Ferroelectr. Freq. Control*, vol. 50, no. 6, pp. 676–685, 2003.
- [17] T. E. Gómez Álvarez-Arenas, F. Montero, M. Moner, E. Rodríguez, A. Roig, and E. Molins, "Viscoelasticity of silica aerogels at ultrasonic frequencies," *Appl. Phys. Lett.*, vol. 81, no. 7, pp. 1198–1200, 2002.
- [18] I. Akseli and C. Cetinkaya, "Air-coupled non-contact mechanical property determination of drug tablets," *Int. J. Pharm.*, vol. 359, no. 1–2, pp. 25–34, 2008.
- [19] T. E. Gómez Álvarez-Arenas, "Simultaneous determination of the ultrasound velocity and the thickness of solid plates from the analysis of thickness resonances using air-coupled ultrasound," *Ultrasonics*, vol. 50, no. 2, pp. 104–109, 2010.
- [20] T. E. Gómez Álvarez-Arenas, H. Calás, J. Ealo Cuello, A. Ramos Fernández, and M. Muñoz, "Noncontact ultrasonic spectroscopy applied to the study of polypropylene ferroelectrets," *J. Appl. Phys.*, vol. 108, no. 7, art. no. 074110, 2010.
- [21] T. Gómez Álvarez-Arenas, J. Benedito, and E. Corona, "Non-contact ultrasonic assessment of the properties of vacuum-packaged dry-cured ham," in *Proc. IEEE Ultrasonics Symp.*, 2009, pp. 2541–2544.
- [22] P. F. Scholander, H. T. Hammel, E. D. Bradstreet, and E. A. Hemmingsen, "Sap pressure in vascular plants," *Science*, vol. 148, no. 3668, pp. 339–346, 1965.
- [23] D. Zimmermann, R. Reuss, M. Westhoff, P. Geßner, W. Bauer, E. Bamberg, F.-W. Bentrup, and U. Zimmermann, "A novel, non-invasive, online-monitoring, versatile and easy plant-based probe for measuring leaf water status," *J. Exp. Bot.*, vol. 59, no. 11, pp. 3157–3167, 2008.
- [24] P. S. Wilson and K. H. Dunton, "Laboratory investigation of the acoustic response of seagrass tissue in the frequency band 0.5–2.5 kHz," *J. Acoust. Soc. Am.*, vol. 125, no. 4, pp. 1951–1959, 2009.
- [25] M. Fukuhara, "Acoustic characteristics of botanical leaves using ultrasonic transmission waves," *Plant Sci.*, vol. 162, no. 4, pp. 521–528, 2002.
- [26] T. E. Gómez Álvarez-Arenas, D. Sancho-Knapik, J. J. Peguero-Pina, and E. Gil-Pelegrín, "Noncontact and noninvasive study of plant leaves using air-coupled ultrasounds," *Appl. Phys. Lett.*, vol. 95, no. 19, art. no. 193702, 2009.
- [27] D. Sancho-Knapik, T. E. Gómez Álvarez-Arenas, J. J. Peguero-Pina, and E. Gil-Pelegrín, "Air-coupled broadband ultrasonic spectroscopy as a new non-invasive and non-contact method for the determination of leaf water status," *J. Exp. Bot.*, vol. 61, no. 5, pp. 1385–1391, 2010.
- [28] D. Sancho-Knapik, T. E. Gómez Álvarez-Arenas, J. J. Peguero-Pina, and E. Gil-Pelegrín, "Relationship between ultrasonic properties and structural changes in the mesophyll during leaf dehydration," *J. Exp. Bot.*, vol. 62, no. 10, pp. 3637–3645, 2011.
- [29] T. E. Gómez Álvarez-Arenas, D. Sancho-Knapik, J. J. Peguero-Pina, and E. Gil-Pelegrín, "Determination of plant leaves water status using air-coupled ultrasounds," in *Proc. IEEE Ultrasonics Symp.*, 2009, pp. 771–774.
- [30] L. M. Brekhovskikh, *Waves in Layered Media*. New York, NY: Springer, 1960.
- [31] J. Stor-Pellinen, E. Häggström, T. Karppinen, and M. Luukkala, "Air-coupled ultrasonic measurement of the change in roughness of paper during wetting," *Meas. Sci. Technol.*, vol. 12, no. 8, pp. 1336–1341, 2001.
- [32] T. E. Gómez Álvarez-Arenas, "Acoustic impedance matching of piezoelectric transducers to the air," *IEEE Trans. Ultrason. Ferroelectr. Freq. Control*, vol. 51, no. 5, pp. 624–633, 2004.
- [33] L. J. Gibson and M. F. Ashby, *Cellular Solids*. New York, NY: Cambridge Univ. Press, 1997.





Contents lists available at ScienceDirect

**Agricultural and Forest Meteorology**journal homepage: [www.elsevier.com/locate/agrformet](http://www.elsevier.com/locate/agrformet)**Microwave L-band (1730 MHz) accurately estimates the relative water content in poplar leaves. A comparison with a near infrared water index ( $R_{1300}/R_{1450}$ )**

Domingo Sancho-Knapik<sup>a</sup>, Javier Gismero<sup>b</sup>, Alberto Asensio<sup>b</sup>, José Javier Peguero-Pina<sup>c</sup>, Victoria Fernández<sup>d</sup>, Tomás Gómez Álvarez-Arenas<sup>e</sup>, Eustaquio Gil-Pelegrín<sup>a,\*</sup>

<sup>a</sup> Unidad de Recursos Forestales, Centro de Investigación y Tecnología Agroalimentaria, Avda. Montaña, 930, Gobierno de Aragón, 50059 Zaragoza, Spain

<sup>b</sup> Univ Politecn Madrid, Grp Microondas & Radar, Dept Señales Sistemas & Radiocomunicac, E-28040 Madrid, Spain

<sup>c</sup> Departament de Biología, Universitat de les Illes Balears, Carretera de Valldemossa, km 7.5, 07071, Palma de Mallorca, Balears, Spain

<sup>d</sup> Forest Genetics and Ecophysiology Research Group, E.T.S. Forest Engineering, Technical University of Madrid, Ciudad Universitaria s/n, 28040 Madrid, Spain

<sup>e</sup> Departamento de Señales, Sistemas y Tecnologías Ultrasónicas. Instituto de Acústica, C.S.I.C., 28002 Madrid, Spain

**ARTICLE INFO****Article history:**

Received 11 June 2010

Received in revised form 19 January 2011

Accepted 27 January 2011

**Keywords:**

L-band

Microwaves

Near infrared reflectance

Plant water status

Poplar clones

**ABSTRACT**

In this study the estimation of reflectivity at 1730 MHz (L-band), measured with a microwave digital cordless telephony (DCT) patch antenna, is presented as an easy-to-handle and non-destructive new method to assess the relative water content (RWC) of poplar leaves and filter discs at different levels of dehydration. The accuracy of this new method has been contrasted with the  $R_{1300}/R_{1450}$  index, determined by a portable near infrared (NIR) spectrometer. The close correlations found between RWC and the reflectivity at a frequency of 1730 MHz, both for filters and leaves, indicate that microwave determinations are rather independent of the physical properties of the material analysed. On the contrary, the differences found between poplar leaves and leaf filters in the relationships established between RWC and the  $R_{1300}/R_{1450}$  index demonstrate a strong influence of the properties of the material in NIR reflectance measurements, specifically as they relate to changes in leaf thickness during dehydration. It should be noted that the amount of energy received by the leaf for the microwave technique (0.1 mW) was much lower than that received for the measuring of the  $R_{1300}/R_{1450}$  index (2.5 W). Moreover, *R*-square coefficients were higher for microwaves than for the  $R_{1300}/R_{1450}$  index. The use of a technologically simple, low cost and portable device, based on a microwave DCT patch antenna, could yield a solid support for the development of a commercial apparatus enabling the determination of plant water status under field conditions.

© 2011 Elsevier B.V. All rights reserved.

**1. Introduction**

Poplars can be considered one of the main agro-forestry resources for biomass production (Meiresonne et al., 1999) and carbon sequestration (McKenney et al., 2004). Specifically, these species have been widely planted and cultivated in southern Europe (Sixto et al., 2007). The existence of atmospheric drought prevailing during the vegetative period in many arid or semi-arid regions of the world, increase significantly the rate of water consumption by the plant (Tognetti et al., 2009). Therefore, many commercial tree plantations are frequently irrigated in order to maintain the physiological activity and achieve a good production (Migliavacca et al.,

2009). To prevent excessive water consumption in a global scene of decreased water availability, several methods have been developed to maximize the water use efficiency in agricultural and horticultural crops, highlighting the need for new methods of accurate irrigation scheduling and control (Jones, 2004). It has been suggested that the use of plant "stress sensing" including both water status and plant response measurements are the main approaches to implement adequate irrigation scheduling, rather than only estimating the soil moisture status directly (Jones, 1990, 2004, 2007).

Assessment of plant water status can be achieved via measuring the energy status (e.g., water potential) or by monitoring the amount of water (i.e., relative water content) (Jones, 2007). On the other hand, direct estimation of plant stress sensing can be carried out by evaluating physiological parameters based on stomatal closure, such as by porometry (Vilagrosa et al., 2003), by thermal imaging (Grant et al., 2006; Suarez et al., 2009), or by assessing the development of energy dissipation mechanisms which induce spectral reflectance changes around the green part of the spectrum (Peguero-Pina et al., 2008; Suarez et al., 2009).

**Abbreviations:** DCT, digital cordless telephony; MWR<sub>1730</sub>, microwave reflectivity at 1730 MHz (L-band); NIR, near infrared; PLT, percentage of loss of thickness; R, reflectance; RWC, relative water content.

\* Corresponding author. Tel.: +34 976 716394; fax: +34 976 716335.

E-mail address: egilp@aragon.es (E. Gil-Pelegrín).

Alternative methods for plant stress sensing based on the response of the plant material to a certain stimulus have also been proposed, since the physical properties of plant tissues have been found to vary according to the degree of hydration. In this way, Gómez Álvarez-Arenas et al. (2009) and Sancho-Knapik et al. (2010) suggested that ultrasound resonances are sensitive to leaf microstructure and water content, and they provided evidence that changes in leaf relative water content and water potential can be accurately estimated by the corresponding changes in the acoustic properties of the leaf.

A more classical approach is based on the study of near infrared reflectance (NIR) and, specially, the so-called water bands. Carter (1991) and Carter and McCain (1993) found that a decrease in leaf water content was generally associated with an increase in reflectance throughout the 400–2500 nm wavelength range spectrum. Since then, several authors employed different techniques concerning infrared frequencies (e.g. Peñuelas et al., 1993; Seelig et al., 2008a,b; Sims and Gamon, 2003). More recently, Wu et al. (2009) used normalized indices based on reflectance ( $R$ ) at 1200, 1450 and 1950 nm and related them to the vegetation water content at the leaf scale. Following a similar procedure, Seelig et al. (2009) obtained a correlation for the ratio of reflectances between 1300 and 1450 nm ( $R_{1300}/R_{1450}$  index) and the relative water content (RWC) of cowpea and bean leaves. Although Seelig et al. (2009) concluded that the  $R_{1300}/R_{1450}$  index may be used as feedback-signal in precision irrigation control, they pointed out that IR reflectances are influenced by leaf thickness, which implies that this should be taken into account during the measurements. Recent advances in infrared technologies may lead to the widespread use of this technique as a tool to measure leaf water status. Stemming from the complex and fairly expensive equipment mainly designed for laboratory use, some portable and more affordable models are nowadays available, which allow to work at the same wavelength even under field conditions (Zimmer et al., 2004).

Lower electromagnetic frequency ranges for measuring plant water status have also been tested (Jördens et al., 2009). A time domain reflectometry (TDR) method to estimate leaf disk water status was implemented by Martínez et al. (1995). Measurements were carried out on the X-band (7–12 GHz) using a complex and expensive laboratory equipment. The low dynamic margin of an oscilloscope may limit the application of the method, since lower magnitudes cannot be accurately determined. More recently, Menzel et al. (2009) described a non-invasive technique based on measuring dielectric properties changes in a microwave cavity resonator induced by the plant material inserted inside the system. Such method enabled measuring the water content of the whole plant, but it involved certain drawbacks associated with the complexity of the experimental set up and its low portability, which prevented this technique from being used for measuring dynamic changes in single leaves and from use under field conditions.

In spite of the good results obtained by Martínez et al. (1995) and Menzel et al. (2009) relating to the use of microwaves to estimate plant water status, the complexity of the experimental set up prevented the applicability of such methods for the development of practical tools to characterize plant water status under field conditions so far. Therefore, the main objective of this study was to combine the potential effectiveness of the frequency range of microwaves with a technology simple and portable device. For this purpose a microwave digital cordless telephony (DCT) patch antenna, commonly used in mobile phone technology was employed to measure the reflectivity at a frequency of 1730 MHz (hereafter MWR<sub>1730</sub>) of poplar leaves at different RWC. A second objective was to compare the accuracy of the new method with the  $R_{1300}/R_{1450}$  index for the same materials, as measured by a portable NIR spectrometer.

## 2. Materials and methods

### 2.1. Plant material

Measurements were performed on mature *Populus × euramericana* (Dode.) Guinier leaves. In the early morning, branches were collected from the north side of the trees, placed in plastic bags and carried to the laboratory. Once there, leaf petioles were re-cut under water to avoid embolism and kept immersed until full leaf rehydration for 24 h at 4 °C. Special care was taken to prevent leaf oversaturation, by detecting eventual water outflow from the sample when water potential ( $\Psi$ ) was equal to zero (Kubiske and Abrams, 1991). After rehydration, one set of ten leaves was destined for the measurement with the microwave technique and other set of ten leaves used for NIR measurements. Leaves were weighed and measured at constant time intervals at different levels of RWC, starting at full saturation (turgid weight, TW). Leaf dry weight (DW) was estimated after keeping the plant material in a stove (24 h, 60 °C). The RWC was then calculated following the expression:  $RWC = (FW - DW)/(TW - DW)$ , being FW the sample fresh weight.

In addition, all the measurements described in this study were also performed on filter papers (homogeneous cellulosic material; Whatman 3; diameter 125 mm; thickness 0.39 mm). Three millilitres of DI water were added to each filter in order to achieve a full water saturation state. Immediately thereafter, filters were introduced in a water-saturated atmosphere at room temperature. Twenty four hours later, one set was measured by the microwave technique while the other was assessed by IR following exactly the same procedure as described above for plant leaves. The disc weight after saturation (SW), the disc fresh weight (FW) and the oven-dried disc weight (after 24 h, 60 °C) were used for the calculation of a RWC equivalent to that calculated for leaves.

### 2.2. The microwave digital cordless telephony (DCT) patch antenna technique: experimental set-up and procedure

The set up consisted of a microwave generator (oscillator), which feeds its signal to the antenna through a splitter device (3 dB hybrid coupler). The splitter allows to obtain at its output two identical signals with respect to power (half of the input power), but with a phase difference of 90° (Fig. 1). The following basic properties of this splitter must be taken into consideration:

- The generator is always loaded with the same impedance, meaning it always delivers the same power to the splitter–antenna set.
- Power fed into the antenna through the two output branches of the splitter is ideally radiated (ideal situation in which the antenna is perfectly matched to the splitter) using a  $50\Omega$  reference impedance.
- Possible power reflections from the antenna back to the splitter at ports 2 and 3 (Fig. 1) are fully routed to port 4, which can be measured, for instance, with a rectifier diode.

In practice, elements inside the dashed box (Fig. 1) are an integral part of a typical microwave instrument: a vector network analyzer (VNA; E8364A 45 MHz to 50 GHz, PNA Series, Agilent Technologies Inc., Santa Clara, USA). This instrument feeds microwave energy into port 1 and allows the simultaneous measurement of both, the power reflected at port 1 (splitter matching) and the power flowing in port 4 (power reflected from the antenna). In a first calibration process, it was checked that the antenna was working properly at the desired frequency which implied that both powers must be low enough (i.e., the generator delivers its power and there is no reflection).

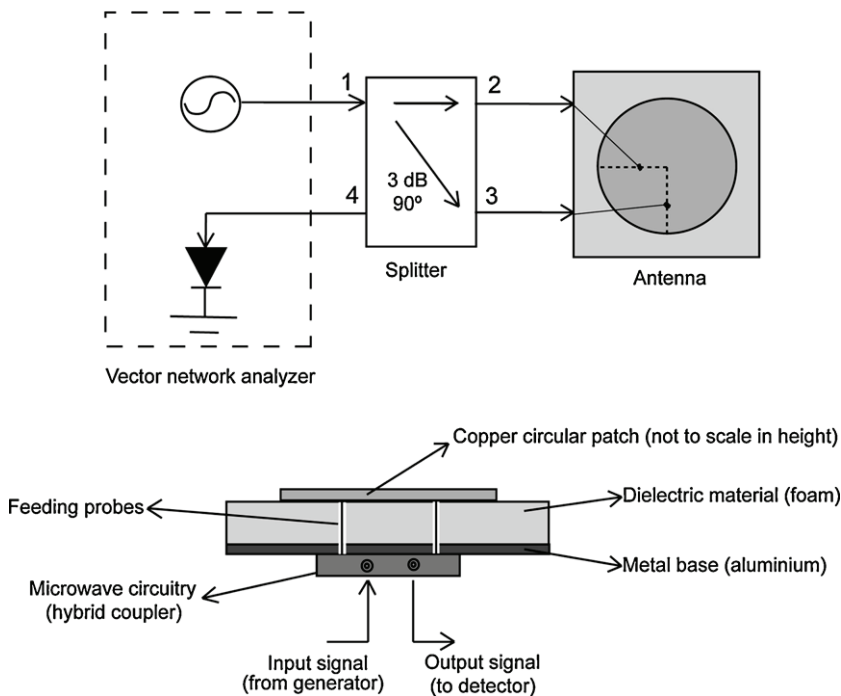


**Fig. 1.** Schematic representation of the experimental set-up of the microwave patch antenna technique.

After calibration, and with no material under test being present at the microwave patch antenna, the impedance of the antenna is perfectly matched to the main circuitry. Under this condition, no electrical wave reflections will occur within the circuitry, and the corresponding electrical reflectivity coefficient, as determined by the VNA, will be low. The presence of water at the vicinity of the antenna, however, will alter the antenna's impedance. The resulting mismatch of impedances is produced by inserting a thin tissue (the sample) with a different dielectric constant from the one the antenna was designed for (air). The value of the sample dielectric constant is highly influenced by its water content (Martínez et al., 1995), so the corresponding VNA reflectivity coefficient will be a direct function of the amount of water being present at or near the antenna.

### 2.3. Measured parameters

The  $R_{1300}/R_{1450}$  index ( $R_{1300}/R_{1450}$ ), which was used as NIR parameter, measures the proportion of light that is reflected from leaves, i.e., leaf reflectance at the spectral region around 1450 nm with respect to the spectral region at approximately 1300 nm (Seelig et al., 2009). These reflectances were obtained by illuminating the leaves using a Polychromix MobiLight light source (500 mA, 2.5 W, Polychromix, USA) and measuring the spectral reflectance region from 930 to 1690 nm using a Polychromix DTS NIR Spectrometer (Polychromix, USA). On the other hand, the parameter  $MWR_{1730}$ , which was determined by the microwave DCT patch antenna technique, is the reflectance coefficient at 1730 MHz, frequency commonly used in DCT antennae (see the experimental set-up described above for details).

The possible influence of the sample thickness on the  $R_{1300}/R_{1450}$  index at different levels of RWC (Seelig et al., 2009), both in leaves and filter discs, was estimated by measuring the thickness through the dessication process by using a digital contact sensor GT-H10L coupled to an amplifier GT-75AP (GT Series, Keyence Corporation, Japan). This ultra-low force sensor (having a measuring force of 0.2 N when installed facing up) applies a clamp pressure of 7 kPa, which is ca. 10 times lower than the one used by Zimmermann

et al. (2008) for similar purposes. Thereby, it is ensured that leaf thickness measurements were not disturbed due to an excess of pressure applied to the leaf. Leaf thickness was standardized calculating the percentage loss of thickness (PLT) per sample, expressed as the ratio between the thickness measured for every particular RWC and the thickness determined at full turgor.

### 2.4. Statistical analysis

For leaves and filters, RWC was plotted against both,  $R_{1300}/R_{1450}$  and  $MWR_{1730}$  values. Data were fitted to models and regression analyses were performed with the statistical programme SAS version 8.0 (SAS, Cary, NC, USA).

## 3. Results

In Fig. 2 data concerning the relationships between  $R_{1300}/R_{1450}$  against the RWC (Fig. 2A) and  $MWR_{1730}$  against the RWC (Fig. 2B) for the filter paper discs are presented. Data were fitted to an exponential model for the filters measured by NIR and to a linear model for the results derived from the microwave technique.

Values from poplar leaves measured with NIR reflectance were fitted to a linear segmented model because it explained the variability of the measured data better than a simple model (Fig. 3A). On the other hand, those values obtained by the microwave technique were subjected to a linear model (Fig. 3B). The segmented model in Fig. 3A is a non-linear model that fits a curve compound of two lineal models with different slopes. The point at which the switch between the two functions occurs is called a joint-point (Schabenberger and Pierce, 2002). In this case the RWC value of the joint-point calculated was  $0.917 \pm 0.022$ . From this value to a value of  $RWC = 1$ , the slope of the lineal model was approximately zero while the slope of the other lineal model (from  $RWC = 0.917$  to 0.250) was 3.39.

Fig. 4 shows the relationship between RWC and the PLT of samples (either leaves or filter paper discs). For both, filter papers and leaves, it was observed that leaf thickness decreased as a result of a decrease in RWC. For filter papers, the PLT decreased linearly

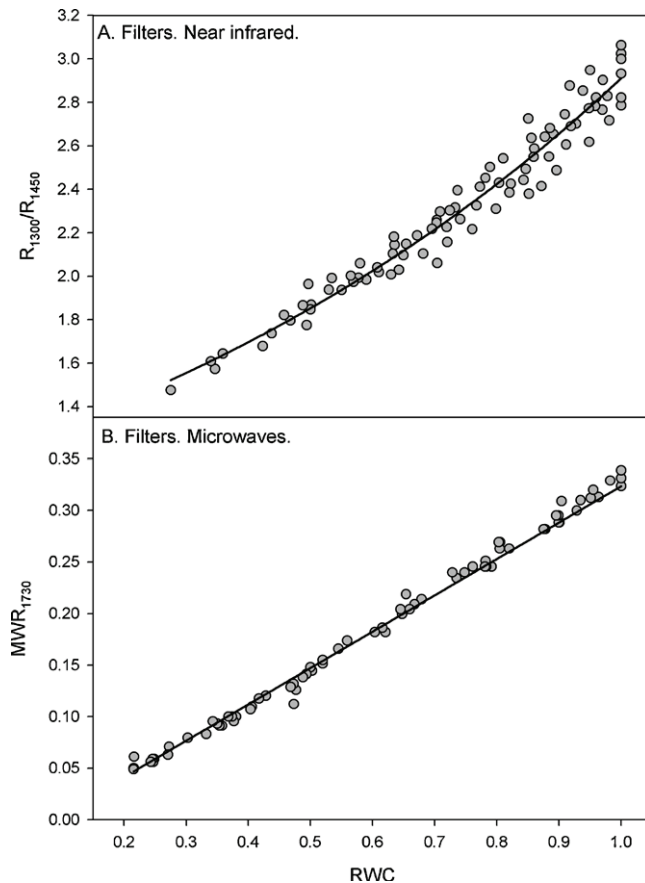


**Fig. 2.** Relationships between the relative water content (RWC) and (A) the  $R_{1300}/R_{1450}$  index for NIR and (B)  $MWR_{1730}$  for microwaves measured on filter paper discs.

ranging from 1 to 0.9 for a decrease in RWC between 1 to approximately 0.25. However, such correlation was not linear for leaves. For the same RWC range indicated above, the decrease in PLT varied between 1 and 0.72.

The regression coefficients of the relationships established for filter papers and leaves are presented in Table 1. For filters, the coefficient correlation ( $R^2$ ) obtained for NIR was 0.96 ( $p < 0.0001$ ) (Fig. 2A), while the resulting  $R^2$  for the data recorded by the microwave technique (Fig. 2B) was 0.99 ( $p < 0.0001$ ). For leaves, the  $R^2$  recorded by NIR (Fig. 3A), was 0.94 ( $p < 0.0001$ ) while the  $R^2$  for the data recorded by the microwave method (Fig. 3B) was 0.98 ( $p < 0.0001$ ). In addition, results indicate that for the microwave technique higher  $F$ -ratios and lower standard errors (SE) of the estimation were recorded in contrast to the NIR method.

**Table 1**

Statistical parameters of the relationships between the relative water content and the near infrared (NIR) or Microwave, either for filter papers and leaves.  $n$  is the number of data points observed;  $F$ -ratio is the ratio of the variance explained by a factor to the unexplained variance;  $R^2$  is the  $R$ -squared; S.E. of Est. is the standard error of the estimation.

	Filter papers		Poplar leaves	
	NIR	Microwave	NIR	Microwave
$n$	87	81	137	124
$F$ -ratio	2289	14703	728	7548
$p$ -Value	<0.0001	<0.0001	<0.0001	<0.0001
$R^2$	0.9642	0.9951	0.9426	0.9849
S.E. of Est.	0.03253	0.00651	0.0219	0.00394

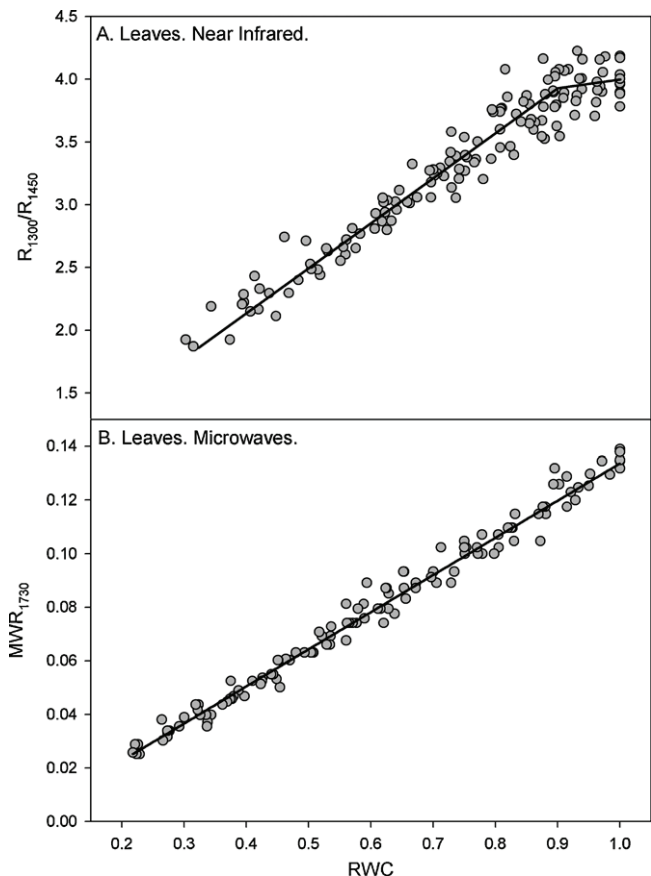


**Fig. 3.** Relationships between the relative water content (RWC) and (A) the  $R_{1300}/R_{1450}$  index for NIR and (B)  $MWR_{1730}$  for microwaves measured on poplar leaves.

#### 4. Discussion

In this study, an easy-to-handle and non-destructive microwave-based technique for the estimation of water content of a material was investigated, with special regard to plant leaves. An experimental set up mainly composed by a standard DTC antenna and a network vector analyser was used to estimate the water content of an homogeneous (filter paper discs)

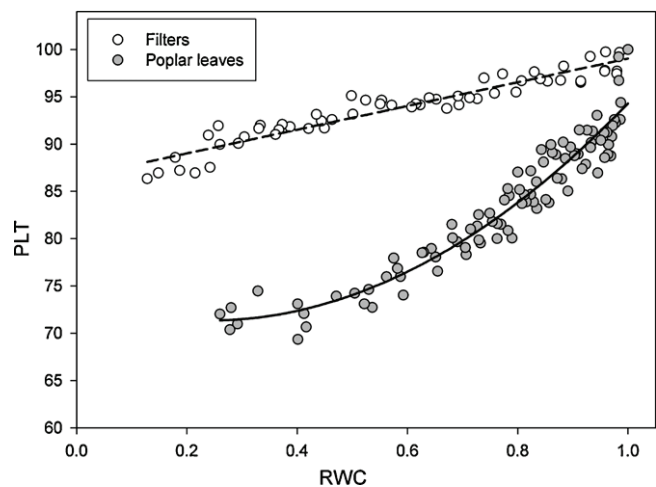


**Fig. 4.** Relationship between the relative water content (RWC) and the percentage loss of thickness (PLT) for filter papers and poplar leaves.

and an heterogeneous (*Populus × euramericana* leaves) material, contrasting the results with the  $R_{1300}/R_{1450}$  index.

The method assessed the dielectric property of the two materials analysed and established very good correlations between RWC and reflectance at a frequency of 1730 MHz, both for filters and leaves, using a very low amount of energy (0.1 mW). Although leaves are more heterogeneous than filters, the accuracy of microwaves for the estimation of RWC was almost the same for both materials (Table 1). The small differences found could be attributable to the irregular structure of plant leaves, in contrast to the structural homogeneity of the filters used in this study. In spite of this fact, the technique may be considered quite independent of the physical properties of the material.

The frequency employed in this investigation is included in the L-band of the microwave spectrum, which has been previously used for remote sensing studies of the vegetation biomass and soil-moisture content (Ferrazzoli et al., 1992), and more recently for the study of vegetation water content at the field level (Notarnicola and Posa, 2007). In contrast, this study proved an accurate determination of plant water status at the leaf level, using a more simple methodology than the one described by Martínez et al. (1995) and Menzel et al. (2009) for plant leaves and shoots, respectively. The use of this simple device became possible due to recent advances in telecommunications technology, especially related to the development of digital cordless telephony (DCT). Consequently, it is possible that a commercial portable tool for the determination of plant water status under field conditions based on our device could be developed.

On the other hand, the accuracy of this new method was compared to the near infrared  $R_{1300}/R_{1450}$  index in this investigation. It should be noted the absence of changes in this index at high leaf RWC values (Fig. 3A). This fact could be explained by the strong changes found in leaf thickness at high RWC values (Fig. 4), which may counteract the changes in near reflectance values due to leaf water losses (Seelig et al., 2009). For this reason, although Seelig et al. (2008a) established a linear relationship, we have used a segmented model in order to distinguish the two phases in the relationship between RWC and the  $R_{1300}/R_{1450}$  index. Therefore, the absence of changes in this index at leaf RWC values above the joint-point of the segmented model (Fig. 3A) prevents its use for the estimation of leaf RWC above this point.

Although both techniques can be used for the accurate estimation of leaf water content, the microwave-based procedure shows a certain number of advantages. First, coefficients of correlation were slightly higher for microwaves than for the  $R_{1300}/R_{1450}$  index (Table 1). For this reason, although near infrared reflectance might be used for plant physiological studies under field conditions, it can also be suitable to assess plant materials under an industrial point of view (e.g. quality control). Furthermore, the amount of energy received by the leaf is only 0.1 mW for the microwave technique, which is much lower than that applied by the spectrometer used in this study for the measuring of the  $R_{1300}/R_{1450}$  index (2.5 W).

## 5. Conclusions

In this study it has been shown that the changes in RWC of poplar leaves can be accurately determined by assessing changes in reflectivity at a frequency of 1730 MHz (L-band). The use of a technologically simple, low cost and portable device, based on a microwave digital cordless telephony (DCT) patch antenna, could yield a solid support for the development of a commercial portable tool for the determination of plant water status under field conditions in the future. This new technique, although tested on a specific poplar clone, can also be applied to other poplar clones and tree

species with similar leaf size dimensions. The use of microwaves to estimate changes in leaf water status in species with smaller leaves would imply the application of other frequency ranges, which demands the development of different types of antennas.

## Acknowledgements

This study was partially supported by INIA project SUM2008-00004-C03-03 (Ministerio de Ciencia e Innovación). Financial support from Gobierno de Aragón (A54 research group) is also acknowledged. Work of José Javier Peguero-Pina is supported by a "Juan de la Cierva"-MICIIN post-doctoral contract.

## References

- Carter, G.A., 1991. Primary and secondary effects of water content on the spectral reflectance of leaves. *Am. J. Bot.* 78, 916–924.
- Carter, G.A., McCain, D.G., 1993. Relationship of leaf spectral reflectance to chloroplast water content determined using NMR microscopy. *Remote Sens. Environ.* 46, 305–310.
- Ferrazzoli, P., Paloscia, S., Pampaloni, P., Schiavon, G., Solimini, D., Coppo, P., 1992. Sensitivity of microwave measurements to vegetation biomass and soil-moisture content—a case-study. *IEEE T. Geosci. Remote* 30, 750–756.
- Gómez Álvarez-Arenas, T.E., Sancho-Knapik, D., Peguero-Pina, J.J., Gil-Pelegrín, E., 2009. Noncontact and noninvasive study of plant leaves using air-coupled ultrasonics. *Appl. Phys. Lett.* 95, 193702.
- Grant, O.M., Tronina, L., Chaves, M.M., 2006. Exploring thermal imaging variables for the detection of stress responses in grapevine under different irrigation regimes. *J. Exp. Bot.* 58, 815–825.
- Jones, H.G., 1990. Plant water relations and implications for irrigation scheduling. *Acta Hort.* 278, 67–76.
- Jones, H.G., 2004. Irrigation scheduling: advantages and pitfalls of plant-based methods. *J. Exp. Bot.* 55, 2427–2436.
- Jones, H.G., 2007. Monitoring plant and soil water status: established and novel methods revisited and their relevance to studies of drought tolerance. *J. Exp. Bot.* 58, 119–130.
- Jördens, C., Scheller, M., Breitenstein, B., Selmar, D., Koch, M., 2009. Evaluation of leaf water status by means of permittivity at terahertz frequencies. *J. Biol. Phys.* 35, 255–264.
- Kubiske, M.E., Abrams, M.D., 1991. Seasonal, diurnal and rehydration-induced variations of pressure–volume relations in *Pseudotsuga menziesii*. *Physiol. Plant.* 83, 107–116.
- Martínez, M., Artacho, J.M., Forniés-Marquina, J.M., Letosa, J., García-Gracia, M., Gil, E., 1995. Dielectric behaviour by T.D.R. of the water status in a vegetal leaf. *OHD Biennial Colloquium Digest* 13, 330–333.
- McKenney, D.W., Yemshanov, D., Fox, G., Ramlal, E., 2004. Cost estimates for carbon sequestration from fast growing poplar plantations in Canada. *Forest Policy Econ.* 6, 345–358.
- Meiresonne, L., Nadezhdin, N., Cermak, J., Van Slycken, J., Ceulemans, R., 1999. Measured sap flow and simulated transpiration from a poplar stand in Flanders (Belgium). *Agr. Forest Meteorol.* 96, 165–179.
- Menzel, M.I., Tittmann, S., Bühler, J., Preis, S., Wolters, N., Jahnke, S., Walter, A., Chlubek, A., Leon, A., Hermes, N., Offenhäuser, A., Gilmer, F., Blümner, P., Schurr, U., Krause, H.J., 2009. Non-invasive determination of plant biomass with microwave resonators. *Plant Cell Environ.* 32, 368–379.
- Migliavacca, M., Meroni, M., Manca, G., Matteucci, G., Montagnani, L., Grassi, G., Zenone, T., Teobaldelli, M., Godel, I., Colombo, R., Seufert, G., 2009. Seasonal and interannual patterns of carbon and water fluxes of a poplar plantation under peculiar eco-climatic conditions. *Agr. Forest Meteorol.* 149, 1460–1476.
- Notarnicola, C., Posa, F., 2007. Inferring vegetation water content from C- and L-band SAR images. *IEEE T. Geosci. Remote* 45, 3165–3171.
- Peguero-Pina, J.J., Morales, F., Flexas, J., Gil-Pelegrin, E., Moya, I., 2008. Photochemistry, remotely sensed physiological reflectance index and de-epoxidation state of the xanthophyll cycle in *Quercus coccifera* under intense drought. *Oecologia* 156, 1–11.
- Peñuelas, J., Filella, I., Biel, C., Serrano, L., Save, R., 1993. The reflectance at the 950–970 nm region as indicador of plant water status. *Int. J. Remote Sens.* 14, 1887–1905.
- Sancho-Knapik, D., Gómez Álvarez-Arenas, T., Peguero-Pina, J.J., Gil-Pelegrín, E., 2010. Air-coupled broadband ultrasonic spectroscopy as a new non-invasive and non-contact method for the determination of leaf water status. *J. Exp. Bot.* 61, 1385–1391.
- Schabenberger, O., Pierce, F.J., 2002. Contemporary Statistical Models for the Plant and Soil Sciences. CRC, Boca Raton.
- Seelig, H.D., Adams, W.W., Hoehn, A., Stodieck, L.S., Klaus, D.M., Emery, W.J., 2008a. Extraneous variables and their influence on reflectance-based measurements of leaf water content. *Irrigat. Sci.* 26, 407–414.
- Seelig, H.D., Hoehn, A., Stodieck, L.S., Klaus, D.M., Adams, W.W., Emery, W.J., 2008b. The assessment of leaf water content using leaf reflectance ratios in the visible, near-, and short-wave-infrared. *Int. J. Remote Sens.* 29, 3701–3713.

- Seelig, H.D., Hoehn, A., Stodick, L.S., Klaus, D.M., Adams III, W.W., Emery, W.J., 2009. Plant water parameters and the remote sensing  $R_{1300}/R_{1450}$  leaf water index: controlled condition dynamics during the development of water deficit stress. *Irrigat. Sci.* 27, 357–365.
- Sims, D.A., Gamon, J.A., 2003. Estimation of vegetation water content and photosynthetic tissue area from spectral reflectance: a comparison of indices based on liquid water and chlorophyll absorption features. *Remote Sens. Environ.* 84, 526–537.
- Sixto, H., Hernández, M.J., Barrio, M., Carrasco, J., Cañellas, I., 2007. Plantaciones del género *Populus* para la producción de biomasa con fines energéticos: revisión. *Inv. Agrar.: Sist. Rec. Forest.* 16 (3), 277–294.
- Suarez, L., Zarco-Tejada, P.J., Berni, J.A.J., Gonzalez-Dugo, V., Fereres, E., 2009. Modelling PRI for water stress detection using radiative transfer models. *Remote Sens. Environ.* 113, 730–744.
- Tognetti, R., Giovannelli, A., Lavini, A., Morelli, G., Fragnito, F., d'Andria, R., 2009. Assessing environmental controls over conductances through the soil-plant-atmosphere continuum in an experimental olive tree plantation of southern Italy. *Agr. Forest Meteorol.* 149, 1229–1243.
- Vilagrosa, A., Bellot, J., Vallejo, V.R., Gil-Pelegrin, E., 2003. Cavitation, stomatal conductance, and leaf dieback in seedlings of two co-occurring Mediterranean shrubs during an intense drought. *J. Exp Bot.* 54, 2015–2024.
- Wu, C., Niu, Z., Tang, Q., Huang, W., 2009. Predicting vegetation water content in wheat using normalized difference water indices derived from ground measurements. *J. Plant Res.* 122, 317–326.
- Zimmer, F., Grueger, H., Heberer, A., Wolter, A., Schenck, H., 2004. Development of a NIR micro spectrometer based on a MOEMS scanning grating. *MEMS MOEMS Micromaching* 5455, 9–18.
- Zimmermann, D., Reuss, R., Westhoff, M., Gebner, P., Bauer, W., Bamberg, E., Bentrup, F.W., Zimmermann, U., 2008. A novel, non-invasive, online-monitoring, versatile and easy plant-based probe for measuring leaf water status. *J. Exp. Bot.* 59, 3157–3167.

## D. RESUMEN

### 1. OBJETIVOS DE INVESTIGACIÓN

En base a lo expuesto en la introducción, el objetivo general de la presente tesis doctoral es el de encontrar y desarrollar nuevos métodos o técnicas para el estudio hídrico de las plantas de manera que no se dañe el material vegetal que se esté midiendo. Por consiguiente, los objetivos de investigación específicos son los que se enumeran a continuación:

- 1) Utilización de la Espectroscopia Ultrasónica de Banda ancha Acoplada al aire sobre hojas de plantas, contemplándola como una técnica no destructiva y relacionando los parámetros ultrasónicos resultantes con el estado hídrico de las hojas.
- 2) Estudio en profundidad de los cambios estructurales que experimenta la hoja en el proceso de deshidratación y observación del efecto que estos cambios producen sobre la señal ultrasónica. Estudio de las correlaciones entre ambos.
- 3) Estudio de las posibles mejoras de la técnica ultrasónica para la obtención de un análisis más detallado de la resonancia de la hoja, así como para facilitar el desarrollo de una técnica más rápida y más robusta.
- 4) Combinación de la potencial efectividad del rango de frecuencias de las microondas (Banda-L) para la medida del contenido hídrico foliar con un dispositivo simple y portátil.

### 2. APORTACIONES DEL DOCTORANDO

Las contribuciones del doctorando para buscar un nuevo método no dañino que permita estudiar el estado hídrico de las plantas, se establecen en lo siguiente:

- Medida de la variación de los parámetros ultrasónicos sobre hojas de varias especies durante el proceso de deshidratación y establecimiento del hecho de que la variación de los parámetros en las hojas siguen una curva tipo sigmoidal con la variación del contenido en agua.
- Incorporación de la tecnología móvil digital en la medida del contenido en agua de hojas a través de la utilización de antenas que trabajan en el rango de las microondas.
- Medida de las hojas por procedimientos universales. Realización de curvas presión-volumen y análisis de las mismas.
- Establecimiento de una correlación directa entre el punto de pérdida de turgencia y el punto de inflexión en las sigmoides que relacionan la frecuencia de resonancia y la constante de elasticidad  $c_{33}$  con el contenido en agua.
- Elaboración de una interpretación de la evolución de los parámetros ultrasónicos con la pérdida de agua en la hoja en función de los cambios observados en la misma.

Además, el doctorando ha aportado la importante tarea de servir de nexo de unión entre los diferentes grupos implicados en este trabajo altamente multidisciplinar (grupos de Ecofisiología, CITA; de Señales, Sistemas y Tecnologías Ultrasónicas, CSIC y de Microondas y Radar, UPM). Fruto del estudio de las diferentes temáticas implicadas y de su contacto directo con los grupos que las desarrollan, el doctorando ha aportado una perspectiva interdisciplinar entre las diferentes áreas y una comprensión de conceptos en los tres grupos, permitiendo el diseño óptimo y el seguimiento de los experimentos; la interpretación y discusión de los resultados y la posterior publicación de los mismos.

### **3. METODOLOGÍA UTILIZADA**

Para el primer objetivo de la tesis, *utilización de la Espectroscopía Ultrasónica de Banda ancha Acoplada al aire sobre hojas relacionando los parámetros ultrasónicos con su estado hídrico*, se llevó el material vegetal a máxima hidratación y con el instrumental ultrasónico se fueron midiendo las hojas en varios estados de hidratación. El principal parámetro ultrasónico resultante de estas medidas fue la frecuencia ( $f$ ), la cual fue analizada y relacionada con el contenido relativo en agua (RWC) y con

parámetros fisiológicos derivados de las curvas presión-volumen: Punto de pérdida de turgencia (*TLP*) y modulo máximo de elasticidad de pared ( $\varepsilon_{max}$ ).

En cuanto al segundo de los objetivos, *estudio en profundidad de los cambios estructurales en el proceso de deshidratación y observación del efecto sobre la señal ultrasónica*, se procedió a observar y a evaluar los cambios que ocurrían en las hojas en diferentes puntos del proceso de deshidratación mediante medidas ultrasónicas, fisiológicas (curvas presión-volumen), medidas independientes de espesor y densidad, cálculo y estimaciones de la velocidad de resonancia (*v*), el factor de calidad (*Q*) y la constante de elasticidad ( $c_{33}$ ) y medida de cambios estructurales a nivel celular a través de la microscopía electrónica.

El tercero de los objetivos, *estudio de las mejoras de la técnica ultrasónica para la obtención de un análisis más detallado así como para facilitar el desarrollo de una técnica más rápida y más robusta*, fue realizado a través de medir simultáneamente la fase y la magnitud de la señal ultrasónica, de la mejora del ajuste de la curva de resonancia teórica sobre la experimental y de la resolución del problema inverso para obtener directamente el espesor y la densidad de la hoja así como la velocidad y la atenuación de la señal. Además se profundizó en el estudio de la constante de elasticidad  $c_{33}$ .

Por último, el cuarto de los objetivos, *combinación del rango de frecuencias de las microondas para medir el contenido hídrico foliar con un dispositivo simple y portátil*, se desarrolló mediante el uso de una antena inalámbrica de microondas empleada comúnmente en la tecnología de los teléfonos móviles. Con ella se procedió a la medida de la reflectividad en las hojas a una frecuencia determinada de la banda-L. Como en los anteriores objetivos, la reflectividad obtenida se relacionó con el RWC de la hoja en el momento de la medida. Además, para evaluar la calidad de esta técnica, se comparó con una técnica comercial en la que se midió la reflectancia en el rango del infrarrojo.

### 3.1 Espectroscopía ultrasónica de banda ancha acoplada al aire

El montaje experimental de la técnica ultrasónica (Figura 1) consistió en dos transductores piezoeléctricos acoplados al aire (emisor y receptor; Imagen 1) que trabajaban en un rango de frecuencias determinado con un diámetro de radiación de 20 mm. Estos transductores se dispusieron enfrentados entre si a una cierta distancia cuya variación no interfirió en la medida.

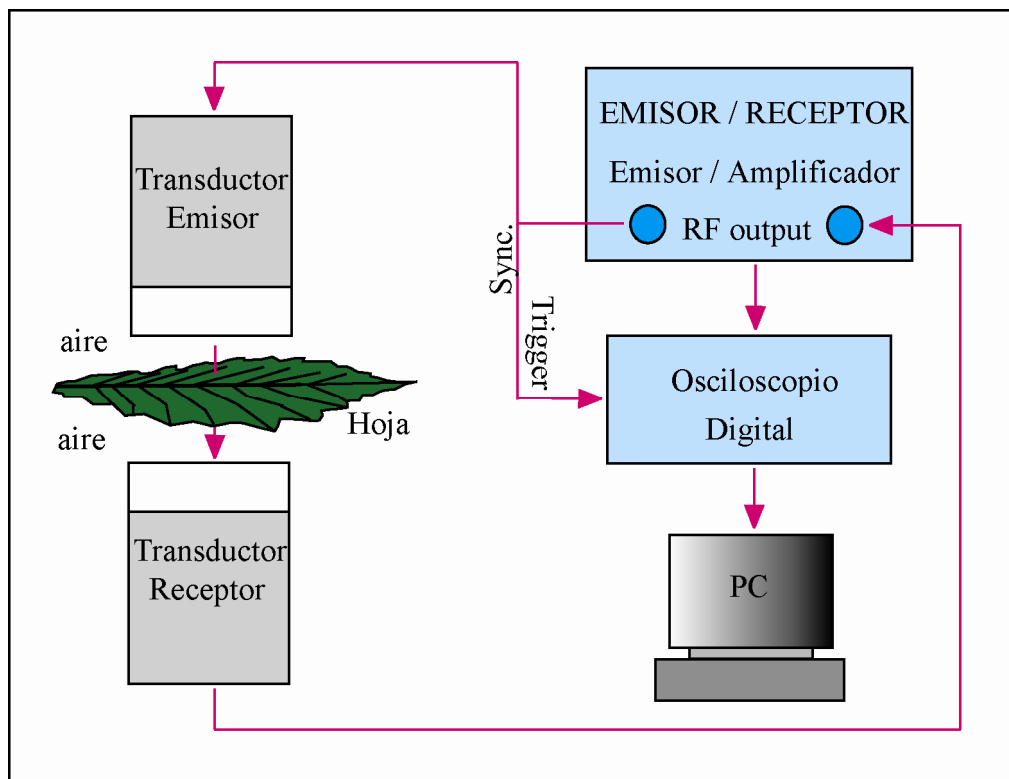
Entonces se aplicó, a través de un emisor-receptor Panametrics 5077 (Olympus USA), una señal (semicírculo de onda cuadrada sintonizado a la frecuencia central de los transductores) eléctrica (100-400 V) al transductor emisor, el cual convertía la señal eléctrica en un pulso ultrasónico que emitía al aire. El receptor recolectaba esta señal ultrasónica y la volvía a convertir en una señal eléctrica, que era amplificada y filtrada analógicamente en el mismo Panametrics 5077. Finalmente, un osciloscopio (Tektronix 5052 TDS, Tektronix Inc., USA) digitalizaba esta señal, reducía el ruido (filtrado digital), efectuaba una Transformación Rápida de Fourier tanto en magnitud como en fase y transfería los datos a un ordenador. La señal de disparo del osciloscopio era proporcionada por el mismo Panametrics 5077.



Imagen 1: Detalle de los transductores

El procedimiento experimental fue el siguiente. En primer lugar, el transductor receptor media directamente la señal transmitida por el emisor sin interponer ninguna muestra entre ellos. Esta medida proporcionaba la calibración del sistema permitiendo normalizar la respuesta de la banda de frecuencia tanto en magnitud como en fase. Entonces la hoja, sujetada con soportes durante unos segundos, se colocaba entre los dos transductores de forma que la señal incidiera ortogonalmente sobre la superficie de la hoja. En ningún momento fue necesario un contacto físico entre la hoja y los transductores. Cuando la onda ultrasónica impactaba contra la hoja, parte de la energía

era reflejada mientras que el resto era transmitida propagándose a través de la hoja hasta llegar a su cara posterior. Entonces otra parte de la energía volvía a ser reflejada mientras el resto era transmitida (señal transmitida) por el aire al transductor receptor. Este proceso se repetía para cada una de las múltiples reflexiones internas en la hoja hasta que la atenuación de los ultrasonidos en el material producía el decaimiento de la reverberación. La transmisión estaba formada entonces, por la señal transmitida más la contribución de todas las reverberaciones que se producían dentro de la hoja y que eran finalmente, transmitidas al aire a partir de la cara posterior de la hoja. Cuando todas estas reverberaciones llegaban a la cara posterior de la hoja en fase entre ellas y en fase con la señal transmitida, la energía transmitida era máxima produciéndose lo que se llamamos una resonancia en la dirección del espesor.



**Figura. 1: Representación esquemática de la técnica de Espectroscopía ultrasónica de banda ancha acoplada al aire**

El parámetro ultrasónico directamente medido fue el pulso transmitido en el dominio del tiempo. A partir de esta medida, la transformada de Fourier permitió obtener la magnitud y la fase del espectro que dieron lugar a la curva donde se enfrentaban el coeficiente de transmisión y la frecuencia. El principal parámetro que se relacionó con el estado hídrico de la hoja en el momento de la medida, fue el valor de la frecuencia

asociada a la máxima transmitancia en el pico de la curva. Para comparar especies entre sí, fue necesario estandarizar cada valor de frecuencia dividiéndolo por el valor obtenido a máxima hidratación.

Otros parámetros estudiados derivados de las medidas de magnitud y fase fueron la atenuación y la constante macroscópica efectiva de elasticidad ( $c_{33}$ ). Para estimar la atenuación del sonido en las muestras se empleó la inversa del factor de calidad ( $Q$ ), por ser  $1/Q$  directamente proporcional a la atenuación. Un incremento en  $1/Q$  reflejaba un incremento en la irregularidad del camino que recorría la señal. El factor  $Q$  se calculó como el cociente entre la frecuencia de resonancia y la anchura del pico de resonancia medido a 3dB por debajo del valor máximo. Por otro lado  $c_{33}$ , que se refiere a la constante elástica que relaciona tensiones y deformaciones ambas producidas a lo largo del eje Z (dirección del espesor de la hoja) y que viene expresada en MPa, representaba la elasticidad de toda la hoja.  $c_{33}$  fue primeramente estimada utilizando medidas independientes entre sí de frecuencia, espesor y densidad foliar y posteriormente calculada directamente a través de medidas directas de velocidad y densidad.

### 3.2 Análisis de la respuesta espectral de la resonancia

La respuesta elástica en las hojas de las plantas viene principalmente determinada por la cantidad de agua contenida en ellas y por los espacios de aire presentes. La mayor cantidad de agua que contienen las hojas está encerrada dentro de las células de las hojas a una presión mayor que la presión atmosférica debido a la tensión mecánica mantenida por la membrana celular. Esta tensión de la membrana, dentro del denso empaquetamiento de la estructura celular, es el principal responsable de las propiedades elásticas de las hojas. Cuando una hoja plenamente hidratada pierde agua, el volumen de agua que contiene cada célula se reduce y, por consiguiente, la tensión almacenada en la membrana celular también se reduce. A una escala macroscópica estos cambios dan lugar a una deformación y a una pérdida de rigidez y, por lo tanto, es esperable que las constantes elásticas ( $c_{ij}$ ) disminuyan.

El espectro de la primera resonancia en la dirección del espesor fue analizado considerando las hojas como láminas homogéneas con propiedades efectivas. Gómez

Álvarez-Arenas et al. (2009a) propusieron un modelo multi-capa más parecido a la estructura real de las hojas. Sin embargo este modelo fue poco práctico ya que introducía un conjunto mucho más amplio de parámetros y variables que eran difíciles de determinar. Además, el modelo mono-capa proporcionó un ajuste razonable de los datos experimentales siempre que se restringiese el análisis al entorno del primer orden de resonancia. El coeficiente de transmisión ( $T$ ) a incidencia normal para una lámina de material homogéneo contenido en un fluido está determinado por  $T=|\xi|^2$ , donde:

$$\xi = \frac{2r\Gamma}{2r\Gamma \cos(k_2 l) - i(1 + r^2\Gamma^2)\sin(k_2 l)} \quad (1)$$

donde  $l$  es el espesor de la lámina,  $r$  es el cociente entre los vectores de las ondas (fluido o sólido)  $r = k_1/k_2$  y  $\Gamma = \rho_1/(r^2\rho_2)$ , y  $\rho$  la densidad (Brekhovskikh, 1960). La rugosidad de la superficie de la lámina puede ser introducida considerando una modificación en los coeficientes de transmisión y reflexión (Stor-Pellinen et al., 2001). El coeficiente de transmisión fue medido usando una técnica de transmisión directa, y por lo tanto se verifican las siguientes relaciones entre el modulo y la fase del coeficiente de transmisión medidos ( $T$  and  $\Delta\phi$ ) y los calculados  $\xi$  (magnitud:  $|\xi|$  y fase:  $\phi(\xi)$ ):

$$T = |(\xi \exp(\alpha_l l))|^2 \cong |\xi|^2 \quad (2)$$

$$\Delta\phi = \phi(\xi) - lk_1 \quad (3)$$

donde  $\alpha_l$  es el coeficiente de atenuación del aire.

El análisis del espectro de la resonancia experimentalmente medido siguió el procedimiento explicado en Gómez Álvarez-Arenas (2010) y Gómez Álvarez-Arenas et al. (2010). Utilizando las ecuaciones (4) y (5), este procedimiento nos permitió obtener una primera estimación de la velocidad ultrasónica ( $v_2$ ) y del espesor ( $l$ ) a partir de los valores medidos de la posición de la frecuencia en la primera resonancia ( $f_{TR}$ ) y del valor de la fase ( $\Delta\phi$ ) a esa frecuencia  $\Delta\phi(f_{TR}) = \Delta\phi_1$ .

$$v_2(f_{TR}) = 2f_{TR}l \quad (4)$$

$$v_2(f_{TR}) = l/(l/v_1 - \Delta\phi_1/(2\pi f_{TR})) \quad (5)$$

donde  $v_1$  es la velocidad de la onda ultrasónica en el fluido donde está inmerso el disco (aire en este caso). En este trabajo, se consideró  $\rho_2^0 = 900 \text{ kg/m}^3$  como una primera estimación de la densidad de las hojas. La atenuación de las ondas ultrasónicas en el disco a una  $f_{TR}$  ( $\alpha_2^0(f_{TR})$ ) se estimó a través de la impedancia y del factor- $Q$  de la resonancia (Gómez Álvarez-Arenas, 2003a; Gómez Álvarez-Arenas, 2003b). La variación de la atenuación con la frecuencia ( $\alpha(f)$ ) fue descrita por la siguiente ley potencial, como se hizo en trabajos anteriores para numerosos materiales porosos y tejidos biológicos (Gómez Álvarez-Arenas et al., 2002; Gómez Álvarez-Arenas et al., 2009b):

$$\alpha'_2(f) = \alpha_2^0 \left( \frac{f}{f_{TR}} \right)^{1.5} \quad (6)$$

Dado el relativamente estrecho rango de frecuencias donde se realizaron las medidas se asumió que la velocidad de los ultrasonidos no variaba con la frecuencia.

Los valores de  $v_2^0$ ,  $\alpha_2^0(f)$ ,  $\rho_2^0$  y  $l^0$  obtenidos se consideraron una primera aproximación. Entonces se calculó  $k_2$  de acuerdo con la ecuación (7).

$$k_2(f) = \frac{\omega}{v_2} + i\alpha_2(f) \quad (7)$$

donde, en este caso,  $v_2 = v_2^0$  y  $\alpha_2(f) = \alpha'_2(f)$ .

Estos valores fueron introducidos en la ecuación (1) calculando  $\xi$ . A partir de  $\xi$  se obtuvo  $T(f)^{theo} = |\xi|^2$  y  $\Delta\phi(f)^{theo} = \phi(\xi) - lk_1$ . La estimación de la bondad del ajuste vino dada por  $\tau^T$  y  $\tau^\phi$ , definido como:

$$\tau^T = \frac{1}{N} \sum_{n=1}^N \left( \left( T(f_n)^{exp} - T(f_n)^{theo} \right) / T(f_n)^{exp} \right)^2 \quad (8.a)$$

$$\tau^\phi = \frac{1}{N} \sum_{n=1}^N \left( \left( \Delta\phi(f_n)^{exp} - \Delta\phi(f_n)^{theo} \right) / \Delta\phi(f_n)^{exp} \right)^2 \quad (8.b)$$

donde  $f_n$  son las frecuencias en el que  $T$  y  $\Delta\phi$  son medidas y  $N$  es el número de medidas (longitud del vector  $f_n$ ).

Para mejorar el ajuste se variaron los valores de velocidad, atenuación, espesor y densidad. Para cada grupo de estos valores se calculó  $T$  y después se estimó la bondad

de ajuste (Ecuación 8). Como resultado final se escogió el grupo de parámetros que mejor ajuste presentó. Para evitar cambiar los cuatro parámetros simultáneamente, se diseñó un procedimiento basado en el conocimiento del efecto que cada uno de estos parámetros produce sobre  $T$  estableciendo el procedimiento en dos etapas principales. En la primera solo se variaron la atenuación y la densidad teniendo como criterio de optimización la Ecuación (8a). En la segunda etapa, se variaron la velocidad y el espesor de tal manera que se mantuvo constante la localización de la frecuencia de resonancia. Como criterio de optimización de la segunda fase se utilizó la Ecuación (8b). El procedimiento se muestra en la Figura 2.

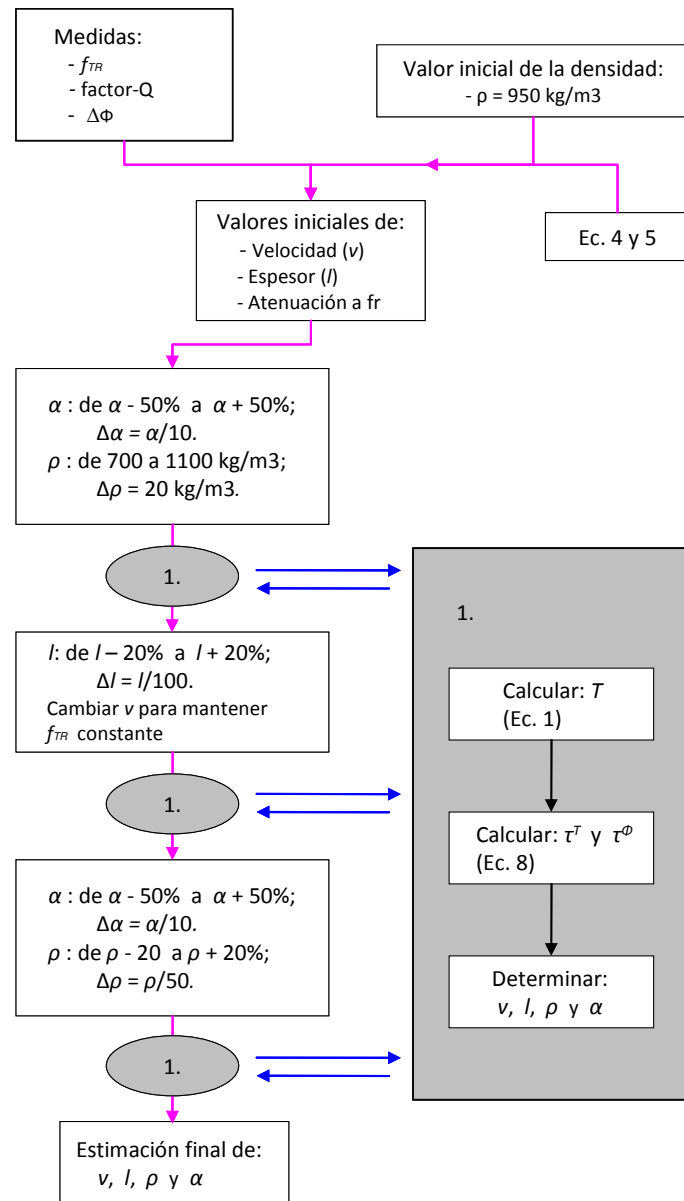


**Figura 2:** Procedimiento para calcular los valores de la velocidad, espesor, densidad y atenuación de la hoja a partir de la magnitud y fase medidas del coeficiente de transmisión y de la expresión teórica del coeficiente de transmisión para discos homogéneos.

Estas operaciones se realizaron en una función del programa matemático MATLAB que se cargaba a través del propio Windows del osciloscopio que se utilizó para realizar las medidas. Las operaciones se ejecutaban justo después de la medida y por eso nos permitieron obtener, prácticamente en tiempo real, la estimación de los parámetros efectivos de la hoja. El valor de esta simple rutina de ajuste fue que se ejecutaba lo suficientemente rápido para que el análisis completo de la resonancia pudiera ser realizado *in situ* y casi en tiempo real. Además fue suficientemente eficaz y proporcionó bastante bien la curva de ajuste para las medidas que se realizaron. La experiencia mostró que los resultados finales no dependían de los valores iniciales propuestos, pero el tiempo de procesado aumentaba cuando los valores iniciales eran poco precisos o cuando el intervalo de variación de las magnitudes tenía que ser ampliado.

### 3.3 La antena de microondas de telefonía móvil digital

El dispositivo experimental consistió básicamente en un generador de microondas (oscilador), una antena y un dispositivo separador. El generador inyectaba su salida a la antena a través de un dispositivo separador, el cual permitía obtener dos señales idénticas de energía (cada una con la mitad de energía de la entrada) pero con una diferencia de fase de 90°. Estas dos salidas de energía se inyectaban a la vez en la antena la cual la recibía y la radiaba al exterior. La posible energía que se reflejaba en la antena por ambas entradas era recogida por el detector de una forma cuantitativa. En la práctica (Imagen 2; Figura 3), se utilizó un Analizador de Redes Vectorial (VNA, E8364A 45MHz a 50 GHz, PNA Series, Agilent Technologies Inc., Santa Clara, USA), que alimentaba de energía al resto del dispositivo a través del puerto 1 (Figura 3) y permitía medir simultáneamente la energía reflejada por el separador (a través del puerto 1) y la reflejada por la antena (puerto 4).

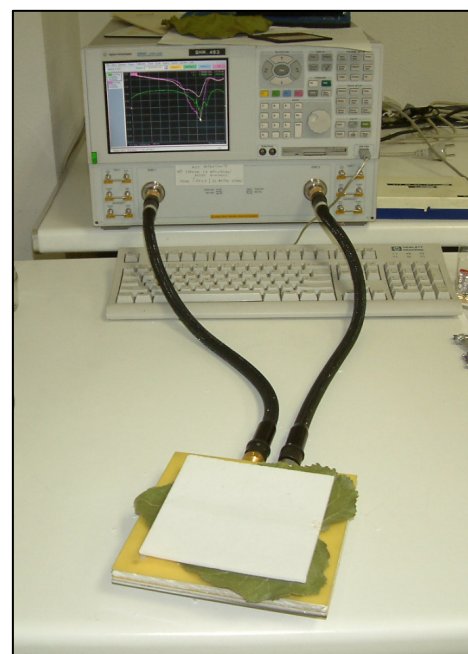


Imagen 2: Detalle del sistema de medida de microondas

En una primera calibración se comprobaba que la antena funcionara correctamente a la frecuencia deseada. Esto implicaba comprobar que las entradas de energía fueran lo suficientemente bajas y que no existiera reflexión alguna. Después de la calibración, y antes de colocar una muestra sobre la antena para ser medida, no existían reflexiones dentro del circuito. Al colocar la muestra (con diferente valor de constante dieléctrica que la del aire) se producía una perturbación en la señal y por lo tanto una reflexión en la energía radiada por la antena. Como el valor de la constante dieléctrica estaba muy influenciado por su contenido en agua (Martínez et al., 1995), el coeficiente de reflectividad era función directa de la cantidad de agua presente en la antena, por lo que si la muestra se iba deshidratando, la medida de reflexión de la propia muestra iba cambiando y pareciéndose más a la medida inicial del aire.

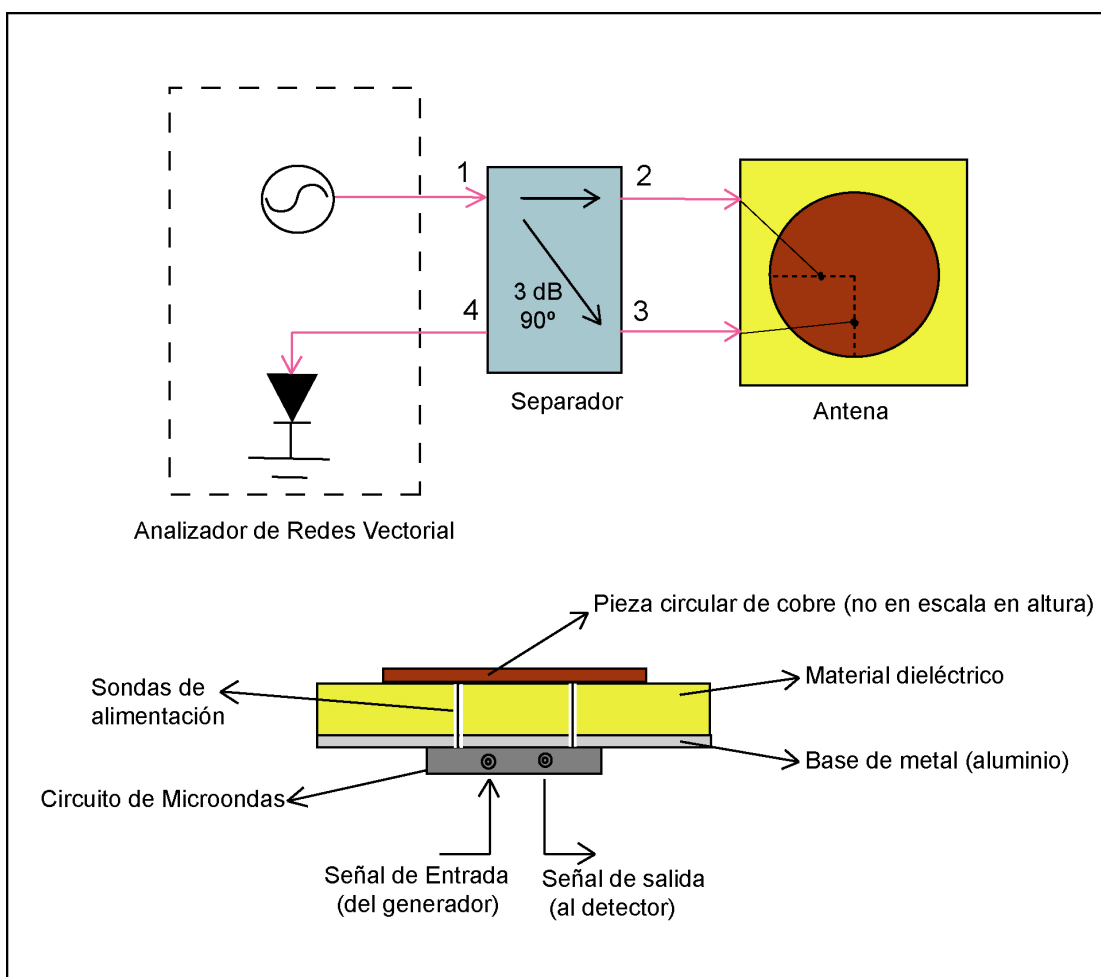


Figura 3: Representación esquemática de la antena y la técnica de microondas

El parámetro medido mediante la técnica de microondas fue el coeficiente de reflectividad a 1730 MHz ( $MWR_{1730}$ ), frecuencia comúnmente utilizada en antenas de telefonía móvil. El índice de infrarrojos con el que  $MWR_{1730}$  se comparó fue el  $R_{1300}/R_{1450}$ , índice que media la reflectancia de la hoja alrededor de la región espectral de 1450 nm con respecto a la de 1300 nm (Seelig et al., 2009). Estas reflectancias fueron obtenidas iluminando las muestras con una fuente de luz Polychromix MobiLight (500 mA, 2,5 W, Polychromix, USA) y midiendo la región del espectro de reflectancias desde 930 a 1690 nm con un Polychromix DTS NIR Spectrometer (Polychromix, USA).

### **3.4 Material vegetal y experimental**

El material vegetal que se utilizó estuvo compuesto por hojas de distinta naturaleza morfológica y fenológica. Las especies arbóreas que se seleccionaron fueron: *Prunus laurocerasus*, *Populus x euroamericana*, *Quercus muehlenbergii*, *Ligustrum lucidum* y *Platanus x hispanica*. De estas especies, se recolectaban a primera hora del día ramas de la parte norte del árbol transportándolas al laboratorio en bolsas de plástico. Una vez ahí, las hojas se cortaban por los peciolos, los cuales estaban sumergidos en agua para evitar el embolismo manteniéndose inmersos durante 24 horas a 4°C para que las hojas alcanzaran la máxima hidratación. Para los experimentos, las hojas se colocaban a temperatura ambiente y se iban dejando secar mientras se pesaban y se obtenían las medidas oportunas a diferentes niveles de contenido relativo en agua (RWC) desde un estado inicial de saturación o plena hidratación (TW). El peso seco de la hoja (DW) se obtenía después de mantener el material en una estufa (24 h, 60 °C). RWC se calculó mediante la siguiente expresión:  $RWC = (FW - DW) / (TW - DW)$ , siendo FW el peso fresco de la muestra en cada una de las medidas.

Como material experimental adicional se utilizaron filtros de papel de material celulósico homogéneo (Whatman 3; diámetro 125mm; espesor 0.39 mm) para la comparación de las medidas de *P. x euroamericana* en la técnica de microondas. A estos filtros se les añadieron tres mililitros de agua destilada para lograr un estado de saturación e inmediatamente después fueron introducidos en una atmósfera saturada de agua a temperatura ambiente para su estabilización.

### **3.5 Curvas presión-volumen**

Las curvas presión-volumen (curvas P-V) fueron determinadas siguiendo el método descrito en estudios anteriores (Dreyer et al., 1990; Corcuera et al., 2002; Brodribb y Holbrook, 2003) utilizando una cámara de presión tipo Scholander. Los parámetros analizados de estas curvas fueron: el potencial hídrico foliar en el punto de pérdida de turgencia, el módulo de elasticidad de la pared celular, la máxima turgencia y el contenido en agua en el punto de pérdida de turgencia. En algún caso, la perdida de agua simplásrica fue calculada para obtener el diagrama de Höfler y en algún otro, se analizaron los cambios dinámicos que se producía en el modulo de elasticidad de pared asociados a los cambios en la presión de turgencia.

### **3.6 Espesor y densidad**

Los valores independientes del espesor de las hojas fueron medidos utilizando un micrómetro convencional y un sensor digital GTH10L acoplado a un amplificador GT-75AP (GT Series, Keyence Corporation, Japan). Este sensor de ultra baja presión (fuerza de medida de 0.2 N cuando se instala boca arriba) aplicaba una presión de 7kPa suficiente para la medida sin provocar alteraciones en las características intrínsecas de la hoja por una excesiva presión. La densidad ( $\text{kg/m}^3$ ) fue calculada como el cociente entre el peso de la hoja y el volumen de la misma. El volumen ( $\text{m}^3$ ) fue calculado como el producto entre el espesor (m) y el área ( $\text{m}^2$ ), obteniendo ésta a través de imágenes digitales y posterior análisis mediante el programa de dominio público NIH Image.

### **3.7 Microscopio electrónico de barrido por congelación**

El microscopio electrónico de barrido por congelación (LTSEM, DSM 960 Zeiss, Alemania) se utilizó para observar hojas de *Quercus muehlenbergii* en tres diferentes niveles de contenido relativo en agua: a plena turgencia, alrededor del punto de turgencia y por debajo del punto de turgencia. Las secciones transversales frescas de las hojas se congelaron en Nitrógeno líquido, se cubrieron con oro, y seguidamente se observaron con esta técnica microscópica. Las imágenes fueron analizadas utilizando el programa de dominio público NIH Image. Posteriormente se midió la longitud y el

espesor de 20 células del parénquima en empalizada y otras 20 del parénquima esponjoso para cada uno de los tres estadios de contenido en agua.

### 3.8 Análisis estadísticos

En un primer análisis la relación entre la frecuencia ( $f$ ) y el contenido en agua (RWC) se ajustó a una función cúbica  $RWC = y_0 + af + bf^2 + cf^3$ , calculando el punto de pérdida de turgencia como el punto de inflexión de la ecuación. Posteriormente esta relación se ajustó a una curva logística de cuatro parámetros  $f = a + (b - a)/(1 + (RWC/c)^d)$  debido principalmente a que el punto de inflexión ( $c$ ) estaba ya incluido en el modelo y porque además dicha función describe perfectamente la evolución entre dos estados en equilibrio: en nuestro caso antes y después del punto de pérdida de turgencia. Por otra parte, también se utilizaron otros modelos como los lineales segmentados o los polinomios cuadrados para ajustar otros tipos de variables como el factor-Q, el espesor o la densidad con el RWC.

El test t de Studen't se utilizó para comparar los parámetros derivados de las curvas P-V con los obtenidos de las medidas ultrasónicas. También se realizaron ANOVAs para comparar la evolución del espesor y longitud de las células del parénquima esponjoso y en empalizada al disminuir RWC y el test de Tukey HSD para realizar múltiples comparaciones entre los diferentes estados de hidratación de las células. Todos los análisis estadísticos y gráficos mostrados fueron realizados con el programa SAS versión 8.0 (SAS, Cary, NC, USA) y con el programa SigmaPlot versión 8.0 (SPSS, Chicago, IL, USA).

## 4. PRINCIPALES RESULTADOS

A continuación se exponen los resultados más importantes que aparecen en el contenido de los artículos presentados. Entre ellos cabe destacar las relaciones de los parámetros físicos con el RWC y con las variables fisiológicas.

En la Figura 4 se representa la relación entre la frecuencia y el coeficiente de transmisión para una hoja de *P. x euroamericana* y *P. laurocerasus* a diferentes niveles de RWC. Para ambas especies al disminuir el RWC, se observó una caída de los valores máximos de transmitancia y un desplazamiento de toda la curva hacia valores de frecuencia más bajos. Aparte de estos cambios que se producían en el pico de la curva, cabe mencionar también los cambios que ocurrían en la propia forma de la curva. Al disminuir en RWC, apareció más ruido en la señal de la transmitancia y la curva se ensanchaba si se observaba a una determinada distancia vertical constante del pico. De este modo, las curvas con un RWC de 0,80 y 0,85 para *P. x euroamericana* y de 0,83 y 0,85 para *P. laurocerasus* mostraron una mayor dispersión y un mayor ensanchamiento que las curvas obtenidas con mayores valores de RWC (Figura 4).

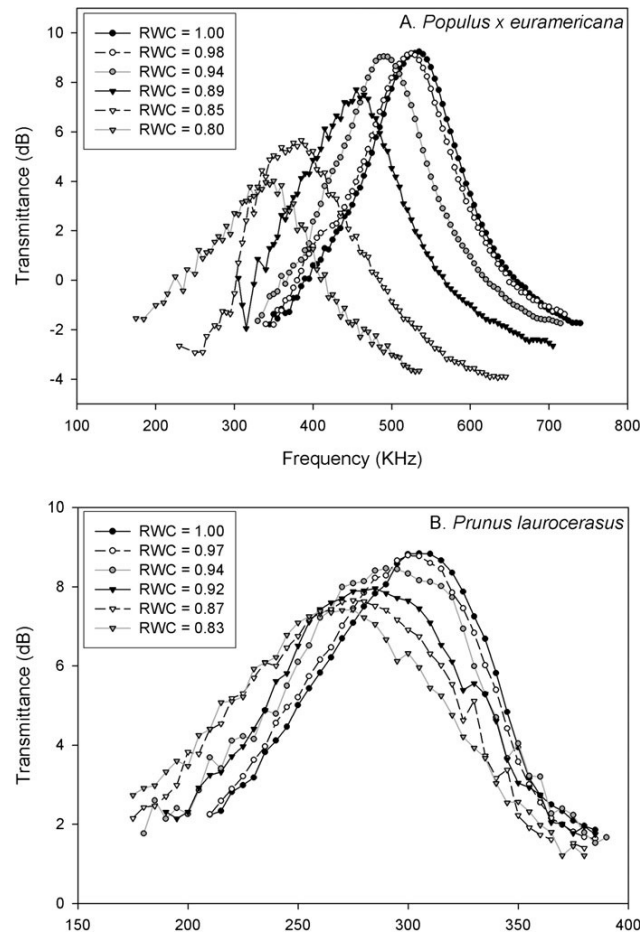


Figura 4: Relación entre la frecuencia (KHz) y la transmittancia (dB) para (A) *Populus x euramerica* y (B) *Prunus laurocerasus* para una hoja de cada especie a diferentes niveles de RWC.

La Figura 5 muestra la relación entre la media de los valores de la frecuencia estandarizada y RWC tanto para hojas de *P. x euroamericana* como para hojas de *P. laurocerasus*. Esta relación se ajustó a una función cúbica ( $R^2 = 0.99$ ,  $P < 0,0001$  para ambas especies), la cual se caracterizaba por la existencia de un punto de inflexión. En el experimento, el punto de inflexión determinó un cambio en la evolución de la frecuencia al disminuir RWC. Este punto puede ser comparado con el punto de intersección de la ecuación lineal de dos fases para la relación entre el potencial hídrico foliar y el RWC encontrado por Brodribb y Holbrook (2003). Estos autores consideran

que el punto de intersección puede ser asociado con el punto de perdida de turgencia, lo que ocurriría con el punto de inflexión en la relación frecuencia-RWC. Para *P. x euroamericana*, el valor de RWC en el punto de perdida de turgencia ( $RWC_{TLP}$ ) fue de  $0,89 \pm 0,01$  mientras el valor obtenido por las curvas P-V fue de  $0,88 \pm 0,01$ . Para *P. laurocerasus* el valor de  $RWC_{TLP}$  fue de  $0,89 \pm 0,01$  para ambas técnicas. Estos valores para cada especie no resultaron estadísticamente diferentes a  $P < 0,05$ .

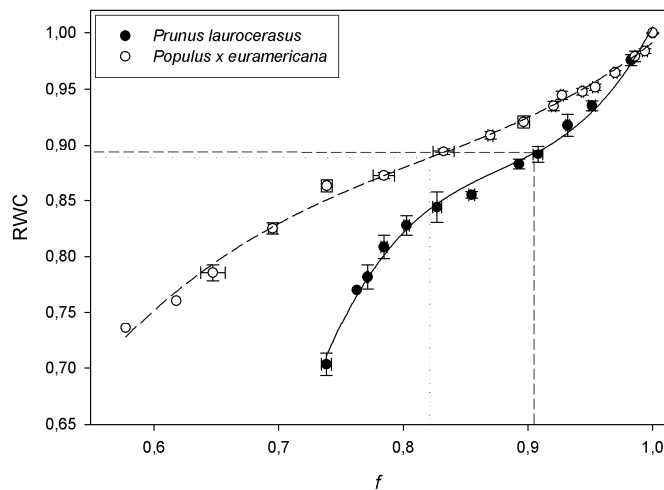


Figura 5: Relación entre la frecuencia estandarizada ( $f$ ) y el contenido relativo en agua ( $RWC$ ) para *Populus x euramericana* y *Prunus laurocerasus*. Datos expresados como medias  $\pm SE$  de diez hojas para cada especie.

En la Figura 6 se representa la relación entre los valores medios de la frecuencia y  $\Psi$  tanto para hojas de *P. x euroamericana* como para hojas de *P. laurocerasus*. Estas relaciones también se ajustaron a una función cúbica ( $R^2 = 0.99$ ,  $P < 0,0001$  para ambas especies). Aunque la relación para *P. x euroamericana* pudo haberse ajustado también a una ecuación lineal ( $R^2 = 0.97$ ,  $P < 0,0001$ ), se consideró la función cúbica por reflejar mejor la relación.

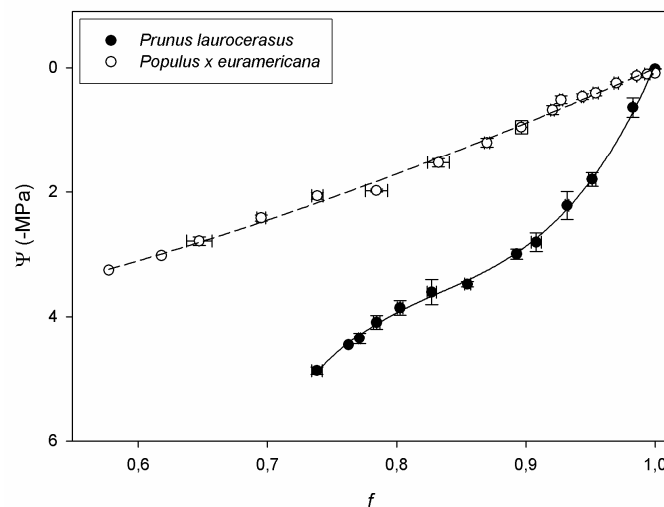
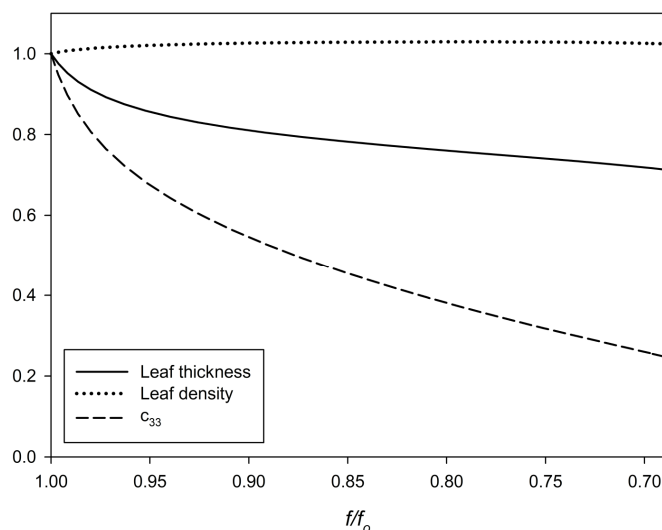


Figura 6: Relación entre la frecuencia estandarizada ( $f$ ) y el potencial hídrico ( $\Psi$ ) para *Populus x euramericana* y *Prunus laurocerasus*. Datos expresados como medias  $\pm SE$  de diez hojas para cada especie.

La figura 7 muestra la influencia de la estimación de la constante macroscópica de elasticidad ( $c_{33}$ ), el espesor foliar y la densidad de la hoja sobre la frecuencia estandarizada para hojas de *Quercus muehlenbergii*. Se puede observar que el  $c_{33}$  es el principal factor que afectó a los cambios en la frecuencia. En cuanto a los otros dos factores, el espesor afectó suavemente a las variaciones en la frecuencia solo a altos valores de ésta (i.e. a altos valores de RWC, antes del punto de perdida de turgencia), mientras que la densidad siempre tuvo una influencia despreciable.

La Figura 8 compara las relaciones entre los cambios del modulo de elasticidad de pared ( $\varepsilon$ ) y la estimación de la constante macroscópica de elasticidad con los cambios en la presión de turgencia. Ambos parámetros disminuyen de forma similar, desde plena turgencia hasta el punto de perdida de turgencia.



**Figura 7:** Variación de la constante macroscópica de elasticidad ( $c_{33}$ ), el espesor y la densidad foliares sobre la frecuencia estandarizada ( $f/f_0$ ) para *Quercus muehlenbergii*. Todas las variables han sido estandarizadas mediante la división de cada valor por el valor a RWC = 1,00.

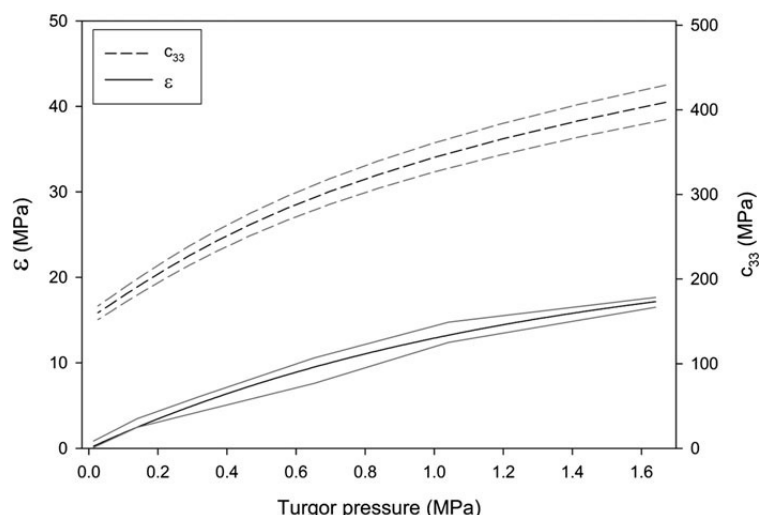


**Figura 8:** Relaciones entre la presión de turgencia (turgor pressure) y el modulo de elasticidad de pared ( $\varepsilon$ , en línea continua) y entre la presión de turgencia y la constante macroscópica de elasticidad ( $c_{33}$ , en línea discontinua) para *Quercus muehlenbergii*. Las líneas grises representan respectivamente los errores estándar de  $\varepsilon$  y  $c_{33}$ .

La Imagen 3 muestra cortes de hojas de *Quercus muehlenbergii* realizadas con el microscopio electrónico de congelación. La disminución en el espesor de la hoja medida fue causada por la reducción de la anchura y longitud de las células de los mesófilos, tanto en el de empalizada como en el del esponjoso. Este proceso puede observarse en los tejidos foliares a plena turgencia (Imagen 3A, C) y a  $RWC = 0.72$  (Imagen 3B, D). Además, la Imagen 3D muestra la deformación experimentada por las células del mesófilo cuando se sobrepasa el punto de perdida de turgencia.

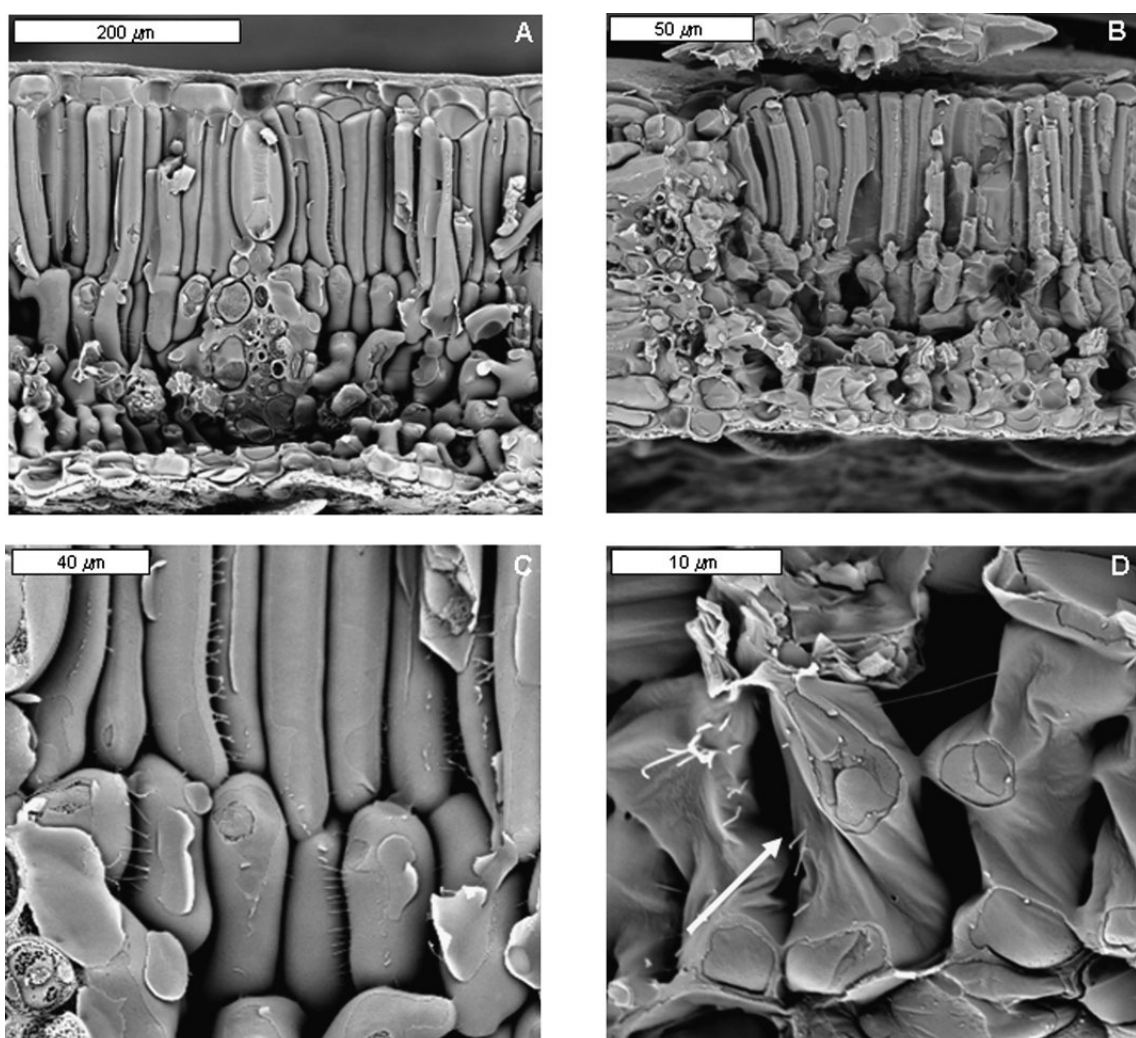


**Imagen 3:** Hojas de *Quercus muehlenbergii* realizadas por el Microscopio electrónico de congelación a plena turgencia (A, C) y a  $RWC=0,72$  (B, D). Las flechas blancas indican el fenómeno de deformación de las células.

La Figura 9 muestra el espectro de la fase y de la magnitud teóricas (línea continua) y experimentales (puntos) del coeficiente de transmisión ultrasónico frente a la

frecuencia de la primera resonancia en la dirección del espesor a diferentes niveles de RWC para una hoja de *Platanus hispanica*. Así mismo se observó un similar comportamiento para las demás hojas y especies medidas. Estos espectros fueron procesados de acuerdo con el procedimiento explicado en el apartado *III.2 Análisis de la respuesta espectral de la resonancia*, para obtener la variación con RWC de: 1) el desplazamiento relativo de la frecuencia de resonancia, 2) el espesor de la hoja, 3) la densidad foliar, 4) la velocidad de los ultrasonidos en la hoja y 5) el coeficiente ultrasónico de atenuación en la hoja. La constante elástica  $c_{33}$ , como se mencionó anteriormente, se calculó a partir de esta velocidad y densidad procedentes del análisis. La variación de  $c_{33}$  con RWC (Figura 10) muestra una relación sigmoidal, típica de la transición entre dos estados, y similar a la variación de la frecuencia y RWC. Esto demuestra que la disminución de la frecuencia de resonancia debido al descenso en RWC es provocado por la reducción de la rigidez elástica de la hoja.

Por otro lado, hay que destacar que las variaciones observadas en  $c_{33}$  con RWC son mayores que las observadas con la frecuencia o con la velocidad. Esto es debido a que en las variaciones de  $c_{33}$  se excluye la influencia del espesor y la densidad. Esto sugiere que la medida de  $c_{33}$  puede proporcionar mejores estimaciones de RWC en las hojas.

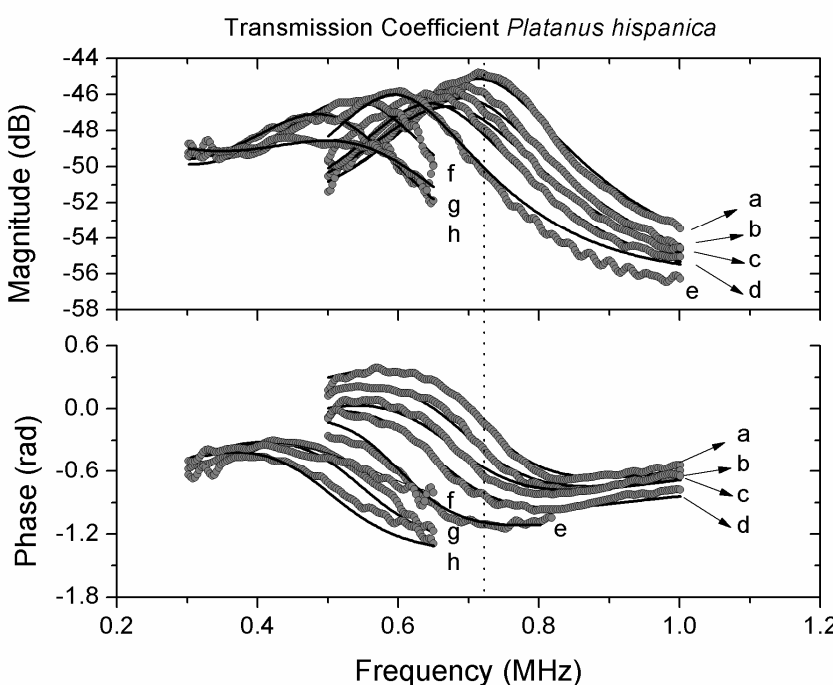
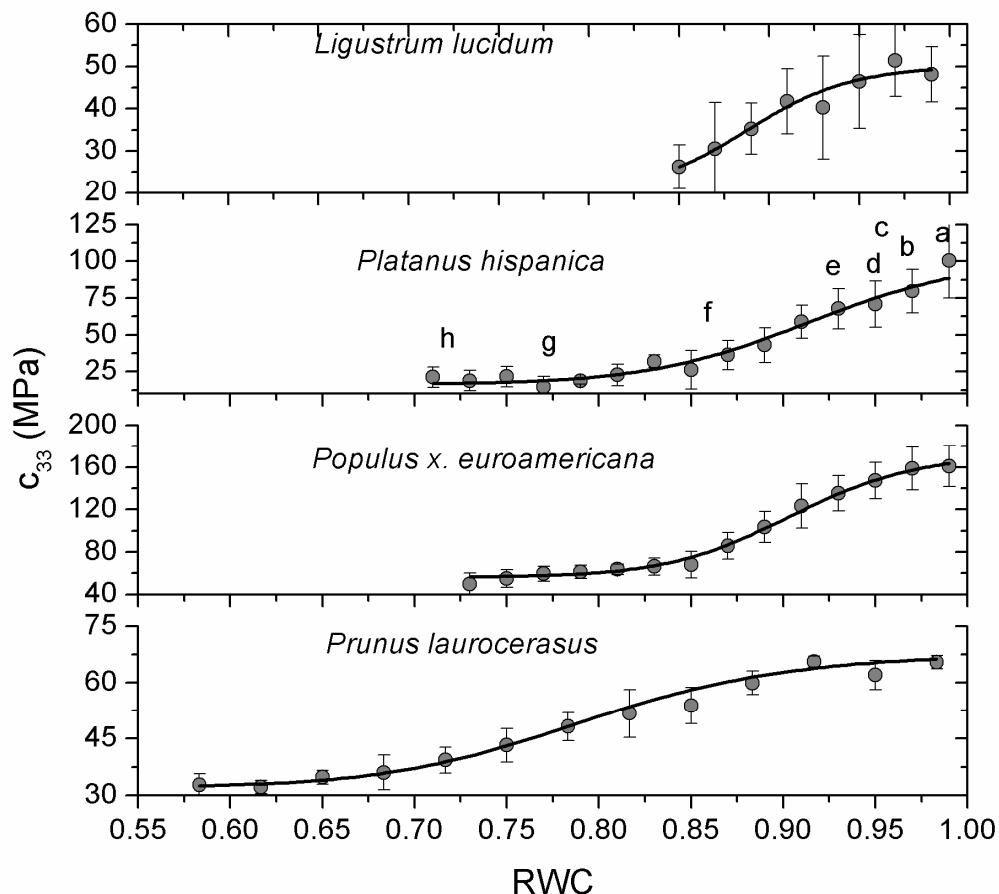
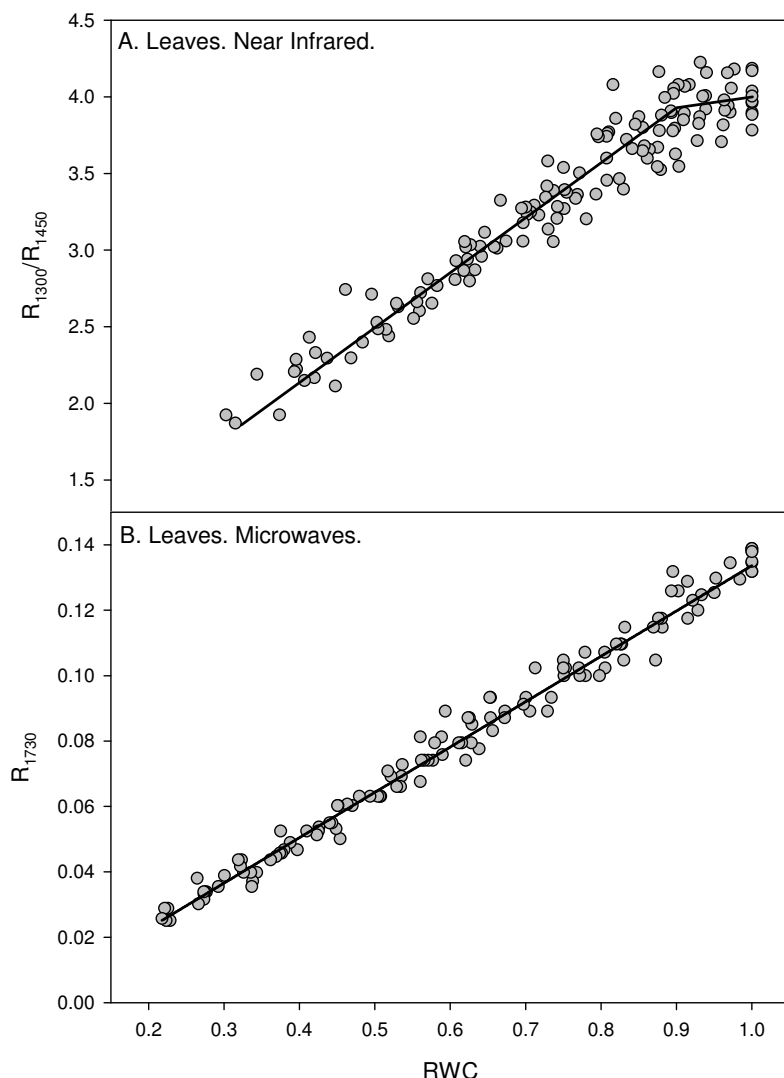


Figura 9: Respuesta espectral (magnitud, arriba y fase, abajo) de la primera resonancia en la dirección del espesor de una hoja de *Platanus hispanica* a diferentes valores de contenido relativo en agua (RWC): a= 1,00; b= 0,97; c= 0,95; d= 0,94; e= 0,92; f= 0,85; g= 0,77; h= 0,72.



**Figura 10:** Variación de la constante macroscópica de elasticidad ( $c_{33}$ ) con el contenido relativo en agua (RWC). Para *Platanus hispanica*, las letras a-h indican el valor de RWC para las resonancias que se muestran en la Figura 9.

Por último, en la Figura 11, se muestran los datos que se refieren a las relaciones entre  $R_{1300}/R_{1450}$  y RWC (Figura 11A) y  $MWR_{1730}$  frente RWC (Figura 11B) medidos sobre hojas de *P. x euroamericana*. Los datos medidos con infrarrojos fueron ajustados mediante un modelo segmentado mientras que los procedentes de la técnica de microondas se ajustaron a un modelo lineal. El modelo segmentado es un modelo no lineal compuesto por dos modelos lineales de diferentes pendientes. El punto en el que coinciden los dos modelos es conocido como punto de encuentro (Schabenberger and Pierce, 2002). En este caso el valor de RWC en el punto de encuentro fue  $0,917 \pm 0,022$ . Desde este valor al valor de  $RWC = 1$ , la pendiente del modelo lineal fue aproximadamente cero mientras que la pendiente del otro modelo (desde  $RWC = 0,917$  a 0,250) fue 3,39. Los coeficientes de regresión  $R^2$  fueron de 0,94 ( $P < 0,0001$ ) para la técnica infrarrojos y de 0,98 ( $P < 0,0001$ ) para la de microondas.



**Figura 11:** Relación entre el contenido relativo en agua (RWC) y (A) el índice  $R_{1300}/R_{1450}$  de infrarrojos y (B) el índice  $MWR_{1730}$  de las microondas. Valores obtenidos en hojas de *Populus x euroamericana*.

## 5. CONCLUSIONES FINALES

La Espectroscopía ultrasónica de banda ancha acoplada al aire ha demostrado ser una prometedora técnica para la determinación del punto de pérdida de turgencia de las hojas calculado como el punto de inflexión de la relación entre la frecuencia y el contenido relativo en agua durante un proceso de deshidratación. Por encima del punto de pérdida de turgencia, la variación en  $c_{33}$  es el principal factor que explicaría el descenso encontrado en la frecuencia. Este descenso de  $c_{33}$  puede ser atribuido a la perdida de tensión en las membranas celulares debido a la disminución del volumen de la célula provocado por la reducción de la cantidad de agua que contienen. Por otro

lado, por debajo de este punto, serían los cambios físicos encontrados en el mesófilo los que provocarían las variaciones en las propiedades ultrasónicas de la hoja.

El mejor análisis de la curva de resonancia ha llevado a cabo una mejor aproximación de la magnitud y de la fase de resonancia de las hojas. Esto ha permitido obtener, de manera directa, valores reales de  $c_{33}$  alcanzando un mejor conocimiento de este parámetro. Por un lado, las variaciones relativas observadas en  $c_{33}$  son mayores que las variaciones observadas en la frecuencia de resonancia, la velocidad, la densidad o el espesor, y por otro, a través de la variación de  $c_{33}$  también se podría estimar el punto de perdida de turgencia. Por lo tanto  $c_{33}$  puede ser un buen indicador del estado de la hoja y estudiar sus variaciones puede ser un mejor procedimiento del estudio del contenido en agua de las hojas.

Las principales ventajas de esta técnica sobre el análisis clásico de las curvas presión-volumen son su simplicidad y su mayor rapidez además de realizarse de forma no destructiva y sin contacto entre la muestra y el instrumental. Además, la habilidad de registrar cambios rápidos en los valores de turgencia bajo condiciones de libre transpiración de la hoja, puede constituir una herramienta de relevante importancia para el estudio de procesos dinámicos asociados a esta variable.

Esta tesis muestra también como los cambios en el contenido en agua de las hojas de chopo pueden ser determinados exactamente a través de los cambios en la reflectividad a una frecuencia del rango de las microondas de 1730 MHz. El uso de un dispositivo portátil, de bajo coste y tecnológicamente simple, basado en una antena de microondas de telefonía móvil digital, podría servir en el futuro como soporte para el desarrollo de una herramienta comercial portátil para determinar el estado hídrico de las plantas en campo. Esta otra técnica, aunque solo ha sido probada en un específico clon de chopo, puede ser aplicada a otros clones y a otras especies con similares dimensiones foliares. Emplear esta técnica en especies con hojas más pequeñas implicaría el uso de otros rangos de frecuencias y el desarrollo de otros tipos de antena.

## 6. PERSPECTIVAS

En base a los satisfactorios resultados que se presentan en la tesis, se están planteando nuevos estudios y posibilidades para el mejor conocimiento de las técnicas y su relación con el estado hídrico de las hojas. En cuanto a la técnica espectroscópica de ultrasonidos, *i)* se quiere incrementar el número de especies medidas incluyendo especies agrícolas como *Vitis vinifera*, *Malus domestica* o *Pyrus communis*, *ii)* se aspira a establecer una mejor relación entre  $\varepsilon$  y  $c_{33}$ , y *iii)* se quieren realizar nuevos estudios sobre la medida y la importancia de las ondas de cizalladura en las hojas o sobre la medida de las constantes de elasticidad en las otras dos direcciones de la hoja ( $c_{31}$  y  $c_{32}$ ). Por otra parte, para la técnica de microondas, además de seguir profundizando en sus bases teóricas y ampliar el número de especies medidas, se espera mejorar el instrumental de medida *i)* utilizando antenas de menor tamaño y forma variable, *ii)* buscando otros rangos de frecuencias que sean mas efectivos y *iii)* utilizando analizadores de redes portátiles.

## 7. BIBLIOGRAFÍA

- Azcón-Bieto J, Talón M.** 2000. Fundamentos de Fisiología Vegetal. McGraw-Hill/Interamericana de España, Aravaca, Madrid.
- Barrs HD.** 1965. Comparison of water potentials in leaves as measured by two types of thermocouple psychrometers. Australian Journal of Biological Sciences 18, 36-52.
- Barrs HD.** 1968. Determination of water deficits in plant tissues. In: Kozlowski TT, ed. Water deficits and plant growth, Vol. I. Academic Press, London and New York.
- Boyer JS.** 1966. Isopiestic technique: measurement of accurate leaf water potentials. Science 154, 1459-60.
- Boyer JS, Knippling EB.** 1963. Isopiestic technique for measuring leaf water potentials with a thermocouple psychrometer. Proceedings of the National Academy of Sciences 54, 1044-51.
- Brekhovskikh LM.** Waves in layered media, New York, 1960.
- Brodrribb TJ, Holbrook NM.** 2003. Stomatal closure during leaf dehydration, correlation with other leaf physiological traits. Plant Physiology 132, 2166-2173.
- Carter GA.** 1991 Primary and secondary effects of water content on the spectral reflectance of leaves. American Journal of Botany 78, 916-924.
- Corcuera L, Camarero JJ, Gil-Pelegrín E.** 2002. Functional groups in *Quercus* species derived from the analysis of pressure-volume curves. Trees, Structure and Function 16, 465-472

- Dreyer E, Bousquet F, Ducrey M.** 1990. Use of pressure volume curves in water relations analysis on woody shoots: influence of rehydration and comparison of four European oak species. *Annales des Sciences Forestières* 47, 285-297.
- Fukuhara M, Gupta SD, Okushima L.** 2006. Acoustic characteristics of plant leaves using ultrasonic transmission waves. In: Gupta SD, Ibaraki Y, eds. *Plant tissue culture engineering*. Dordrecht: Springer, 427-439.
- Geitmann A.** 2006. Experimental approaches used to quantify physical parameters at cellular and subcellular levels. *American Journal of Botany* 93, 1380-1390.
- Gómez Álvarez-Arenas TE, Montero F, Moner M, Rodríguez E, Roig A, Molins E.** 2002. Viscoelasticity of silica aerogels at ultrasonic frequencies. *Applied Physics Letters* 81, 1198-1200.
- Gómez Álvarez-Arenas TE.** 2003a. Air-coupled ultrasonic spectroscopy for the study of membrane filters. *Journal of Membrane Science* 213, 195-207.
- Gómez Álvarez-Arenas TE.** 2003b. A non-destructive integrity test for membrane filters based on air-coupled ultrasonic spectroscopy. *IEEE Transactions on Ultrasonics, Ferroelectrics and Frequency Control* 50, 676-685.
- Gómez Álvarez-Arenas TE, Sancho-Knapik D, Peguero-Pina JJ, Gil-Pelegrín E.** 2009a. Determination of Plant Leaves Water Status using Air-Coupled Ultrasounds. *Proceedings IEEE Ultrasonics Symposium*, 771-774.
- Gómez Álvarez-Arenas TE, Benedito J, Corona E.** 2009b. Non-contact ultrasonic assessment of the properties of vacuum-packaged dry-cured ham. *Proceedings IEEE Ultrasonics Symposium*, 2541-2544.
- Gómez Álvarez-Arenas TE.** 2010. Simultaneous determination of the ultrasound velocity and the thickness of solid plates from the analysis of thickness resonances using air-coupled ultrasound. *Ultrasonics* 50, 104-109.
- Gómez Álvarez-Arenas TE, Calás H, Ealo Cuello J, Ramos Fernández A, Muñoz M.** 2010. Noncontact ultrasonic spectroscopy applied to the study of polypropylene ferroelectrets. *Journal of Applied Physics* 108, 074110.
- Haines NF, Bell JC, McIntyre PJ.** 1978. The application of broadband ultrasonic spectroscopy to the study of layered media. *Journal of the Acoustical Society of America* 76, 498-504.
- Jones HG.** 1990. Plant water relations and implications for irrigation scheduling. *Acta Horticulturae* 278, 67-76.
- Jones HG.** 2004. Irrigation scheduling: advantages and pitfalls of plant-based methods. *Journal of Experimental Botany* 55, 2427-2436.
- Jones HG.** 2007. Monitoring plant and soil water status: established and novel methods revisited and their relevance to studies of drought tolerance. *Journal of Experimental Botany* 58, 119-130.
- Kline RA.** 1984. Measurement of attenuation and dispersion using an ultrasonic spectroscopy technique. *Journal of the Acoustical Society of America* 76, 498-504.
- Knippling EB, Kramer PJ.** 1967. Comparison of the dye method with the thermocouple psychrometer for measuring leaf water potentials. *Plant Physiology* 42, 1315-1320.
- Larcher W.** 2003. *Physiological Plant Ecology*. 4th Edition. Ecophysiology and Stress Physiology of Functional Groups. Springer-Verlag, Berlin.

- Lintilhac PM, Wei C, Tanguay JJ, Outwater JO.** 2000. Ball tonometry: a rapid, non-destructive method for measuring cell turgor pressure in thin-walled plant cells. *Journal of Plant Growth Regulation* 19, 90-97.
- Martinez M, Artacho JM, Forniés-Marquina JM, Letosa J, García Gracia, Gil E.** 1995 Dielectric behaviour by T.D.R. of the water status in a vegetal leaf. OHD Biennial Colloquium Digest, 13.
- McBurney T.** 1992. The relationship between leaf thickness and plant water potential. *Journal of Experimental Botany* 43, 327-335.
- Menzel MI, Tittmann S, Bühler J, Preis S, Wolters N, Jahnke S, Walter A, Chlubek A, Leon A, Hermes N, Offenhäuser A, Gilmer F, Blümller P, Schurr U, Krause HJ.** 2009. Non-invasive determination of plant biomass with microwave resonators. *Plant, Cell and Environment* 32, 368-379.
- Nobel PS.** 1983. Biophysical Plant Physiology and Ecology. WH Freeman, San Francisco.
- Passiourara JB.** 1982. Water in the soil-plant-atmosphere continuum. In Encyclopedia of Plant Physiology. New Series, Vol. 12B (eds Lange OL, Nobel PS, Osmond CB, Ziegler H). Springer-Verlag, Berlin.
- Pearcy RW, Ehleringer JR, Mooney HA, Rundel PW.** 1991. Plant Physiological Ecology. Field methods and instrumentation. Chapman and Hall, London.
- Pialucha T, Guyott CCH, Cawley P.** 1989. Amplitude spectrum method for the measurement of phase velocity. *Ultrasonics* 27, 270-279.
- Sachse W, Pao YH.** 1978. On the determination of phase and group velocities of dispersive waves in solids. *Journal of Applied Physics* 49, 4320-4327.
- Santos JE, Douglas JJ, Corberó JM, Lovera OM.** 1990. A model for wave propagation in a porous medium saturated by a two-phase fluid. *Journal of the Acoustical Society of America* 87, 1439-1448.
- Schabenberger O, Pierce FJ.** 2002. Contemporary statistical models for the plant and soil sciences. CRC Press. Boca Raton, FL.
- Schollander PF, Hammel HT, Bradstreet ED, Hemmingsen EA.** 1965. Sap pressure in vascular plants. *Science* 148, 339-345.
- Seelig HD, Hoehn A, Stodieck LS, Klaus, Adams III WW, Emery WJ.** 2009. Plant water parameters and the remote sensing  $R_{1300}/R_{1450}$  leaf water index: controlled condition dynamics during the development of water deficit stress. *Irrigation Science* 27, 357-365.
- Slatyer RO.** 1967. Plant-Water Relationships. Academic Press, London.
- Slavík B.** 1974. Methods of Studying Plant Water Relations. Berlin, Springer.
- Spanner DC.** 1951. The Peltier effect and its use in measurements of suction pressure. *Journal of Experimental Botany* 2, 145468.
- Stor-Pellinen J, Hæggström E, Karppinen T, Luukkala M.** 2001. Air-coupled ultrasonic measurement of the change in roughness of paper during wetting. *Measurement Science and Technology* 12, 1336-1341.
- Tognetti R, Giovannelli A, Lavini A, Morelli G, Fragnito F, d'Andria R.** 2009. Assessing environmental controls over conductances through the soil-plant-atmosphere continuum in an experimental olive tree plantation of southern Italy. *Agricultural and FOREST Meteorology* 149, 1229-1243.

- Torii T, Okamoto T, Kitani O.** 1988. Non-destructive measurement of water content of a plant using ultrasonic technique. *Acta Horticulturae* 230, 389-396.
- Turner NC.** 1981. Techniques and experimental approaches for the measurement of plant water status. *Plant and Soil* 58, 339-366.
- Tyree MT, Hammel HT.** 1972. The measurement of the Turgor pressure and the water relations of plants by the pressure-bomb technique. *Journal of Experimental Botany* 23, 267-282.
- Tyree MT, Jarvis PG.** 1982. Water in tissues and cells. In *Encyclopedia of Plant Physiology. New Series*, Vol. 12B (eds Lange OL, Nobel PS, Osmond CB, Ziegler H). Springer-Verlag, Berlin.
- Wu C, Niu Z, Tang Q, Huang W.** 2009. Predicting vegetation water content in wheat using normalized difference water indices derived from ground measurements. *Journal of Plant Research* 122, 317-326.
- Wullschleger SD, Oosterhuis DM.** 1987. Electron microscope study of cuticular abrasion on cotton leaves in relation to water potential measurements. *Journal of experimental Botany* 38, 660-667.
- Zimmer F, Grueger H, Heberer A, Wolter A, Schenk H.** 2004. Development of a NIR micro spectrometer based on a MOEMS scanning grating. *MEMS MOEMS Micromaching* 5455, 9-18.
- Zimmermann D, Reuss R, Westhoff, Gebner P, Bauer W, Bamberg, Bentrup FW, Zimmermann U.** 2008. A novel, non-invasive, online-monitoring, versatile and easy plant-based probe for measuring leaf water status. *Journal of Experimental Botany* 59, 3157-3167.

## E. APÉNDICES



## APÉNDICE 1: Factor de impacto y Área temática de las revistas

<b>Revista</b>	<b>Factor de impacto</b>	<b>Área temática</b>
Journal of Experimental Botany	4,818	Plant Science
IEEE Transactions on Ultrasonics, Ferroelectrics and Frequency Control	1,462	Acoustics Engineering, Electrical & Electronic
Agricultural and Forest Meteorology	3,228	Agronomy Forestry Meteorology & Atmospheric Science



## APÉNDICE 2: Justificación de la contribución del doctorando

**Artículo I.** *Sancho-Knapik D, Gómez Álvarez-Arenas T, Peguero Pina JJ, Gil-Pelegrín E. 2010. Air-coupled broadband ultrasonic spectroscopy as a new non-invasive and non-contact method for the determination of leaf water status. Journal of Experimental Botany 61, 1385-1391.*

La contribución del doctorando Domingo Sancho en este primer trabajo fue la colaboración en el planteamiento inicial y posterior, la utilización del instrumental ultrasónico para la obtención de la variable *frecuencia de resonancia de la hoja*, la obtención de las variables fisiológicas *Contenido relativo en agua* y *potencial hídrico*, el análisis de éstos parámetros y la búsqueda de las relaciones entre ellos estableciendo una correlación directa entre el *punto de pérdida de turgencia* y el punto de inflexión en las sigmoides que las relacionan, realización de los análisis estadísticos, colaboración en la redacción del artículo, colaboración en las correcciones requeridas por los evaluadores de la revista y presentación y discusión de los resultados al Dr MT Tyree.

**Artículo II.** *Sancho-Knapik D, Gómez Álvarez-Arenas T, Peguero-Pina JJ, Fernández V, Gil-Pelegrin E. 2011. Relationship between ultrasonic properties and structural changes in the mesophyll during leaf dehydration. Journal of Experimental Botany 62, 3637-3645.*

La contribución del doctorando en este segundo trabajo fue la colaboración en el planteamiento, la utilización del instrumental ultrasónico para la obtención de las variables *frecuencia de resonancia* y *factor-Q*, la estimación de la *constante elástica macroscópica* de la hoja, la obtención de las variables fisiológicas *contenido relativo en agua, espesor y densidad*, colaboración en la obtención del *modulo de elasticidad de pared*, el análisis de éstos parámetros y la búsqueda de las relaciones entre ellos elaborando una interpretación de la evolución con la pérdida de agua en la hoja en función de los cambios observados en la misma, colaboración en la realización de los análisis estadísticos, colaboración en la redacción del artículo y colaboración en las correcciones requeridas por los evaluadores de la revista.

**Artículo III.** *Sancho-Knapik D, Calás H, Peguero-Pina JJ, Ramos Fernández A, Gil-Pelegrín E, Gómez Álvarez-Arenas T. 2012. Air-coupled ultrasonic resonant spectroscopy for the study of the relationship between plants leaves elasticity and their water content. IEEE Transactions on Ultrasonics, Ferroelectrics and Frequency Control 59, 319-325.*

La contribución del doctorando en este tercer trabajo fue la colaboración en el planteamiento inicial, la utilización del instrumental ultrasónico para la obtención de las variables *frecuencia de resonancia* y *constante elástica macroscópica* en un número más amplio de especies vegetales, la obtención del *contenido relativo en agua* y colaboración en la redacción del artículo.

**Artículo IV.** *Sancho-Knapik D, Gismero J, Asensio A, Peguero-Pina JJ, Fernández V, Gómez Álvarez-Arenas T, Gil-Pelegrín E. 2011. Microwave L-band (1730 MHz) accurately estimates the relative water content in poplar leaves. A comparison with a near infrared water index (R1300/R1450). Agricultural and Forest Meteorology 151, 827-832.*

Por último, la contribución del doctorando en este cuarto trabajo fue la colaboración en el planteamiento inicial y posterior, la utilización de la antena de microondas y del dispositivo de infrarrojos para la obtención de las variables físicas tanto en las hojas como en los filtros, análisis de las medidas y búsqueda de su relación con el contenido hídrico relativo, medida de la variación del espesor con la variación del contenido hídrico, realización de los análisis estadísticos, colaboración en la redacción del artículo y colaboración en las correcciones requeridas por los evaluadores de la revista.

## Noncontact and noninvasive study of plant leaves using air-coupled ultrasounds

T. E. Gómez Álvarez-Arenas,<sup>1,a)</sup> D. Sancho-Knapik,<sup>2</sup> J. J. Peguero-Pina,<sup>2</sup> and E. Gil-Pelegrín<sup>2</sup>

<sup>1</sup>*Instituto de Acústica, CSIC, Serrano 144, 28006 Madrid, Spain*

<sup>2</sup>*Unidad de Recursos Forestales, CITA, Gobierno de Aragón, Apdo. 727, 50080 Zaragoza, Spain*

(Received 3 July 2009; accepted 21 October 2009; published online 11 November 2009)

Plant leaves are studied by the analysis of the magnitude and phase spectra of their thickness mechanical resonances. These resonances appear at ultrasonic frequencies and have been excited and sensed using air-coupled ultrasounds. In spite of the complex leaf microstructure, the effective medium approach can be applied to solve the inverse problem, at least in the vicinity of the first thickness resonance. Results suggest that these resonances are sensitive to leaf microstructure, composition water content and water status in the leaf. © 2009 American Institute of Physics. [doi:10.1063/1.3263138]

Plant leaves are key elements of the structure of life as it is there where the photosynthesis takes places. In addition, they are the last stage of an important and intriguing plant mechanism that permits to lift water from the soil up to the canopy. This is commonly described by the cohesion-tension theory, recently been tested in synthetic trees.<sup>1</sup> The knowledge of the way plant leaves operate, its mechanical and microstructural properties can be useful for the design of biologically inspired materials and is attracting a growing interest.<sup>2–5</sup>

In the context of plant physiology, it is extremely interesting to develop noninvasive procedures to monitor the dynamic of water movement through the plant in the context of the plant-soil-atmosphere continuum model.<sup>6</sup> Applications in this field demand sensors capable of monitoring water in the plant directly and online. Available techniques present serious difficulties as they are either too laborious or the equipment are too complex or automation is not possible or they are not fully noninvasive (see Ref. 7).

Ultrasonic techniques have shown very strong capabilities for materials noninvasive and nondestructive inspection. These techniques have also been applied to study plant leaves.<sup>8,9</sup> However, these techniques cannot be used to study variations of the water content or the turgor pressure in the leaf for water immersion was used. Use of air-coupled ultrasounds is promising. Among many different applications, air-coupled ultrasounds have been used for the study of synthetic membranes.<sup>10,11</sup> As these membranes exhibit some similarities with plant leaves, try to adapt that technique to plant leaves seems reasonable. Toward this end, it was necessary to modify the technique to avoid the necessity to independently measure the thickness, which is not acceptable in this case.

Let us consider two transducers located facing each other. First, transmission from transmitter directly into the receiver is measured, both magnitude and phase spectra ( $I_0(\omega)$  and  $\phi_0(\omega)$ , respectively- $\omega$ : angular frequency-) are calculated and stored. Then the leaf is put in between the transducers at normal incidence. Magnitude- $I(\omega)$ - and phase- $-\phi(\omega)$ - spectra of the transmitted signal are again calculated.

Hence, the insertion loss [ $M=I(\omega)/I_0(\omega)$ ] and the phase shift [ $\Phi=\Delta\phi=\phi(\omega)-\phi_0(\omega)$ ] are obtained.

The ratio ( $\xi$ ) of transmitted to incident wave potentials for normal incidence on a homogeneous and isotropic plate can be analytically calculated (see, for example, Refs 10–12). Transmission coefficient ( $T$ ), is defined as the ratio of transmitted to incident energy fluxes, and is given by  $T=|\xi|^2$ . The plot of  $T$  versus frequency - $T(f)$ - shows a pattern of thickness resonances located at:

$$\omega_n = 2\pi v(\omega_n) n / 2h, \quad n = 1, 2, 3, \dots, \quad (1)$$

where  $v$  is the velocity in the plate and  $h$  is the thickness. For our experimental set-up, following relations hold:  $T=M^2$  and  $\Phi=\phi(\xi)-h\omega/v_a$ , where  $\phi(\xi)$  is the phase of  $\xi$ .

If  $h$  is known and  $T(f)$  is measured (at least one resonance is observed), solution of the inverse problem permits us to obtain the following:  $v$ ,  $\alpha$ , and density.<sup>10,11</sup> On the contrary, when reverberations in the plate are either negligible or can be filtered out, then  $v(\omega)$  can be obtained directly from  $\Delta\phi$ ,  $h$ , and  $v_f$  (the velocity of ultrasounds in the fluid where the plate is immersed)<sup>13,14</sup>

$$v(\omega) = h/(h/v_f - \Delta\phi/\omega). \quad (2)$$

Presence of reverberations inside the plate introduces a phase shift and  $\xi$  becomes a complex magnitude.<sup>12</sup> This invalidates the use of Eq. (2). However, at  $\omega=\omega_n$  and if dissipation in the plate can be neglected,  $\xi$  is real valued, and both phase spectra with and without reverberations coincide. Therefore, Eq. (2) holds at resonance. From Eqs. (1) and (2) and measured  $\omega_1$  and  $\Delta\phi_1$ , velocity ( $v$ ) and thickness ( $h_{us}$ ) can be obtained.  $\omega_1$  can be measured from the frequency location of either the maximum of  $M$  or the point of inflection of  $\Delta\phi$ . Attenuation coefficient at  $\omega_1=2\pi f_1$ ,  $-\alpha(f_1)$ —is calculated from the measured  $Q$ -factor of the resonance and the density is calculated from the minimum value of  $T$ , as explained in Refs 10 and 11. These data are used to calculate the theoretical prediction for  $T$ . Fitting of the theoretical values into the experimental data is performed by considering a power law for the variation of the attenuation coefficient;  $\alpha(f)=\alpha(f_1)\times(f/f_1)^m$ ,  $1 < m < 2$ , commonly used for different viscoelastic and porous materials.<sup>15</sup> Then,  $m$  is the unique fitting pa-

<sup>a)</sup>Electronic mail: tgomez@ia.cetef.csic.es.

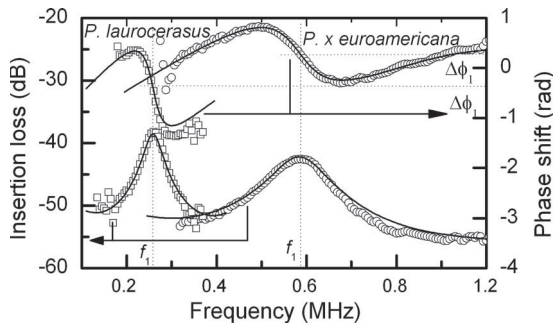


FIG. 1. Theoretical (solid line) and experimental insertion loss and phase shift vs frequency for a *P. Laurocerasus* and a *P. x Euroamericana* leaf.

parameter. This nonnegligible attenuation may displace the resonant frequency away from the condition given in Eq. (1), this may require to recalculate the values of  $v$  and  $h$  along the fitting procedure.

Ten different leaves of two evergreen species: *Prunus laurocerasus* and *Ligustrum lucidum* and two deciduous: *Platanus x hispanica* and *Populus x euroamericana* were studied. The leaf life-span influences the composition of the leaf; a longer life-span implies a higher percentage of resinous substances in order to make the leaf harder and more resistant; this feature is expected to affect the leaf ultrasonic properties. Average densities were; 780 Kg/m<sup>3</sup>, 950 Kg/m<sup>3</sup>, 870 Kg/m<sup>3</sup>, and 780 Kg/m<sup>3</sup>, respectively. In all cases, leaf cross-section is a four-layered structure: upper epidermis, palisade parenchyma (PP), spongy mesophyll (SM), and lower epidermis. Epidermis is a dense packing of flat cells with an external waxy cuticle, PP is a dense packaging of elongated cells (normal to the leaf plane) and the SM is a loose arrangement of cells with large intercellular spaces filled with air and moisture. Typical thickness ratio SM/PP is approximately ≈2, <1, ≈1, and ≈1 for *Prunus*, *Ligustrum*, *Populus*, and *Platanus*, respectively. The overall ultrasonic properties of the leaves are expected to be largely determined by the SM layer, where porosity is very high,  $\alpha$  should be very large and  $v$  very low.

Three pairs of air-coupled transducers (center frequency of 0.25, 0.75, and 1.2 MHz, circular aperture and diameter of 25, 20, and 20 mm, respectively) were used.<sup>15,16</sup> Transmitter-receiver separation was between 1 and 2 cm and leaves were located at normal incidence. Variations of the resonances when the ultrasound beam is scanned over the leaf surface were negligible. Figure 1 shows measured and calculated (assuming the leaf as a plane homogeneous and isotropic plate)  $M$  and  $\Delta\phi$  in the vicinity of the first thickness resonance. One interesting feature is that plant leaves, though being a complex, anisotropic, and heterogeneous material, provide a first thickness resonance that is well described by the theory for isotropic and homogeneous plates. Obtained leaf parameters from the analysis of the first thickness resonance appear in Table I. In addition, thickness was measured using a micrometer — $h_{\text{microm}}$ —(error ± 5 μm).  $h_{\text{us}}$  is very close to  $h_{\text{microm}}$ , differences can be accounted for by the fact that the leave deforms under the pressure of the micrometer. Table I shows, for a given specie, a certain link between leaf thickness and  $v$  and  $\alpha$ , which suggests a close relationship between the ultrasonic parameters and either the leaf development stage or the presence of a polluted environment, which can give rise to a reduction of the PP layer. In addi-

TABLE I. Measured properties of two different leaves of each specie.

Sample	$h_{\text{microm}}$ (μm)	$h_{\text{us}}$ (μm)	$v$ (air) (m/s)	$v$ (water) (m/s)	$f_1$ (KHz)	$\alpha(f_1)$ Np/m
<i>Prunus</i>	425	464 ± 10	255 ± 5	419	275 ± 4	910 ± 10
	445	475 ± 25	270 ± 15	409	283 ± 4	800 ± 70
<i>Ligustrum</i>	345	370 ± 5	196 ± 3	298	265 ± 4	790 ± 10
	540	552 ± 6	287 ± 3	348	260 ± 4	416 ± 10
<i>Populus</i>	250	250 ± 3	365 ± 5	436	730 ± 4	1420 ± 40
	280	295 ± 2	351 ± 5	416	598 ± 4	1140 ± 50
<i>Platanus</i>	190	214 ± 2	275 ± 5	512	640 ± 4	3200 ± 100
	235	232 ± 8	369 ± 9	570	805 ± 4	2070 ± 100

tion, deciduous and evergreen species exhibit different ultrasonic properties.

As expected, measured  $v$  and  $\alpha$  are similar to those obtained for porous membranes.<sup>10,11</sup> Under the action of the ultrasounds the fibers bend and the vacuoles deform as solid spheres in the Hertz problem. These deformation modes, common in porous media, give rise to low elastic moduli and hence, to low ultrasonic velocity.<sup>17</sup>

To determine whether the leaf layered structure has any influence on  $T(f)$ , *Prunus* and *Ligustrum* leaves were measured at higher frequencies, see Fig. 2. Theoretical predictions encounter some of the following problems: the periodicity of the resonances is altered and the value of  $T(f)$  in between resonances is lower than predicted. This behavior is typical of a multilayered plate, where as frequency increases, resonances of sublayers may become apparent, as well as the coupling between them. It is also interesting that the increase of the damping with the frequency is much more pronounced for the *Prunus* than for the *Ligustrum* leaf. Both are evergreen species but the *Prunus* leave exhibit a thicker SM layer.

To determine velocity of shear waves, incidence angle of the ultrasonic beam on the leaf was changed,<sup>18</sup> however, no evidence of shear waves was observed. Finally, the leaves were measured using a conventional water immersion and through transmission ultrasonic technique at 1.00 and 2.25 MHz (see Table I). Differences between ultrasonic velocities from different techniques can be explained considering that leaves rehydrates when they are immersed in water. To verify this, additional measurements were performed using a dry contact technique (at 0.25 MHz) on five *Prunus* leaves. Av-

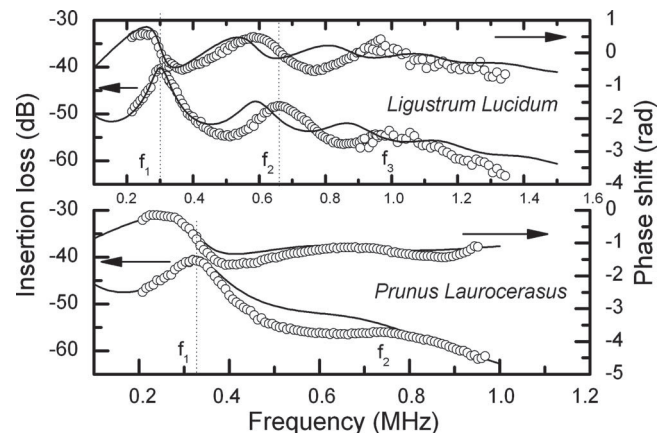


FIG. 2. Theoretical (solid line) and experimental insertion loss and phase shift vs frequency for a *P. Laurocerasus* and a *L. Lucidum* leaf.

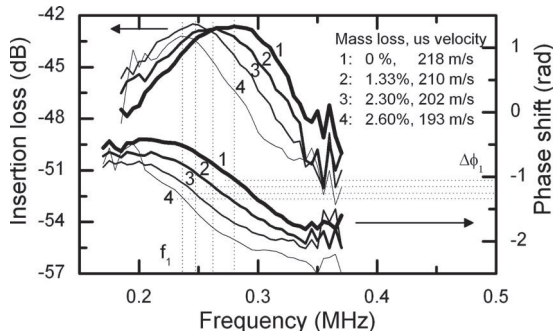


FIG. 3. Evolution of experimental insertion loss and phase shift vs frequency of a *P. Laurocerasus* leaf as water content decreases.

eraged velocity was  $293 \pm 35$  m/s, which agree with the value obtained with the air-coupled technique.

Finally, Fig. 3 shows that the response of the first thickness resonance of a *Prunus* leaf changes as it is left to dry at ambient conditions. A similar behavior was found in the other species. Loss of water is measured by weighing the leaf with a high precision balance. As water evaporates the resonance frequency and the velocity decreases while the attenuation increases. Initially (mass loss  $<2.0\%$ ) no thickness variation is observed ( $400 \pm 15$   $\mu\text{m}$ ), from 2.0% to 2.6% of mass loss, thickness reduces steadily down to 360  $\mu\text{m}$ . This velocity decrease can be explained by an increase of the compressibility of the cells that build up the leaf structure due to a loss of pressure in the vacuole membrane produced by the loss of water, that is, a decrease of the turgor pressure. Calculated values of the compressibility are 37.3, 34.1, 31.25, and 28.4 MPa, respectively.

The research presented demonstrate the possibility to excite and sense thickness resonances of plant leaves using air-coupled ultrasonic spectroscopy and to determine, simultaneously, thickness and velocity and attenuation coefficient of ultrasounds. Response of the first thickness resonance is well described by assuming the leaf as homogeneous and isotropic; deviation of higher resonance orders from this behavior can be attributed to the layered structure of the leaf.

Measurements suggest a close relationship between ultrasonic parameters and leaf development stage or environmental conditions. Evergreen and deciduous species present different ultrasonic properties that can be attributed to variations of leaf morphology and composition that depends on the leaf life-span. In addition, for similar species, the attenuation coefficient is larger and increases more rapidly with the frequency for those leaves having the thicker SM. Finally, ultrasound velocity and attenuation shows a great sensitivity to variations of the leaf water content, mainly due to the variations of turgor pressure associated to the changes in the water content.

- <sup>1</sup>T. D. Wheeler and A. D. Stroock, *Nature (London)* **455**, 208 (2008).
- <sup>2</sup>R. T. Borno, J. D. Steinmeyer, and M. M. Maharbiz, *Appl. Phys. Lett.* **95**, 013705 (2009).
- <sup>3</sup>W. Barthlott and C. Neinhuis, *Planta* **202**, 1 (1997).
- <sup>4</sup>Z. M. Liu, W. J. Wu, and B. R. Hu, *Sci. China, Ser. E: Technol. Sci.* **51**, 1902 (2008).
- <sup>5</sup>Z. Guo, W. Liu, and B.-L. Su, *Appl. Phys. Lett.* **93**, 201909 (2008).
- <sup>6</sup>M. Tyree, *Handbook of functional plant ecology* (Marcel Dekker, New York, 1999), pp. 221–268.
- <sup>7</sup>D. Zimmermann, R. Reuss, M. Westhoff, P. Geßner, W. Bauer, E. Bamberg, F.-W. Bentrup, and U. Zimmermann, *J. Exp. Bot.* **59**, 3157 (2008).
- <sup>8</sup>M. Fukuhara, *Plant Sci.* **162**, 521 (2002).
- <sup>9</sup>P. S. Wilson and K. H. Dunton, *J. Acoust. Soc. Am.* **125**, 1951 (2009).
- <sup>10</sup>T. E. Gómez Álvarez-Arenas, *J. Membr. Sci.* **213**, 195 (2003).
- <sup>11</sup>T. E. Gómez Álvarez-Arenas, *IEEE Trans. Ultrason. Ferroelectr. Freq. Control* **50**, 676 (2003).
- <sup>12</sup>L. M. Brekhovshikh, *Waves in Layered Media* (Academic Press, New York, 1960).
- <sup>13</sup>T. E. Gómez Álvarez-Arenas, S. de la Fuente, and I. González, *Appl. Phys. Lett.* **88**, 221910 (2006).
- <sup>14</sup>W. Sachse and Y. H. Pao, *J. Appl. Phys.* **49**, 4320 (1978).
- <sup>15</sup>T. E. Gómez Álvarez-Arenas, *IEEE Trans. Ultrason. Ferroelectr. Freq. Control* **51**, 624 (2004).
- <sup>16</sup>T. E. Gómez Álvarez-Arenas and I. González Gómez, *Appl. Phys. Lett.* **90**, 201903 (2007).
- <sup>17</sup>L. J. Gibson and M. F. Ashby, *Cellular Solids* (Cambridge University Press, Cambridge, 1999), pp. 92–110.
- <sup>18</sup>T. E. Gómez Álvarez-Arenas, F. Montero, M. Moner, E. Rodríguez, A. Roig, and E. Molins, *Appl. Phys. Lett.* **81**, 1198 (2002).



# Determination of Plant Leaves Water Status using Air-Coupled Ultrasounds

Tomás Gómez Álvarez-Arenas

Instituto de Acústica,

Spanish Scientific Research Council , CSIC

Madrid, Spain

[tgomez@ia.cetef.csic.es](mailto:tgomez@ia.cetef.csic.es)

**Abstract**— Water in plants is studied by analyzing the magnitude and the phase spectra of the first thickness resonance of their leaves. These resonances appear at ultrasonic frequencies and have been excited and sensed using air-coupled ultrasounds. In spite of the complex leaf microstructure, the resonances of the leaves can be well described by the resonances of either a homogeneous and isotropic solid plate or a four-layered composite. Results reveal that these resonances are strongly sensitive to leaf microstructure, water content and water status in the leaf. As the technique is completely non-contact and non-invasive, it offers a unique possibility to study the complex dynamic behaviour of water in plants and the water exchange between the plant and the atmosphere across the leaves.

**Keywords-component;** *plant leaves; air-coupled ultrasound, spectral analysis, thickness resonance.*

## I. INTRODUCTION.

Plant leaves are key elements of the structure of life as it is there where the photosynthesis takes place; through the leaves the plants interchange gases, water vapour and energy with the atmosphere. In this sense, they are the last stage of an important and intriguing plant mechanism that permits to lift water from the soil up to the canopy. The cohesion-tension theory commonly accepted to describe this mechanism is based on the reduction of pressure in the leaf due to evaporation and the appearance of large negative pressures that stretches the water in the capillaries. This mechanism has recently been tested in synthetic trees [1]. Recently, a synthetic leaf has been proposed to harvest energy from evaporation-driven flows. [2]

Figure 1 shows a schematic cross section of the structure of a leaf made up of four layers: upper epidermis (densely packed cells with very thick walls and a waxy cuticle), palisade parenchyma, spongy mesophyll and lower epidermis. In addition, leaves also contain veins. In the spongy mesophyll there are large spaces between cells that contain moist air and allow diffusion of carbon dioxide. Stomata in the lower epidermis permit the exchange of moisture and carbon dioxide between the leaf and the atmosphere. Unlike stretched water in the plant capillaries, water contained on leaf cells (vacuoles) is subjected to positive pressures. This is due to the elastic energy stored in the vacuole membrane. This mechanism is responsible for the turgor pressure which maintains the leaf (and in some cases the whole plant) rigid.

D. Sancho-Knapik, J. J. Peguero-Pina and E. Gil-

Pelegrín.

Unidad de Recursos Forestales

CITA, Gobierno de Aragón

Zaragoza, Spain

In the context of plant physiology it is extremely interesting to develop non-invasive procedures to monitor the dynamic of water movement through the plant and from the plant into the atmosphere, in the context of the plant-soil-atmosphere continuum model. This is also interesting for the optimization of water supplies. These applications demand sensors capable of monitoring water content of the plant directly and online. Available techniques present serious difficulties as they are either too laborious or the equipment too complex or automation is not possible or they are not fully non-invasive.

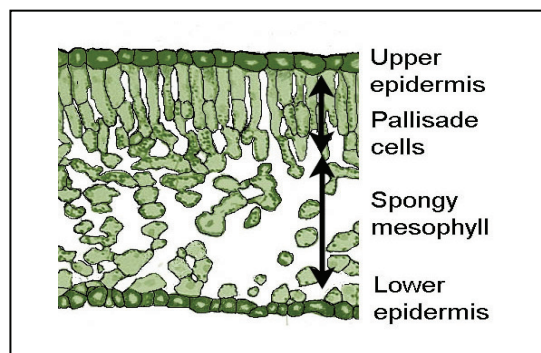


Figure 1. Cross-section of the leaf

Recently, Fukuhara [3] measured velocity and attenuation of ultrasounds in plant leaves. However, this technique presents the drawback of using water as coupling medium. This water penetrates in the leaves and modifies their acoustic properties (see Ref. [4]). More recently [4], we have used air-coupled ultrasounds to excite and sense the first order thickness resonance of leaves of different plants. The spectral response of the transmission coefficient in the vicinity of the first thickness resonance (both magnitude and phase) is well described by the theory of sound transmission through a homogeneous solid plate. Solution of the inverse problem permitted the authors to obtain, simultaneously, velocity and attenuation of ultrasounds in the leaf and the thickness of the leaf. Finally, it was experimentally demonstrated that small variation of water content in the leaf give rise to a measurable frequency shift of the leaf thickness-resonance.

In this paper, we investigate the possibility of using a more detailed model based on a four layered representation of the

Financial support from the “Ministerio de Ciencia e Innovación” in Spain (DPI2008-05213/DPI) is acknowledged

cross-section of the leaf. These layers correspond to the leaf structure shown in Fig. 1.

## II. EXPERIMENTAL SET-UP AND MATERIALS.

Ultrasonic transmitter and a receiver specially designed for efficient transmission/reception to/from the air, were positioned in opposition. Transmitter is driven by a negative square semi cycle tuned to the centre frequency of the transducers. So it launches an ultrasonic signal that travels across the air-gap between transmitter and receiver transducer and is eventually received by the receiver. This converts the ultrasonic signal into electrical, it is then amplified and filtered. Afterwards it is displayed and digitized in a digital oscilloscope.

The measuring procedure is as follows. First the signal received without any sample is acquired; FFT (magnitude and phase) is calculated and stored as reference. Then the sample is put in between the transducers at normal incidence, and the procedure is repeated, hence we calculate the phase shift ( $\Delta\phi$ ) and the insertion loss. Two pairs of special air-coupled transducers with centre frequency of 0.25 and 0.75 MHz were employed. Thickness was measured using a micrometer (error  $\pm 5 \mu\text{m}$ ).

Leaves from *Prunus laurocerasus*, *Ligustrum lucidum*, *Platanus x hispanica* and *Populus x euroamericana* were studied; for each species ten different leaves were measured.

## III. MODEL FOR SOUND TRANSMISSION THROUGH A PLANT LEAVE.

Thickness resonances of solid plates have been used in the context of air-coupled ultrasound with the purpose to increase the amount of transmitted energy [5]. For a homogeneous and isotropic plate the amplitude ratio of transmitted to incident wave potentials for normal incidence is given by:

$$\xi = \frac{-2Z_1 Z_2}{2Z_1 Z_2 \cos(kh) + i(Z_1^2 + Z_2^2) \sin(kh)} \quad (1)$$

where  $Z_1$  and  $Z_2$  are the acoustic impedances of the plate and the surrounding fluid,  $h$  the thickness of the plate and  $k$  the wave number. The first thickness resonance appears at a frequency given by the following relation:

$$v(\omega_0) = 2\omega_0 h / 2\pi \quad (2)$$

where  $v$  is the velocity of sound in the plate and  $\omega_0$  the angular frequency of the first thickness resonance. So if the proper combination of transducer frequency band, ultrasound velocity in the material and plate thickness is given, thickness resonances are observed.

Later, these resonances have been used to study the properties of the solid material. The most basic approach is to get an independent measurement of the thickness, and then work out the velocity of the ultrasounds in the solid from the relation given above. A more complete characterization of the solid can be obtained from the analysis of the whole resonance

vs. frequency curve. This procedure is explained in detail and used in [6] and [7]. An important limitation of this method is that the thickness of the plate must be independently measured. In some cases, this is either not possible or not accurate enough. Plant leaves is one of these cases.

However, if both magnitude and phase spectra of the transmission coefficient are simultaneously measured it is possible to overcome this problem and to obtain, simultaneously, both ultrasound velocity and thickness of the plate. This method was developed and tested for different materials and plates by Gómez Álvarez-Arenas [8] and it is based on the fact that at resonance and when attenuation is negligible the following relation is verified:

$$v(\omega_0) = \frac{h}{h/v_f - \Delta\phi/\omega_0} \quad (3)$$

where  $v_f$  is the velocity in the coupling fluid (in this case 340 m/s) and  $\Delta\phi$  is the phase shift. Equation 3 is the relation normally used to work out velocity from the measurement of phase spectrum in a through transmission experiment, [9] which is similar to the Sachse and Pao method [10]. Then, using equations 2 and 3, it is possible to simultaneously obtain both  $v$  and  $h$  from measured  $\omega_0$  and  $\Delta\phi(\omega_0)$ .

Finally,  $v$  and  $h$  so calculated are then used as initial guess to fit the theoretical value of  $T=|\xi|^2$  and  $\Delta\phi$  into the experimentally measured ones. A power law for the variation of the attenuation coefficient with the frequency is assumed:  $\alpha=\alpha_0 f^m$ , where  $1 < m < 2$ . It must be noted that this non-negligible attenuation displaces the resonant frequency away from the condition given by Eq. 1. Further details of the technique can be seen in Refs [4] and [8].

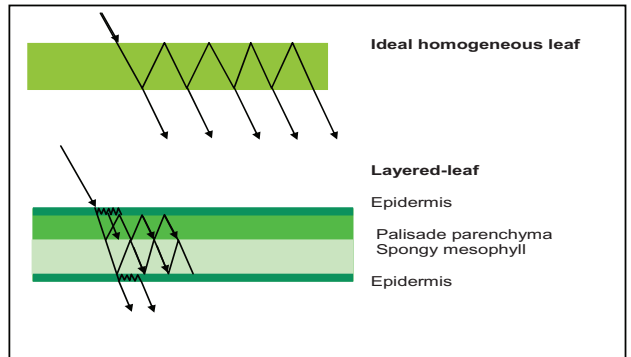


Figure 2. 1-layer and 4-layers models for plant leaves cross-section structure.

The presence of several sub-layers within the plate, having different acoustic properties, modifies the resonances of the plate. This situation is shown in Fig. 2. The main problem of modelling sound transmission through a leaf that presents a four-layered structure is that detailed information about each layer is needed. Unfortunately almost no information about the acoustic properties of these organic tissues is available. What we do know is the typical thickness of each layer and its microstructure or composition. The epidermis contains a very thin layer of a waxy cuticle and the epidermis itself: a layer of densely packed and rigid flattened cells. The pallisade

parenchyma is a less dense packing of elongated cells oriented along the normal direction to the leaf plane. This could be considered a 1-3 connectivity composite of pillar-like cells in a matrix of water and air. The next layer, the spongy mesophyll, presents a foam or spongy-like structure and can be considered a 0-3/3-3 connectivity composite. [11] This is made of less densely packed rounded cells and large spaces between them to allow diffusion of carbon dioxide, oxygen and water vapour. The elastic stiffness of the cells in these two layers are largely determined by the pressure of water inside them.

Determination of the properties of each of these layers lies out of the scope of this work; however, it is possible to propose a rough estimation of the properties of each of them. Let us consider a typical *Prunus laurocerasus* leaf:  $h=450 \mu\text{m}$ ,  $v=255 \text{ m/s}$ ,  $\rho = 785 \text{ Kg/m}^3$ ,  $\alpha(f_0)=740 \text{ Np/m}$ ,  $f_0 = 0.30 \text{ MHz}$  and a linear variation of the attenuation coefficient with the frequency (ref. 4). The calculated transmission coefficient (magnitude and phase) is shown in Fig. 3. Now we assumed a four-layered composite leaf, and that attenuation in all layers varies linearly with the frequency. For the upper layer and the lower layers (wax and epidermis) we considered a  $h = 12 \mu\text{m}$ ,  $\rho = 900 \text{ Kg/m}^3$ , (in between density of water and density of wax) and a velocity of sound similar to the velocity in water: 1500 m/s, finally,  $\alpha(f_0)=50 \text{ Np/m}$ . For the pallisade parenchyma, thickness is 200  $\mu\text{m}$ , now we are using velocity and density values similar to those observed in microporous polymer films with similar structure:  $v= 405 \text{ m/s}$ ,  $\alpha(f_0)=600 \text{ Np/m}$  and  $\rho = 900 \text{ Kg/m}^3$ . Finally, for the spongy mesophyll, the most complex layer from the acoustic point of view, we worked out its properties so that the global density of the four-layered model be equal to the density of the single layer model. A similar procedure was followed to determine the velocity and the attenuation coefficient, obtained result for the spongy mesophyll layer are:  $h=226 \mu\text{m}$ ,  $v=173 \text{ m/s}$ ,  $\rho = 624 \text{ Kg/m}^3$ ,  $\alpha(f_0)=929 \text{ Np/m}$ .

Calculated transmission coefficient for this composite structure is shown in Fig. 3. There are three main differences. First, there is a frequency shift. Second, the insertion loss predicted by the multilayered model is larger. Third, the regular resonance pattern observed in the one-layer model is distorted in the four layered model: periodicity is lost and the resonance pattern completely disappears at high frequencies. All these effects are the result of the multilayered structure.

It is interesting to try to fit the resonance peak calculated with the one-layered model into the calculated values with the four-layered model. In some sense, this is what we do when we try to fit the one-layered model into the experimental data (of a four layered leaf). Result is shown in the inset in Fig 3. Best fitting is obtained for the following material parameters in the 1-layer model:  $h=492 \mu\text{m}$ ,  $v=212 \text{ m/s}$ ,  $\rho = 785 \text{ Kg/m}^3$ ,  $\alpha(f_0)=1400 \text{ Np/m}$  and a quadratic variation of the attenuation coefficient with the frequency. That is, the result of fitting the 1-layer model first thickness resonance to the 4-layered composite first thickness resonance is that estimated attenuation coefficient in the 1 layer model is much larger than the actual value in the four-layered model, velocity somewhat lower and thickness slightly larger. In addition, the 1-layer model fails to reproduce the shape of the resonance curve at

high frequencies. This deviation of the parameters estimated with the 1-layer model related to the more precise parameter estimation of the 4-layered model has to be considered if leaf properties are going to be measured. However, this is not so important when relative variations of the leaf properties are to be studied; one example is the study of the variations of the leaf water content as it is shown below.

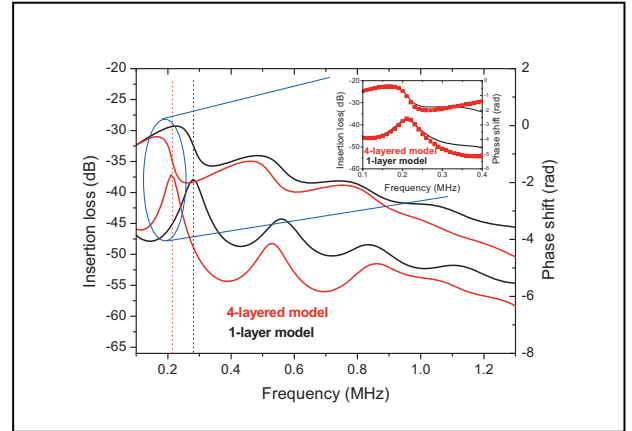


Figure 3. Coefficient of transmission (magnitude and phase) vs. frequency of a *Prunus* leaf.

#### IV. EXPERIMENTAL RESULTS.

Figure 4 shows measured and calculated T and  $\Delta\phi$  for two cases. One interesting feature is that the 1-layer model provides a good fitting into the experimental results, at least in the vicinity of the first thickness resonance.

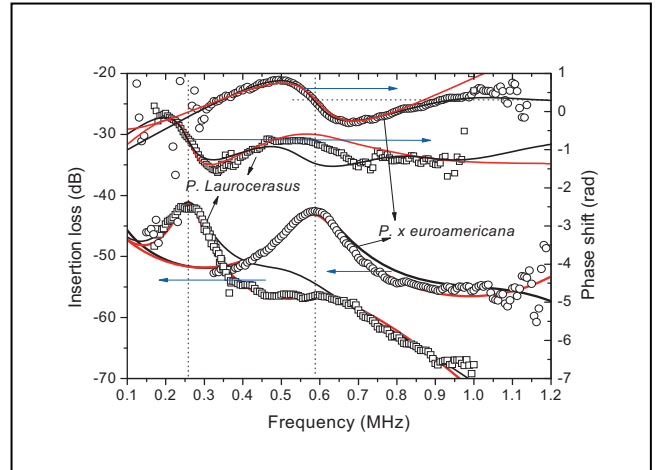


Figure 4. Experimental (dots) transmission coefficient vs. frequency of *P. Laurocerasus* and *P. x euroamericana* leaves. Solid line represents the theoretical predictions: Black 1-layer model, Red: 4-layers model.

Obtained ultrasound velocity and thickness from the 1-layer model for all the studied cases appear in Table I. Two cases for each species are show: the thickest and the thinnest leaves. Relationship between ultrasonic properties and thickness can be interpreted as the result of a close link between the ultrasonic properties and the leaf development stage. Ultrasonically measured thickness is very close to the thickness

measured with a micrometer, observed differences can be accounted for either by the fact that the leave deforms under the pressure of the micrometer or by the error of using a 1-layer model (in comparison with the real 4-layered leaf structure). Four-layers model parameters are summarized in Tables II and III. Calculated IL and phase appear in Fig. 4. As frequency increases the 4-layers model fits better into the experimentally observed behaviour.

TABLE I. MEASURED LEAF PROPERTIES.

Specie	$h$ (micrometer) ( $\mu\text{m}$ )	$h$ (ultrasound) ( $\mu\text{m}$ )	$v$ (m/s)
<i>P. laurocerasus</i>	425	$464 \pm 10$	$255 \pm 5$
	445	$475 \pm 25$	$270 \pm 15$
<i>L. lucidum</i>	345	$370 \pm 5$	$196 \pm 3$
	540	$552 \pm 6$	$287 \pm 3$
<i>P. x euroamericana</i>	250	$250 \pm 3$	$365 \pm 5$
	280	$295 \pm 2$	$351 \pm 5$
<i>P. x hispanica</i>	190	$214 \pm 2$	$275 \pm 5$
	235	$232 \pm 8$	$369 \pm 9$

TABLE II. *P. LAUROCERASUS* PARAMETERS FOR THE 4-LAYER MODEL

Layer	$h$ ( $\mu\text{m}$ )	$\rho$ ( $\text{Kg/m}^3$ )	$v$ (m/s)	$\alpha_0$ (Np/m)
Epidermis	12	900	1500	50
Palisade p.	251	950	450	350
Spongy m.	200	555	210	900

TABLE III. *P. X EUROAMERIC.* PARAMETERS FOR THE 4-LAYER MODEL.

Layer	$h$ ( $\mu\text{m}$ )	$\rho$ ( $\text{Kg/m}^3$ )	$v$ (m/s)	$\alpha_0$ (Np/m)
Epidermis	12	900	1500	50
Palisade p.	157	950	550	800
Spongy m.	121	600	300	1460

Finally, location and shape of the first thickness resonance spectral response change as water evaporates. Fig. 5 shows IL and phase for the first thickness resonance of a *Prunus* and a *Populus* leaves left to dry at ambient conditions. Loss of water is measured by weighing the sample with a high precision balance. As water evaporates the resonance frequency shifts towards lower values. A similar behaviour was found in the other species. For cases shown in Fig. 5, velocity is 218, 210, 202 and 193 m/s, respectively, while thickness remains constant. This velocity decrease can be explained by an increase of the compressibility of the arrangement of vacuoles that build up the leaf structure due to a loss of pressure in the vacuole membrane produced by the loss of water.

## V. CONCLUSIONS.

The technique presented permitted us to determine, simultaneously, thickness of plant leaves and velocity and attenuation coefficient of ultrasounds. The low values of the velocity can be linked to the microstructure of the leaf: air, fibres and water filled vacuoles. Measurements obtained from different leaves suggest a close relationship between ultrasound velocity and leaf development stage. Two models, 1-layer and 4-layers, have been proposed. The 4-layers model gives a more accurate description of the experimental data, though a more

complete knowledge of the leaf is required. The 1-layer model is simpler and provides a reasonably good description of the first thickness resonances, at least in the vicinity of the resonant frequency. In addition, ultrasound velocity shows a great sensitivity to any variation of the water content and water status in the leaf. The possibility of monitoring water content changes in a transpiring leaf will provide is of great importance for plant physiologists.

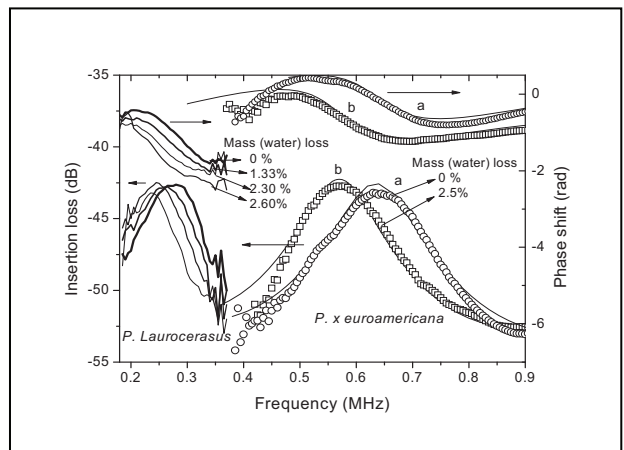


Figure 5. Variation of the first thickness resonance vs. frequency (magnitude and phase) as leaves lose water due to evaporation.

## VI. REFERENCES

- [1] T. D. Wheeler and A. D. Stroock, "The transpiration of water at negative pressure in a synthetic tree," *Nature*, no. 455, pp. 208, August 2008.
- [2] R. T. Borno, J. D. Steinmeyer, M. M. Maharbiz, "Charge-pumping in a synthetic leaf for harvesting energy from evaporation-driven flows," *Appl. Phys. Lett.*, no. 95, pp. 013705, 2009.
- [3] M. Fukuhara, "Acoustic characteristics of botanical leaves using ultrasonic transmission waves," *Plant Sci.* vol. 162, pp. 521-528, 2002
- [4] T. E. Gómez, D. Sancho-Knapik, J. J. Peguero-Pina and E. Gil-Pelegrín, "Non-destructive and non-invasive method for the study of plant leaves," unpublished..
- [5] D. W. Schindel and D. A. Hutchins, "Through-thickness characterization of solids by wideband air-coupled ultrasounds," *Ultrasonics*, vol. 33(1), pp. 11-17, 1995.
- [6] T. E. Gómez, "Air-coupled ultrasonic spectroscopy for the study of membrane filters," *J. Membr. Sci.* vol. 213, pp. 195-207, 2003.
- [7] T. E. Gómez, "A nondestructive integrity test for membrane filters based on air-coupled ultrasonic spectroscopy," *IEEE Trans. Ultrason., Ferroelect., Freq. Contr.*, vol 50 (6), pp. 676-685, 2003.
- [8] T. E. Gómez, "Simultaneous determination of the ultrasound velocity and the thickness of solid plates by using through-transmitted and wide-band airborne ultrasonic pulses," *Ultrasonics*, *in press*.
- [9] T. E. Gómez, S. de la Fuente, I. González, "Simultaneous determination of apparent tortuosity and microstructure length scale and shape: application to rigid open-cell foams," *Appl. Phys. Lett.* vol. 88, pp. 221910, 2006.
- [10] W. Sachse and Y. H. Pao, "On the determination of phase and group velocities of dispersive waves in solids," *J. Appl. Phys.*, vol. 49, pp. 4320-4327, 1978.
- [11] T. E. Gómez, A. J. Mulholland, G. Hayward, J. Gomatam, "Wave propagation in 0-3/3-3 connectivity composites with complex microstructure," *Ultrasonics*, vol. 38, pp. 897-907, 2000.



